MASTER'S DISSERTATION

ON THE BULK VISCOSITY AND SHEAR INDUCED DISPERSION IN MAGNETOHYDRODYNAMIC FLOWS

Leonardo Afonso da Silva Inácio

Brasília, May 9, 2024

UNIVERSITY OF BRASÍLIA

FACULTY OF TECHNOLOGY
DEPARTMENT OF MECHANICAL ENGINEERING

UNIVERSITY OF BRASÍLIA
Faculty of Technology
Department of Mechanical Engineering

MASTER'S DISSERTATION

ON THE BULK VISCOSITY AND SHEAR INDUCED DISPERSION IN MAGNETOHYDRODYNAMIC FLOWS

Leonardo Afonso da Silva Inácio

Dissertation submitted to the Department of Mechanical Engineering in partial fulfillment of the requirements for the degree of Master of Mechanical Sciences

Examining Committee

Francisco Ricardo da Cunha, PhD
Advisor (ENM-UnB)

André von Borries Lopes, PhD
Internal Member (ENM-UnB)

William Roberto Wolf, PhD
External Member (FEM-Unicamp)

Brasília, May 9, 2024

FICHA CATALOGRÁFICA

Inácio, L. A. S.
On the Bulk Viscosity and Shear Induced Dispersion in Magnetohydrodynamic Flows
[Distrito Federal] 2024.
xxii, 91p. (ENM/FT/UnB, Mestrado, Ciências Mecânicas, 2024.
Dissertação de Mestrado - Universidade de Brasília.
Faculdade de Tecnologia.
Departamento de Engenharia Mecânica.
Palavras-chave:

1. Escoamentos Magnetohidrodinâmicos	2. Gradiente de pressão
3. Campo magnético	4. Segundo coeficiente de viscosidade
5. Fluido condutor	6. Dispersão hidrodinâmica
I. ENM/FT/UnB	II. Título (série)

REFERÊNCIA BIBLIOGRÁFICA

Inácio, L. A. S. (2024). On the Bulk Viscosity and Shear Induced Dispersion in Magnetohydrodynamic Flows. Dissertação de Mestrado, Publicação ENM.DM - XXX.XXX, Departamento de Engenharia Mecânica, Universidade de Brasília, Brasília, Distrito Federal, xxii, 91p.

CESSÃO DE DIREITOS

This work is dedicated to my parents, Edmar and Mirian, and to my love, Isabelle.

“Physical laws should have mathematical beauty.”
(Paul Adrien Maurice Dirac)

“We are trying to prove ourselves wrong as quickly as possible,
because only in that way can we find progress.”
(Richard Feynman)

“Fall in love with some activity, and do it! Nobody ever figures out
what life is all about, and it doesn’t matter. Explore the world.
Nearly everything is really interesting if you go into it deeply enough.”
(Richard Feynman)

Acknowledgements

Primeiramente gostaria de agradecer imensamente ao meu orientador, professor e amigo Francisco Ricardo da Cunha pelo suporte incansável e por forncer sempre o melhor cenário para mim como aluno. Afinal, nada deste trabalho seria possível sem as incontáveis horas de reuniões e orientações, nas quais as dicussões científicas sempre engrandeceram o trabalho e minha formação, sem as majestosas disciplinas ministradas, que forneceram uma base inabalável para meu conhecimento acadêmico, e sem os conselhos gerais, que me engrandeceram no âmbito acadêmico e também no pessoal. Obrigado por tudo, Professor.

Agradeço também ao Professor e amigo André von Borries Lopes, o qual sempre esteve disposto a me ajudar, sempre com o maior entusiasmo. Nunca irei esquecer todos os incentivos e oportunidades para me aprimorar como acadêmico e docente que você me forneceu. Além de todos os conselhos pessoais e profissionais, que posso dizer que foram estritamente essenciais para a minha jornada. Obrigado por tudo.

Agradeço aos meus pais, Edmar e Mirian, e ao meu irmão, Eduardo. Tudo que eu tenho ou sou, eu devo a vocês. De fato, eu ganhei na loteria da família. Eu não mudaria absolutamente nada se pudesse. Agradeço profundamente por todo suporte e amor, afinal, vocês nunca mediram qualquer esforço para dar tudo de si para que eu pudesse ser feliz.

Agradeço profundamente à minha companheira de vida, minha noiva Isabelle. Você traz mais sentido à minha vida, você diariamente aumenta a minha satisfação pessoal com a arte de viver. O seu jeito de olhar o mundo permeia meus dias e me incentiva a correr atrás de tudo que quero viver. Você me inspira. Te agradeço infinitamente, principalmente por você ser você.

Agradeço à todos amigos do grupo VORTEX que de alguma forma me incentivaram e contribuiram para esse trabalho e para minha jornada acadêmica. Igor, Marcos, Matheus, Érick, Yuri, Victor e Olaf, muito obrigado por tudo.

Agradeço à todos os familiares e amigos próximos que me incentivaram e fornece-

ram suporte de alguma forma. Em especial às minhas primas Mariana e Juliana, que sempre me incentivaram na vida acadêmica, aos meus amigos Lucas Rocha, André Cássio e Gabriel Rizzo, que me fizeram companhia em grande parte das minhas escritas acadêmicas, e ao amigo Juan Linhares, que dividiu grande parte do tempo da graduação e do mestrado comigo.

Abstract

Title: On the Bulk Viscosity and Shear Induced Dispersion in Magnetohydrodynamic Flows
Author: Leonardo Afonso da Silva Inácio
Advisor: Francisco Ricardo da Cunha, Prof. Univ (ENM/UnB)
Master in Mechanical Sciences

In this dissertation, we explore two different flows in the context of magnetohydrodynamics (MHD). The first one focus on a study of the bulk viscosity (i.e. the second viscosity coefficient) in a compressible MHD flow, involving magnetoacoustic waves. In the second problem, we examine the phenomenon of shear induced dispersion in an incompressible magnetohydrodynamic flow. The governing equations of both flow problems represent a coupling between hydrodynamics and electrodynamics and the relevant physical parameters of the flow are presented after an appropriate dimensional analysis of these equations. Only few studies in the current literature have explored the effect of a bulk viscosity in compressible flows involving high frequency and propose how to determine this quantity experimentally. Therefore, in the first part of this work, we present a study on a flow of an electrically conducting barotropic gas in the presence of a bulk viscosity. Firstly, an analysis of small perturbations around an equilibrium state results in a system of linearized equations in the wave space. The dispersion relation for magnetic waves are determined in the presence of a bulk viscosity. Secondly, we propose a model to calculate the bulk viscosity in terms of the physical quantities related to magnetoacoustic waves. The results show the behavior of the bulk viscosity as a function of the wavenumber for different magnetic intensity and orientation, revealing how the rate of energy dissipation associated with the bulk viscosity can be controlled by an external magnetic field. In the second part of the work, we examine the phenomenon of shear induced dispersion in a magnetohydrodynamic flow of an incompressible electrically conducting suspension.

The mechanism underlying hydrodynamic dispersion involves symmetry breaking of particle trajectories after collisions. The governing equations are again presented and made non-dimensional by an appropriated scaling analysis. A supplementary diffusion equation based on hydrodynamic particle fluxes associated with both a gradient in particle concentration and a gradient in the shear rate is proposed and discussed. The resulting set of equations is solved analytically by a regular perturbation analysis, as the parameter PeK_c, where Pe is the Peclet number and K_c is the non-dimensional diffusivity associated with the shear-induced dispersion, is considered a small parameter in the coupled channel-flow. The results clearly show substantial variations of the velocity profile and the effective viscosity with the particle diffusivity in a channel-pressure driven flow in the presence of a uniform transversal magnetic field.

Key-words: Magnetohydrodynamic flows, pressure gradient, magnetic field, bulk viscosity, conducting fluid, hydrodynamic dispersion

Resumo

Título: Investigação sobre o Segundo Coeficiente de Viscosidade e Dispersão Induzida por Cisalhamento em Escoamentos Magnetohidrodinâmicos
Autor: Leonardo Afonso da Silva Inácio
Orientador: Francisco Ricardo da Cunha, Prof. Univ (ENM/UnB)
Mestrado em Ciências Mecânicas

Nesta dissertação, são explorados dois escoamentos diferentes no contexto da magnetohidrodinâmica (MHD). O primeiro foca em um estudo da viscosidade expansional (i.e. segundo coeficiente de viscosidade) em um escoamento MHD compressível, envolvendo ondas magnetoacústicas. No segundo problema, o fenômeno de dispersão induzida por cisalhamento é analisado em um escoamento magnetohidrodinâmico incompressível. As equações governantes para ambos os escoamentos representam um acoplamento entre a hidrodinâmica e a eletrodinâmica, e os parâmetros físicos relevantes do escoamento são apresentados depois de uma análise dimensional apropriada das equações. Apenas poucos estudos na atual literatura exploraram os efeitos da viscosidade expansional em escoamentos compressíveis envolvendo alta frequência e propuseram como determinar essa quantidade experimentalmente. Portanto, na primeira parte deste trabalho, é apresentado o estudo do escoamento de um de um gás barotrópico eletricamente condutor na presença da viscosidade expansional. Primeiramente, uma análise de pequenas perturbações em torno de um estado de equilíbrio resulta em um sistema de equações linearizado no espaço de onda. As relações de dispersão para ondas hidromagnéticas são determinadas na presença da viscosidade expansional. Posteriormente, é proposto um modelo para calcular a viscosidade expansional em termos de quantidades físicas relacionadas às ondas magnetoacústicas. Os resultados mostram o comportamento da viscosidade expansional como função do número de onda para diferentes intensidades e orientações magnéticas, mostrando como a taxa de dissipação de energia associada com a viscosidade expansional pode ser controlada por um campo magnético externo. Na segunda parte deste trabalho, o fenômeno de dispersão induzida por cisalhamento é examinado em um escoamento de uma suspensão incompressível eletricamente condutora. O mecanismo por trás da dispersão hidrodinâmica envolve quebra de simetria das trajetórias das partículas após colisões. Uma equação de difusão suplementar baseada no fluxo hidrodinâmico de partículas, associado com os gradientes de concentração de partículas e de taxa de cisalhamento, é proposta e discutida. O conjunto de equações resultantes é resolvida analiticamente através de uma análise de perturbação regular, já que o parâmetro PeK_c, em que Pe é o número de Peclet e K_c é a difusividade adimensional associada com a difusão induzida por cisalhamento, é considerado um parâmetro pequeno no escoamento acoplado em canal. Os resultados mostram claramente variações substanciais do perfil de velocidade e da viscosidade efetiva com a difusividade de partículas em um escoamento movido por pressão em canal na presença de um campo magnético transversal uniforme.

Palavras-chaves: Escoamentos magnetohidrodinâmicos, gradiente de pressão, campo magnético, segundo coeficiente de viscosidade, fluido condutor, dispersão hidrodinâmica

List of Figures

List of Tables

List of symbols

MHD	Magnetohydrodynamics
$\boldsymbol{f}_L$	Lorentz force per unit volume vector field
ρ_e	Electrical charge density scalar field
$\boldsymbol{u}$	Velocity vector field
$\boldsymbol{J}$	Electrical current density vector field
$\boldsymbol{B}$	Magnetic flux density vector field
ρ	Mass density scalar field
$\boldsymbol{x}$	Spacial or Eulerian coordinate
$\boldsymbol{X}$	Material or Lagrangian coordinate
t	Time parametrization variable
δV	Volume of a material element
λ	Molecular length scale
$\delta(\boldsymbol{y})$	Dirac's delta distribution centered on $\boldsymbol{y}$
$d\boldsymbol{S}$	Surface element
$d\boldsymbol{x}$	Line element
$\boldsymbol{F}$	Deformation gradient tensor
J	Jacobian determinant of the transformation $\boldsymbol{x} \rightarrow \boldsymbol{X}$
ε^{ijk}	Levi-Civita permutation symbol
$\mathcal{V}$	Vector space

$\frac{D}{Dt}$	Material or Lagrangian derivative operator
$\boldsymbol{\nabla}$	Nabla differential operator
M	Mass of a subset of the continuum
$\boldsymbol{P}$	Linear momentum of a subset of the continuum
$\boldsymbol{F}$	Total force
$\boldsymbol{F}_B$	Body force
$\boldsymbol{F}_S$	Contact force
$\hat{\boldsymbol{n}}$	Exterior normal vector
$\boldsymbol{b}$	Body force per unit volume
$\boldsymbol{t}$	Traction vector
$\boldsymbol{\sigma}$	Cauchy's stress tensor
$\boldsymbol{L}$	Total angular moment
$\boldsymbol{T}$	Total torque
$\boldsymbol{T}_B$	Torque generated by body forces
$\boldsymbol{T}_S$	Torque generated by surface forces
$\boldsymbol{T}_M$	Magnetic torque
$\boldsymbol{t}_M$	Magnetic torque per unit volume
$\boldsymbol{\epsilon}$	Levi-Civita's third order permutation tensor
$\boldsymbol{Q}$	Orthogonal tensor
p_0	Thermodynamic pressure
$\boldsymbol{I}$	Second order identity tensor
$\boldsymbol{\tau}$	Shear stress tensor
$\boldsymbol{D}$	Symmetric part of the velocity gradient tensor
$\boldsymbol{\eta}$	Fourth order viscosity tensor

p	Mechanical pressure
η_2	Bulk viscosity
η	Dynamic viscosity
x, y, z	Cartesian coordinates
Re	Reynolds number
h	Half of the height of a channel
Q	Flow rate
a	Radius of a tube
c	Speed of light
v	Relative velocity between two frames of reference
$\boldsymbol{\beta}$	Velocity v non-dimensionalized by the speed of light c
$\boldsymbol{\chi}$	4-position vector
$\hat{\boldsymbol{e}}_i$	i-th basis vector
$g_{\mu\nu}$	Components of the 4-dimensional metric tensor
$\Lambda^{\mu}{}_{\nu}$	Components of Lorentz transformation
$\boldsymbol{E}$	Electric field
ϕ_e	Electromagnetic scalar potential
$\boldsymbol{A}$	Electromagnetic vector potential
$\boldsymbol{\mathcal{A}}$	Electromagnetic 4-potential
$\boldsymbol{J}$	Electric current density
$\boldsymbol{\mathcal{J}}$	Electric 4-current
Q_e	Electric charge in a subset of the continuum
ρ_e	Electric charge density
μ_0	Magnetic permeability of the vacuum

$\boldsymbol{F}_L$	Lorentz force
$\boldsymbol{\sigma_e}$	Electrical conductivity tensor
σ_e	Electrical conductivity
ε_0	Electrical permisivity of the vacuum
ν_m	Magnetic diffusivity
Ha	Hartmann number
Re_m	Magnetic Reynolds number
E_m	Euler magnetic number
τ	Relaxation time
ω	Angular frequency
Re_k	Expansional Reynolds number
k	Wavenumber
ξ	Amplification factor
G	Negative of the pressure gradient in flow direction
η_{eff}	Effective viscosity
ϕ	Volume fraction of particles
$\boldsymbol{N}$	Local flux vector field
$\boldsymbol{N}_c$	Down-gradient flux
$\boldsymbol{\mathcal{D}}_c$	Down-gradient diffusivity tensor
$\boldsymbol{\mathcal{D}}_s$	Self-diffusivity tensor
$\boldsymbol{\mathcal{D}}_f$	Flux contribution to the diffusivity tensor
$\dot{\gamma}$	Shear rate
a_p	Radius of a particle
K_c	Diffusivity coefficient of the gradient of volume fraction

K_η	Diffusivity coefficient of the gradient of viscosity
D_t	Translational Brownian diffusivity
$\boldsymbol{N}_b$	Flux due to Brownian motion
k	Boltzmann constant
η_0	Viscosity of the carrier fluid
T	Temperature
A	Transversal area
Pe	Peclet number
η_e	Einstein viscosity for the homogeneous suspension
ϕ_m	Maximum packing volume fraction
$\{\hat{\boldsymbol{e}}_i\}$	Basis vectors
$\{\hat{\boldsymbol{e}}^i\}$	Dual basis vectors
$\delta^i{}_j$	Kronecker delta
$\boldsymbol{g}$	Metric tensor or inner product
$\mathcal{V}^*$	Dual vector space

List of Contents

1 INTRODUCTION

1.1 Overview on Magnetohydrodynamics

Magnetohydrodynamics (MHD) is the study of the interaction between magnetic fields and moving, electrically conducting fluids. Several general applications of magnetohydrodynamics can be cited, like the flow of plasma in astrophysics, MHD turbulence, plasma containment in fusion reactors, materials processing, MHD pumping, magnetohydrodynamics of biological systems and many other well known applications. For these, some good review studies are available in current literature, like the work of Davidson (1999), Knaepen and Moreau (2008), Morley et al. (2000), Rashidi, Esfahani and Maskaniyan (2017), Yiwen et al. (2017) and Gregory et al. (2016). Some specific applications are justified in more details below:

- Plasma flows in astrophysics: Astrophysical phenomena of large scale are full of plasma, the way that some of these can be well described by magnetohydrodynamics. In particular, we cite solar wind, which are currents of charged particles realeased from the solar corona;

- Geodynamo: In a general manner, there is an agreement that the earth's magnetic field is generated by the flow of iron in its core. The mechanical energy is converted in magnetic energy through stretching and twisting of the magnetic field lines (DAVIDSON, 2017).

- Conducting fluids in metallurgical industry: Several metallurgical process, including open problems, can be described by the magnetohydrodynamic theory. In particular, magnetic fields can be used to heat, pump, stir and levitate liquid metals (DAVIDSON, 2017). One problem of industrial nature is the magnetohydrodynamic instabilities arising in aluminum reduction cells. When producing aluminum by electrolysis (most of today's aluminum is produced by this method), interfacial gravity waves are generated. Depending on the configuration of the reduction cell, these tends to grow, limiting the use of more energy-efficient configurations. A solution to control these instabilities, enabling more energy-efficient configurations, would result in significant energy savings in aluminum production, leading to substantial cost reduction (URATA, 1994). Other application of much interest of magnetohydrodynamics is the stirring of liquid metal through application of rotating magnetic fields. One can use such fields, homogenizing the solidification and, as a consequence, the microstructure of the final piece. It is also important to note that a magnetic field can also be used to damp convective currents in such solidification processes. The principal metallurgical applications of MHD are discussed in more depth in the review paper by Davidson (1999).

MHD models the flows of electrically conducting fluids coupling Maxwell's equations with hydrodynamics equations (KNAEPEN; MOREAU, 2008). In this context, the density of free charges is invariably very small, given that if the flow velocity is considerably smaller than the velocity of electrons in the conductor fluid and the fluid is a good conductor, any unbalance between the electrons charges and the positive charges will be removed almost instantaneously by the electric field created by this unbalance (CUNHA, 2012). In this context of very small density of free charges, significantly simplifications can be made in the governing equations, which are usually called MHD simplification. The direct coupling is done introducing the Lorentz force per unit volume, given by

$$\boldsymbol{f_L} = \rho_e \boldsymbol{u} \times \boldsymbol{B} = \boldsymbol{J} \times \boldsymbol{B}, \tag{1.1}$$

as a body force in the dynamic equation for a continuum, i.e. it enters the equation together with gravity as a force per unit volume in the form

$$\boldsymbol{b} = \rho \boldsymbol{g} + \boldsymbol{J} \times \boldsymbol{B}. \tag{1.2}$$

Here, ρ_e is the electric charge density, $\boldsymbol{u}$ is the velocity vector field, $\boldsymbol{J}$ is the electric current density vector field, $\boldsymbol{B}$ is the magnetic vector field, ρ is the mass density scalar field and $\boldsymbol{g}$ is the gravitational vector field. It is important to note that the microstructure of the fluid and its constitutive equation (for the stress tensor) remains unchanged. This justifies the fact that the magnetic effect enters the dynamic equations for the fluid as a body force.

1.2 Magnetohydrodynamic Waves

An important consequence of the coupling between hydrodynamics and eletromagnetic theory is the so called magnetohydrodynamic waves, which was first suggested to exist by ALFVÉN (1942). These are hydromagnetic waves that travel in the conducting fluid. The discovery of magnetohydrodynamic waves was a major breakthrough in plasma physics and its applications to space physics and fusion research (FÄLTHAMMAR, 2007), as it explains several physical phenomena involved. Posteriorly, several studies demonstrated and investigated these waves experimentally (LUNDQUIST, 1949a; LUNDQUIST, 1949b; LEHNERT, 1954; JEPHCOTT, 1959; ALLEN et al., 1959; NAGAO; SATO, 1960; WILCOX; BOLEY; SILVA, 1960). More recently, the majority of the papers published on magnetohydrodynamic waves concerns space physics, more specifically the study of these waves and their effects in solar corona. Several recent good work involving this field can be cited, as an overview of these, we refer to the studies of Moortel and Nakariakov (2012), Sokolov et al. (2013), Okamoto et al. (2007), Ptuskin et al. (2006), Goossens et al. (2009), Goossens, Erdélyi and Ruderman (2011), Vigeesh et al. (2012), Banerjee et al. (2021) and, as a good review paper, Nakariakov and Kolotkov (2020). Although magnetohydrodynamic waves are a well explored topic, only a very limited number of studies approach the bulk viscosity on these. Only Ibánez (2007) have approached topics in this context.

1.3 MHD Internal Flows

Some of the cited applications can take place in MHD internal flows, in special the MHD pumping, heating and damping applications. The field of MHD internal flows has been vastly explored, both in theoretical and experimental manner. Theoretically, this study started with Hartmann (1937), which described entirely the MHD flow between parallel plates with an external field normal to the plates. After him, Shercliff (1952) solved the more general MHD flow in a rectangular duct. Concerning analytical solutions for MHD flows in circular tubes, several papers explore different configurations of electrical conductivity and wall thickness for different limits of the Hartmann number (main nondimensional physical parameter in MHD internal flows, which measure the ratio between Lorentz and viscous forces). The principal studies in this topic are those written by Shercliff (1956), Chang and Lundgren (1961), Uhlenbusch and Fischer (1961), Tanazawa (1962), Gold (1962), Ihara, Matsushima and Tajima (1967) and Samad (1981). This work, together, completely describe the MHD flow in circular tubes with a vertical external magnetic field. Experimentally, the study of internal magnetohydrodynamic flow of liquid is vastly explored, these being initiated with the work of Hartmann and Lazarus (1937). After these authors, internal MHD flows have been vastly explored experimentally in many different situations, like the work by Fraim and Heiser (1968) and Murgatroyd (1953) that explored things like transition to turbulence and by Hunt and Malcolm (1968) that explored electrically driven flows. More recently, experiments with internal MHD flow are done involving different applications and contexts. The internal MHD flows are important to this work because shear induced dispersion will be analyzed in this context.

1.4 Shear-Induced Dispersion

The so-called shear induced dispersion or hydrodynamic dispersion is a dispersion of the particles in a suspension caused by the break of symmetry of particle's trajectory in collisions. This break of symmetry can be caused by several reasons, like the surface roughness of the particles (CUNHA; HINCH, 1996), the shape of the particles (HUDSON, 2003), magnetic interactions (ROURE; CUNHA, 2018), interactions between three particles (WANG; MAURI; ACRIVOS, 1998) and many others.

The studies on this effect of dispersion caused by shear starts with Karnis, Goldsmith and Mason (1966) and Eckstein, Bailey and Shapiro (1977). After the initial studies, many papers explored experimentally and theoretically details of this physical effect on much different physical configuration (LEIGHTON; ACRIVOS, 1987b; LEIGHTON; ACRIVOS, 1987a; SCHAFLINGER; ACRIVOS; ZHANG, 1990; NIR; ACRIVOS, 1990; ACRIVOS et al., 1992; ACRIVOS; MAURI; FAN, 1993; KAPOOR; ACRIVOS, 1995; ZARRAGA; LEIGHTON DAVID T., 2002). These studies have employed scaling arguments to analyze the dispersing effect and have conducted experimental measurements, revealing the consequences of this dispersion induced by shear. Also, they show side effects generate by this dispersion. Cunha and Hinch (1996) develop a model to the self-diffusivity and down-gradient diffusivities in suspensions composed by rough spheres. This model is extended to the study of suspension with magnetic interactions by Roure and Cunha

(2018). As the hydrodynamic dispersion plays a fundamental role on suspension mechanics, constitutive models to treat it in a continuum approach is needed. The first models were proposed by Leighton and Acrivos (1987b) and Phillips et al. (1992). These are based in experimental data and scale analysis of the problem. The model by Phillips et al. (1992) was also modified for more complex cases, like bidisperse suspensions (KRISHNAN; BEIMFOHR; LEIGHTON, 1996) and for curvature-induced migration (KIM; LEE; KIM, 2008). Although the hydrodynamic dispersion has been studied in several different physical configurations, like with magnetic fluids (ROURE; CUNHA, 2018; SINZATO; CUNHA, 2020; SINZATO; CUNHA, 2021; CUNHA; SINZATO; PEREIRA, 2022), as far as we know, it was not explored yet in a electrically conducting suspension in the context of magnetohydrodynamics.

1.5 Objectives

Based on the discussed throughout this section, this work has objectives in two different studies. The first is the study of the effects of a bulk viscosity on magnetohydrodynamic waves and the second is the study of an incompressible electrically conducting suspension of rigid monodisperse spheres in the presence of shear induced dispersion. The specific objectives are listed below:

1. Construct the set of governing equations for the flow of a barotropic gas in the presence of a bulk viscosity and make this set of governing equations non-dimensional, finding the relevant non-dimensional physical parameters that rules the problem;
2. Linearize the set of governing equations for the flow of an barotropic gas using small perturbation around an equilibrium value of the physical quantities;
3. Find the dispersion relations for magnetohydrodynamic waves in the presence of a bulk viscosity;
4. Analyze the effects of the bulk viscosity in the propagation of Alfvén's wave and magnetoacosutic waves with an already existing model for the bulk viscosity, the Landau model (MANDELSHTAM; LEONTOVICH, 1937; LANDAU; LIFSHITZ, 1987);

5. Propose a model to calculate the bulk viscosity coefficient using laboratory experiments with magnetoacoustic waves;

6. Discuss the fluxes for the hydrodynamic dispersion and construct a mathematical model in an unidirectional flow based in a already existing constitutive model;

7. Couple a diffusion equation for these fluxes with the magnetohydrodynamics equations and make all set of governing equations non-dimensional;

8. Solve the set of non-dimensional differential equations for the flow of an electrically conducting dilute monidisperse suspension of rigid spheres in a channel using a regular perturbation analysis;

9. Analyze the results, searching for the effects of the shear induced dispersion on the flow and the effects of an external magnetic field in the flow, in special the effects of this field on the dispersion of particles.

1.6 Organization of the Work

This dissertation is organized in 5 chapters, which are described below:

- Chapter 2 (Theoretical Fundamentals): A construction of the theoretical fundamentals needed thoughout the work, including fluid dynamics, electrodynamics and magnetohydrodynamics fundamentals;

- Chapter 3 (Bulk Viscosity on Magnetohydrodynamic Waves): The full construction of the model to study the effects of a bulk viscosity in MHD waves and the results are presented in this section. Also, in this chapter we work on the objectives 1-5;

- Chapter 4 (Shear Induced Dispersion on MHD Flows): In this chapter we construct the full model to analyze the shear induced dispersion in a channel MHD flow and present the solutions to the model constructed. Also, in this chapter we work on the objectives 6-9;

- Chapter 5 (Conclusion): Finally, this chapter summarize the results obtained throughout the work. Also, in this chapter we discuss possibilities for future work.

As two separate topics are treated in this work, the sequence of reading is not necessarily the exact order of the chapters. Figure 1 shows a organization scheme of the work. In this, the possible sequences of reading are shown.

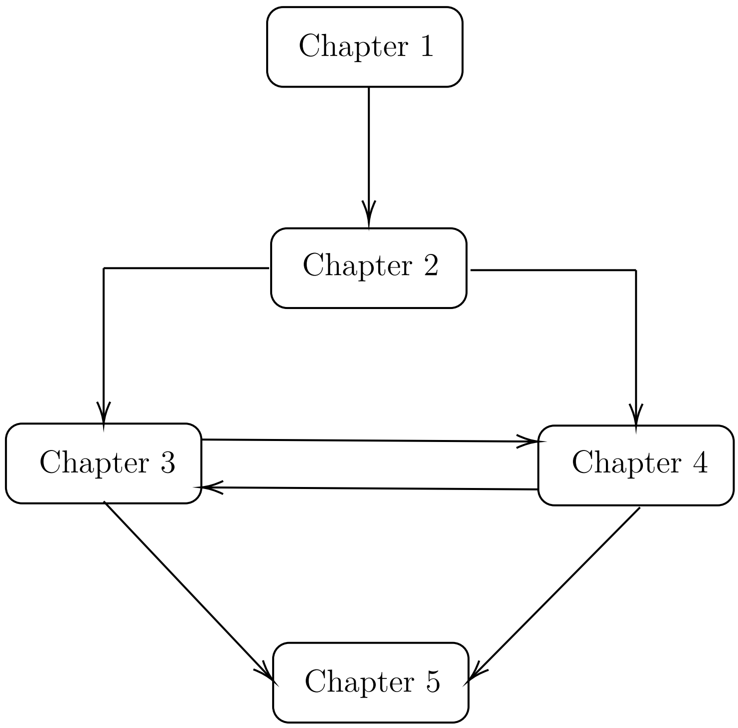

Figure 1 – Organization scheme of the work.

2 THEORETICAL FUNDAMENTALS

2.1 Fluid Dynamics

In this section, we construct the tools of continuum mechanics and, in specific, fluid dynamics, as it is one of the pillars of the work done in this dissertation and will be extensively used.

2.1.1 Continuum Hypothesis

The continuum hypothesis states the possibility of describing physical quantities of a continuous medium as a continuous function of the space point $\boldsymbol{x}$ and of the instant of time t. A property of the continuum, $G(\boldsymbol{x}, t)$, is defined as the volumetric average of a microscopic property in the volume δV contained in the neighborhood of $\boldsymbol{x}$, such that, in the case of mass density,

$$\rho(\boldsymbol{x}, t) = \lim_{\delta V' \to \delta V} \frac{1}{\delta V'} \int_{\delta V'} \sum_{k} m_{(k)} \delta(\boldsymbol{y} - \boldsymbol{x_k}) d\boldsymbol{y}, \tag{2.1}$$

where $m_{(k)}$ is the mass of the k-th molecule in δV, $\boldsymbol{x}_k$ represents the position of the k-th molecule and $\boldsymbol{y}$ is the position vector that reaches each point of δV in the neighborhood of $\boldsymbol{x}$. For this hypothesis be valid mathematically and physically, δV must be big enough to contain a large number of molecules, such that the volumetric average of the properties are well-defined and converges. Also, this volume must be small enough to be considered a point in comparison with the global scale of the continuum, the way the properties are continuous function of $\boldsymbol{x}$, that represents this volume δV. This way, if λ represents a molecular length scale and L a global length scale of the continuum, then δV must satisfy

$$\lambda^3 \ll \delta V \ll L^3. \tag{2.2}$$

The scale in which the continuum hypothesis is valid is called continuum scale and the material portion contained in δV is called a material particle or material element.

2.1.2 Localization Theorem

The localization theorem states that, $f(\boldsymbol{x}, t)$ being a continuous function in the region V, a subset of the three-dimensional Euclidean space $\mathbb{E}^3$, and Ω being an arbitrary volume such that $\Omega \subseteq V$, then, if

$$\int_\Omega f(\boldsymbol{x}, t) dV = 0 \quad \forall\, \Omega \subseteq V, \tag{2.3}$$

we have that

$$f(\boldsymbol{x}, t) = 0 \quad \forall\, \boldsymbol{x} \in \mathcal{V}. \tag{2.4}$$

This theorem can be proved noting that if $f(\boldsymbol{y}, t) \neq 0$ for any $\boldsymbol{y} \in V$, V could not be arbitrary, given that in the region $\Delta \boldsymbol{y} \subset V$ that describes the neighborhood of $\boldsymbol{y}$ the integral would have a non-zero value, characterizing a contradiction. It is important to note that this theorem is a direct consequence of the continuity of f.

2.1.3 Time Evolution of Material Surfaces

Let $d\boldsymbol{S} = dS\boldsymbol{n}$ be a material element of area (contained in the continuum) in a generic time t and $d\boldsymbol{S}_0 = dS_0\boldsymbol{N}$ be the same material element of area in a reference fixed instant of time t_0. Here, $\boldsymbol{n}$ and $\boldsymbol{N}$ are the respective exterior normal vectors. Hence,

$$d\boldsymbol{S} = d\boldsymbol{x}_1 \times d\boldsymbol{x}_2, \tag{2.5}$$

$$d\boldsymbol{S}_0 = d\boldsymbol{X}_1 \times d\boldsymbol{X}_2, \tag{2.6}$$

where $d\boldsymbol{x}_1$ and $d\boldsymbol{x}_2$ are the infinitesimal material lines that generate the material surface and $d\boldsymbol{X}_1$ and $d\boldsymbol{X}_2$ its form in the reference instant of time. Then, using the map $\boldsymbol{\Phi}$ defined by $\boldsymbol{x} = \boldsymbol{\Phi}(\boldsymbol{X}, t)$[1], we have that

$$d\boldsymbol{S} = \left(\frac{\partial \boldsymbol{x}_1}{\partial \boldsymbol{X}_1} \cdot d\boldsymbol{X}_1\right) \times \left(\frac{\partial \boldsymbol{x}_2}{\partial \boldsymbol{X}_2} \cdot d\boldsymbol{X}_2\right), \tag{2.7}$$

[1] Also known as the trajectory of the particle identified by $\boldsymbol{X}$.

where $(\partial \boldsymbol{x}/\partial \boldsymbol{X})_{ij} = \partial x_i/\partial X_j$. But, as $d\boldsymbol{x}_1$ and $d\boldsymbol{x}_2$ are material lines that generate the same material area,

$$\frac{\partial \boldsymbol{x}_1}{\partial \boldsymbol{X}_1} = \frac{\partial \boldsymbol{x}_2}{\partial \boldsymbol{X}_2} = \boldsymbol{F}, \tag{2.8}$$

where $\boldsymbol{F}$ is known as the deformation gradient and $d\boldsymbol{x} = \boldsymbol{F} \cdot d\boldsymbol{X}$. This way, Equation (2.7) can be rewritten as

$$d\boldsymbol{S} = (\boldsymbol{F} \cdot d\boldsymbol{X}_1) \times (\boldsymbol{F} \cdot d\boldsymbol{X}_2)\,. \tag{2.9}$$

On the other hand, the cofactor of the tensor $\boldsymbol{F}$, $\boldsymbol{F}^*$, is also a second order tensor defined by

$$(\boldsymbol{F} \cdot d\boldsymbol{X}_1) \times (\boldsymbol{F} \cdot d\boldsymbol{X}_2) = \boldsymbol{F}^* \cdot (d\boldsymbol{X}_1 \times d\boldsymbol{X}_2)\,. \tag{2.10}$$

Thus (CHANDRASEKHARAIAH; DEBNATH, 1994)

$$\boldsymbol{F}^* = J(\boldsymbol{F}^T)^{-1} = J\boldsymbol{F}^{-T}, \tag{2.11}$$

where J is the Jacobian determinant of the transformation given by the map $\boldsymbol{\Phi}$, i.e.[2]

$$J = \frac{1}{6}\epsilon^{ijk}\epsilon^{lmn}F_{il}F_{jm}F_{kn} = \det \boldsymbol{F}, \tag{2.12}$$

with ϵ^{ijk} being the Levi-Civita permutation symbol. It is important to note that in this work we will use index notation for general systems, including non-orthogonal ones. The introductory mathematical construction to it can be found on section A.1 of the Appendix. Also, in Equation (2.12) Einstein's summation convention[3] has been used and will be used throughout this work, when not it will be explicitly noted. Finally, using Equations (2.9), (2.10) and (2.11),

$$d\boldsymbol{S} = dS_0\boldsymbol{F}^* \cdot \boldsymbol{N} = JdS_0\boldsymbol{F}^{-T} \cdot \boldsymbol{N}, \tag{2.13}$$

which relates the material surface in an arbitrary time with the same material surface in a reference state.

2.1.4 Time Evolution of Material Volumes

Let $d\boldsymbol{x}_1$, $d\boldsymbol{x}_2$ and $d\boldsymbol{x}_3$ be the infinitesimal material lines that generates the volume element dV, such that

$$dV = |d\boldsymbol{x}_1 \cdot d\boldsymbol{x}_2 \times d\boldsymbol{x}_3|\,, \tag{2.14}$$

[2] Latin indexes like i and j can assume the values 1, 2 or 3.
[3] This convention states that every repeated index implies summation on this index.

and $d\boldsymbol{X}_1$, $d\boldsymbol{X}_2$ and $d\boldsymbol{X}_3$ be the reference configuration of these material lines, generating the volume in the reference configuration, dV_0. Then we have

$$\begin{aligned} dV &= |(\boldsymbol{F}\cdot d\boldsymbol{x}_1)\cdot(\boldsymbol{F}\cdot d\boldsymbol{x}_2)\times(\boldsymbol{F}\cdot d\boldsymbol{x}_3)| \\ &= |\det\boldsymbol{F}|\,|d\boldsymbol{X}_1\cdot d\boldsymbol{X}_2\times d\boldsymbol{X}_3| \\ &= JdV_0. \end{aligned} \tag{2.15}$$

The relation given by Equation (2.15) for the material volume is known as the Euler's first relation.

2.1.5 Material Derivative of the Jacobian Determinant

Let $\boldsymbol{S}$ be a second order tensor and $\psi(\boldsymbol{S})$ a functional on second order tensor space $\mathcal{V}\otimes\mathcal{V}$, such that $\psi:\mathcal{V}\otimes\mathcal{V}\to\mathbb{R}$, defined by $\psi(\boldsymbol{S})=\det\boldsymbol{S}$. Here $\mathcal{V}$ represents the three-dimensional inner product space on the continuum and $\mathbb{R}$ the field of real numbers. Then,

$$\frac{D}{Dt}\psi(\boldsymbol{S})=\frac{\partial\psi}{\partial S_{ij}}\frac{DS_{ij}}{Dt}. \tag{2.16}$$

Here $D/Dt=(\partial/\partial t)_{\boldsymbol{X}}=\partial/\partial t+\boldsymbol{u}\cdot\boldsymbol{\nabla}$ represents the Lagrangian or material derivative, which indicates the variation of the properties viewed by the material elements. Performing the derivative $\partial\psi/\partial S_{ij}$, we obtain that $\partial\psi/\partial S_{ij}=S^*_{ij}$ (LIU, 2002). Thus, for the specific case of the deformation gradient tensor, manipulating algebraically,

$$\frac{D}{Dt}\psi(\boldsymbol{F})=(\det\boldsymbol{F})\,\mathrm{tr}\left(\frac{D\boldsymbol{F}}{Dt}\cdot\boldsymbol{F}^{-1}\right), \tag{2.17}$$

where tr() is the trace operator. Finally, substituting Equation (A.15),

$$\frac{DJ}{Dt}=J\boldsymbol{\nabla}\cdot\boldsymbol{u}. \tag{2.18}$$

The expression given by Equation (2.18) is known as Euler's second relation.

2.1.6 Reynolds Transport Theorem

Let $G(\boldsymbol{x},t)$ be a smooth arbitrary tensorial field, $\Omega(t)$ an arbitrary material region on the continuum and Ω_0 this region in a reference time. Then, using Euler's first relation, Equation (2.15),

$$\frac{d}{dt}\int_\Omega GdV=\int_{\Omega_0}\frac{D}{Dt}(GJ)\,dV_0. \tag{2.19}$$

Using Euler's second relation, Equation (2.18),

$$\frac{d}{dt}\int_{\Omega} G dV = \int_{\Omega}\left(\frac{DG}{Dt} + G\boldsymbol{\nabla}\cdot\boldsymbol{u}\right) dV, \tag{2.20}$$

or

$$\frac{d}{dt}\int_{\Omega} G dV = \int_{\Omega}\left[\frac{\partial G}{\partial t} + \boldsymbol{\nabla}\cdot(\boldsymbol{u}G)\right] dV. \tag{2.21}$$

The result presented by Equation (2.21) is known as the Reynolds transport theorem.

2.1.7 Transport Theorem for a Flux Integral

Let $\boldsymbol{P}(\boldsymbol{x},t)$ be a smooth vector field and $\partial\Omega(t)$ an arbitrary material surface of the continuum. Then, using Equation (2.13), the time derivative of the flux integral of $\boldsymbol{P}$ through $\partial\Omega(t)$ can be calculated as

$$\frac{d}{dt}\int_{\partial\Omega}\boldsymbol{P}\cdot\boldsymbol{n}dS = \int_{\partial\Omega_0}\frac{D}{Dt}\left(\boldsymbol{P}\cdot J\boldsymbol{F}^{-T}\right)\cdot\boldsymbol{N}dS_0. \tag{2.22}$$

Using Euler's second relation, Equation (2.18), and the relation deduced in the Appendix A.2, Equation (A.17), we obtain that

$$\frac{d}{dt}\int_{\partial\Omega}\boldsymbol{P}\cdot\boldsymbol{n}dS = \int_{\partial\Omega_0}\left[\frac{D\boldsymbol{P}}{Dt} + \boldsymbol{P}\left(\boldsymbol{\nabla}\cdot\boldsymbol{u}\right) - \boldsymbol{P}\cdot\boldsymbol{\nabla}\boldsymbol{u}\right]\cdot J\boldsymbol{F}^{-T}\cdot\boldsymbol{N}dS_0. \tag{2.23}$$

Therefore, using Equation (2.13) again,

$$\frac{d}{dt}\int_{\partial\Omega}\boldsymbol{P}\cdot\boldsymbol{n}dS = \int_{\partial\Omega}\left[\frac{D\boldsymbol{P}}{Dt} + \boldsymbol{P}\left(\boldsymbol{\nabla}\cdot\boldsymbol{u}\right) - \boldsymbol{P}\cdot\boldsymbol{\nabla}\boldsymbol{u}\right]\cdot\boldsymbol{n}dS, \tag{2.24}$$

or[4]

$$\frac{d}{dt}\int_{\partial\Omega}\boldsymbol{P}\cdot\boldsymbol{n}dS = \int_{\partial\Omega}\left[\frac{\partial\boldsymbol{P}}{\partial t} - \boldsymbol{\nabla}\times\left(\boldsymbol{u}\times\boldsymbol{P}\right) + \boldsymbol{u}\left(\boldsymbol{\nabla}\cdot\boldsymbol{P}\right)\right]\cdot\boldsymbol{n}dS. \tag{2.25}$$

In a physical context, Equation (2.25) represents a purely kinematic relation. In fact, Wald (2022) deduces it from a purely kinematic analysis, considering $\partial\Omega(t)$ in different times infinitesimally close.

2.1.8 Mass Balance Equation

In continuum mechanics, at a reference time the material in the neighborhood of each point of the continuum is defined as a material element. Each material element is labeled with its position $\boldsymbol{X}$ at the reference time and stays the same element throughout

[4] Using the identity given by $\boldsymbol{\nabla}\times(\boldsymbol{u}\times\boldsymbol{P}) = \boldsymbol{u}\left(\boldsymbol{\nabla}\cdot\boldsymbol{P}\right) - \boldsymbol{P}\left(\boldsymbol{\nabla}\cdot\boldsymbol{u}\right) + \left(\boldsymbol{P}\cdot\boldsymbol{\nabla}\right)\boldsymbol{u} - \left(\boldsymbol{u}\cdot\boldsymbol{\nabla}\right)\boldsymbol{P}$.

the time evolution, the way the mass of each material element is conserved. Therefore, if M is the mass of an arbitrary material volume $\Omega(t)$ that is defined by the same particles at every instant of time, we have that

$$\frac{dM}{dt} = \frac{d}{dt}\int_{\Omega} \rho dV = 0, \tag{2.26}$$

where ρ is a positive integrable function $\rho : \mathcal{V} \times \mathbb{R}^+ \to \mathbb{R}^+$ known as the mass density. Using Reynolds transport theorem, given by Equation (2.21),

$$\int_{\Omega} \left[\frac{\partial \rho}{\partial t} + \boldsymbol{\nabla} \cdot (\boldsymbol{u}\rho) \right] dV = 0. \tag{2.27}$$

Finally, by the localization theorem, we obtain that

$$\frac{\partial \rho}{\partial t} + \boldsymbol{\nabla} \cdot (\rho \boldsymbol{u}) = 0. \tag{2.28}$$

Equation (2.28) states the conservation of the mass and is known as the mass continuity equation.

In the special case of incompressible fluids, the mass density is conserved by each material element. Thus, Equation (2.28) reduces to

$$\boldsymbol{\nabla} \cdot \boldsymbol{u} = 0. \tag{2.29}$$

2.1.9 Linear Momentum Balance Equation

Newton's laws of dynamics states that exists a frame of reference, called inertial frame, in which the time variation of the linear momentum of some mass equals the resultant force acting on this mass. Now, consider an arbitrary material volume $\Omega(t)$ formed by the same particles in any instant of time. The surface of this material volume is $\partial\Omega(t)$ and its total linear momentum is characterized by the vector $\boldsymbol{P}(t)$. Hence, applying Newton's laws of dynamics to this part of the continuum,

$$\frac{d\boldsymbol{P}}{dt} = \frac{d}{dt}\int_{\Omega} \rho \boldsymbol{u} dV = \boldsymbol{F}, \tag{2.30}$$

where $\boldsymbol{F}$ represents the total force acting on Ω.

Continuum mechanics assumes that the total force force acting on some part of the continuum can be divided in two parts, body forces and contact forces. The first results from external forces acting within the whole material volume, like Newton's gravitational force. The second acts on the surface of each material element and is a result of molecular interaction. As molecular interactions decays quickly with the distance, in continuum scales they are seen as forces on the surface of the elements. These two are written for the volume Ω described respectively as

$$\boldsymbol{F}_B = \int_{\Omega} \boldsymbol{b} dV, \tag{2.31}$$

$$\boldsymbol{F}_S = \oint_{\partial\Omega} \boldsymbol{t} dS, \tag{2.32}$$

where $\boldsymbol{b}$ is called the body force density (per unit volume) and $\boldsymbol{t}$ is called the surface traction (per unit surface area). While $\boldsymbol{b}$ is a pure vector field, $\boldsymbol{t}$ is not, as in general it must depend on the surface it is acting on, i.e. $\boldsymbol{t} = \boldsymbol{t}(\hat{\boldsymbol{n}}, \boldsymbol{x}, t)$. Thus, $\boldsymbol{t}$ can not appear in the field equations that describe the dynamic of the continuum. Cauchy was the first to solve this problem writing $\boldsymbol{t} = \boldsymbol{t}(\hat{\boldsymbol{n}}, \boldsymbol{x}, t)$ in terms of the traction acting on surfaces whose exterior normal vectors are constant, in special the canonical basis vectors. Thus, using a material tetrahedron defined by a triangular region that intercept each axis that generates the canonical basis, we obtain that (LIU, 2002)

$$\boldsymbol{t}(\hat{\boldsymbol{n}}, \boldsymbol{x}, t) = \hat{\boldsymbol{n}}(\boldsymbol{x}, t) \cdot \boldsymbol{\sigma}(\boldsymbol{x}, t), \tag{2.33}$$

where $\boldsymbol{\sigma}$, defined by $\boldsymbol{\sigma} = \hat{\boldsymbol{e}}_k \otimes \boldsymbol{t}(\hat{\boldsymbol{e}}_k, \boldsymbol{x}, t)$, is the so-called Cauchy's stress tensor. Here, $\hat{\boldsymbol{e}}_k$ denotes the k-th canonical basis vector. Equation (2.33) is known as Cauchy's theorem.

Therefore, using Equations (2.30), (2.31), (2.32) and (2.33),

$$\frac{d}{dt} \int_{\Omega} \rho \boldsymbol{u} dV = \oint_{\partial\Omega} \boldsymbol{n} \cdot \boldsymbol{\sigma} dS + \int_{\Omega} \boldsymbol{b} dV. \tag{2.34}$$

Applying Reynolds transport theorem, given by Equation (2.21), divergence theorem for second order tensors (ARIS, 1989) and localization theorem, this equation reduces to

$$\rho \frac{D\boldsymbol{u}}{Dt} = \rho \left(\frac{\partial \boldsymbol{u}}{\partial t} + \boldsymbol{u} \cdot \boldsymbol{\nabla} \boldsymbol{u} \right) = \boldsymbol{\nabla} \cdot \boldsymbol{\sigma} + \boldsymbol{b}. \tag{2.35}$$

Equation (2.35) is known as Cauchy's equation and represents the linear momentum balance in a continuum. It is important to note that the use of this equation requires a prescription for the stress tensor, which is given by a constitutive relation. Such constitutive relations are characterized by the materials, solids or fluids.

2.1.10 Angular Momentum Balance

Newton's laws of dynamics states that, in a inertial frame, the time variation of the angular momentum of a mass equals the torque acting on it. Now, consider the same material volume defined in subsection 2.1.9 and define its total angular momentum as $\boldsymbol{L}$. Then, we have

$$\frac{d\boldsymbol{L}}{dt} = \frac{d}{dt}\int_{\Omega} \boldsymbol{x} \times \rho \boldsymbol{u} dV = \boldsymbol{T}, \tag{2.36}$$

where $\boldsymbol{T}$ is the total torque acting on $\Omega(t)$.

The total torque is divided into three parts: the torque generated by the body forces, the torque generated by the contact forces, and an extra torque. The latter is a new addition and is only necessary to account for magnetic torques, as it is well-established that magnetic fields apply torques on particles with magnetic moment. These torques are described respectively by

$$\boldsymbol{T}_B = \int_{\Omega} \boldsymbol{x} \times \boldsymbol{b} dV, \tag{2.37}$$

$$\boldsymbol{T}_S = \oint_{\partial\Omega} \boldsymbol{x} \times (\hat{\boldsymbol{n}} \cdot \boldsymbol{\sigma})\, dS, \tag{2.38}$$

$$\boldsymbol{T}_M = \int_{\Omega} \boldsymbol{t}_M dV, \tag{2.39}$$

where $\boldsymbol{t}_M$ is the magnetic torque density (per unit volume). Therefore, using Equations (2.36), (2.37), (2.38) and (2.39),

$$\frac{d}{dt}\int_{\Omega} \boldsymbol{x} \times \rho \boldsymbol{u} dV = \int_{\Omega} \boldsymbol{x} \times \boldsymbol{b} dV + \oint_{\partial\Omega} \boldsymbol{x} \times (\hat{\boldsymbol{n}} \cdot \boldsymbol{\sigma})\, dS + \int_{\Omega} \boldsymbol{t}_M dV. \tag{2.40}$$

Applying the divergence theorem (ARIS, 1989), Reynolds transport theorem and manipulating the expression algebraically, we obtain that

$$\int_{\Omega} \boldsymbol{x} \times \left(\rho \frac{D\boldsymbol{u}}{Dt} - \boldsymbol{\nabla} \cdot \boldsymbol{\sigma} - \boldsymbol{b}\right) dV - \int_{\Omega} (\boldsymbol{\epsilon} : \boldsymbol{\sigma} + \boldsymbol{t}_M)\, dV = 0, \tag{2.41}$$

where $\boldsymbol{\epsilon}$ is the Levi-Civita's third order permutation tensor. Using Cauchy's Equation (2.35) and applying the localization theorem, Equation (2.41) reduces to

$$\boldsymbol{\epsilon} : \boldsymbol{\sigma} = -\boldsymbol{t}_M, \tag{2.42}$$

which is the angular momentum balance equation.

Extra torques are caused, as far as we know, only in magnetic materials. These are a direct effect of the external magnetic field trying to line up the magnetic moments with the external field direction. An example of such materials is ferrofluids, where this extra magnetic torque is present. In cases such magnetohydrodynamics that the fluid does not have magnetic moment, the angular momentum balance equation is just

$$\boldsymbol{\epsilon} : \boldsymbol{\sigma} = \mathbf{0}, \tag{2.43}$$

which is equivalent to say that the stress tensor is a symmetric tensor, i.e. $\boldsymbol{\sigma} = \boldsymbol{\sigma}^T$. As in our context we work only with pure magnetohydrodynamics, from now on we assume the stress tensor to be symmetric.

2.1.11 Constitutive Formalism

It can be noted that, in general, Cauchy's and continuity equations do not fully describe the dynamics of a continuum material, as an expression for the stress tensor is needed. Indeed, a expression for this tensor must be provided, as it describes the details of the response of the material used to deformations. This way, this constitutive relation for $\boldsymbol{\sigma}$ contains intrinsic characteristics of the material used, being it a solid or a fluid.

A constitutive equation can be built and proposed through theoretical models based on the characteristics of the material. One can built it with physical or empirical arguments. Nonetheless, every constitutive equation must obbey some basic physical principles to be consistent, they are (CUNHA, 2021b):

- Causality principle: establishes that the stress in any instant of time must depend, in general, on the deformation states of the material in previous times t'. Hence, a general constitutive equation must relates the stress state in a time t with events in previous times t';

- Locality principle: establishes that only material neighborhood of $\boldsymbol{x}$ can affect the stress state of the material element $\delta V(\boldsymbol{x})$, given by $\boldsymbol{\sigma}(\boldsymbol{x}, t)$;

- Coordinate system invariance: establishes that the functional that defines the stress state in $\boldsymbol{x}$ at time t must be independent of the coordinate system used to describe it. It is equivalent to say that this functional is invariant to the Galilean group;

- Fading memory principle: establishes that events more time separated from t have less influence on the stress state in t;

- Objectivity principle (principle of material frame indifference): establishes that the functional that defines the stress state must be invariant under a general change of frame of reference. Physically it is equivalent to impose that the material characteristics do not depend on the dynamic state of the frame of reference. Consider the general transformation,

$$\boldsymbol{x}^* = \boldsymbol{c}(t) + \boldsymbol{Q}(t) \cdot (\boldsymbol{x} - \boldsymbol{x_0}) \,, \tag{2.44}$$

$$t^* = t + a, \tag{2.45}$$

for some $a \in \mathbb{R}$, $\boldsymbol{x}_0 \in \mathcal{V}$, $\boldsymbol{c}(t) \in \mathcal{V}$ and $\boldsymbol{Q}(t) \in O(\mathcal{V})$, where $O(\mathcal{V})$ is the orthogonal group on $\mathcal{V}$. This transformation is also known as homogenous transformation of Truesdell and Noll (TRUESDELL, 1977). Hence, if $\mathcal{F}$ is the functional describing the stress tensor, based on this principle (CUNHA, 2021a),

$$\boldsymbol{Q}(t) \cdot \mathcal{F}\left\{\theta, \boldsymbol{k}, \boldsymbol{R}\right\} \cdot \boldsymbol{Q}^T(t) = \mathcal{F}\left\{\theta, \boldsymbol{Q}(t) \cdot \boldsymbol{k}, \boldsymbol{Q}(t) \cdot \boldsymbol{R} \cdot \boldsymbol{Q}^T(t)\right\} = \mathcal{F}\left\{\theta^*, \boldsymbol{k}^*, \boldsymbol{R}^*\right\}. \tag{2.46}$$

where θ, $\boldsymbol{k}$ and $\boldsymbol{R}$ are, respectively, scalar, vector and second-order tensor function dependencies of the functional and θ^*, $\boldsymbol{k}^*$ and $\boldsymbol{R}^*$ represents their transformed versions. We call $\mathcal{F}$ the constitutive function or response function of $\boldsymbol{\sigma}(\boldsymbol{x}, t)$.

Applying the constitutive principles exposed, a general constitutive equation for the stress tensor must have the form given by

$$\boldsymbol{\sigma}(t) = \mathcal{F}\left\{\frac{\partial \boldsymbol{x}}{\partial \boldsymbol{X}}(t')\right\}; \quad -\infty < t' < t, \tag{2.47}$$

where the symbol $-\infty$ was used to represent the time history before t. Furthermore, Equation (2.47) must, under a homogenous Trusdell and Noll's transformation, transform accordingly to

$$\boldsymbol{Q}(t) \cdot \mathcal{F}\left\{\frac{\partial \boldsymbol{x}}{\partial \boldsymbol{X}}(t')\right\} \cdot \boldsymbol{Q}^T(t) = \mathcal{F}\left\{\boldsymbol{Q}(t) \cdot \frac{\partial \boldsymbol{x}}{\partial \boldsymbol{X}}(t') \cdot \boldsymbol{Q}^T(t)\right\}. \tag{2.48}$$

2.1.12 Constitutive Model for a Newtonian Fluid

It is known that a fluid at rest just feels normal stresses. Hence, the stress tensor for a static fluid is given by

$$\boldsymbol{\sigma}_0 = -p_0(\boldsymbol{x})\boldsymbol{I}, \tag{2.49}$$

where the scalar field p_0 representing the norm of the normal stresses is called static or thermodynamic pressure. In general, extra stresses should arise as a result of the movement of the fluid, the way we write a general stress tensor for a moving fluid as

$$\boldsymbol{\sigma} = -p_0\boldsymbol{I} + \boldsymbol{\tau}, \tag{2.50}$$

where $\boldsymbol{\tau}$ is the contribution to the stress tensor caused by the movement of the fluid, also called viscous stresses.

The first model for viscous stresses was proposed by Newton. For a simple experiment consisting of two parallel plates with fluid filling the gap, he proposed that, when one of the plates is moving, the stress on the plate should be proportional to the velocity gradient, with the proportion factor being the viscosity η of the fluid. Fluids that obeys Newton's law of viscosity are called Newtonian fluids. Hence, we intend to use a generalization of Newton's law of viscosity to construct a constitutive model for the viscous stress tensor. To do that, first we must note that the pure velocity gradient $\nabla\boldsymbol{u}$ is not a good candidate to construct a constitutive equation, as it is not frame indifferent (CUNHA, 2021a; LIU, 2002). Thus, we use a combination of it, its symmetric part $\boldsymbol{D} = \left[\boldsymbol{\nabla u} + (\boldsymbol{\nabla u})^T\right]/2$, that can be shown to be frame indifferent, the way that

$$\boldsymbol{\tau} = \boldsymbol{\eta} : \boldsymbol{D}, \tag{2.51}$$

where $\boldsymbol{\eta}$ is a fourth order tensor. Equation (2.51) is the most general way of relating two second order tensors linearly. For the case of isotropic and homogeneous fluids, we impose that $\boldsymbol{\eta}$ must be isotropic[5] and homogeneous. Therefore,

$$\eta'_{ijkl} = \eta_{ijkl} \tag{2.52}$$

and, by a direct consequence of Equation (2.52) (LIU, 2002)[6],

$$\eta_{ijkl} = C_1 g_{ij} g_{kl} + C_2 g_{ik} g_{jl} + C_3 g_{il} g_{kj}, \tag{2.53}$$

where C_1, C_2 e C_3 are material constants, η'_{ijkl} represents the components of $\boldsymbol{\eta}$ is a transformed coordinate system and g_{ij} are the components of the metric tensor. Using Equations (2.53) and (2.51) in Equation (2.50) and renaming the material constants, the

[5] Its components are the same in any coordinate system
[6] Note that in Cartesian coordinate system, $g_{ij} = \delta_{ij}$.

stress tensor can be shown to be (BATCHELOR, 1967; LANDAU; LIFSHITZ, 1987)

$$\boldsymbol{\sigma} = -\left(p_0 - \eta_2 \boldsymbol{\nabla} \cdot \boldsymbol{u}\right) \boldsymbol{I} + 2\eta \left[\boldsymbol{D} - \frac{1}{3}\left(\mathrm{tr}\boldsymbol{D}\right) \boldsymbol{I}\right], \tag{2.54}$$

where η is the dynamic viscosity coefficient and η_2 is the second viscosity coefficient. We note that the second viscosity coefficient, or bulk viscosity, can depend on some properties of the flow, like the frequency of some physical phenomena in this flow, and only have significant effect in high frequency cases, as discussed by Landau and Lifshitz (1987). It also important to define a quantity named the mechanical pressure, given by $p = -\mathrm{tr}(\boldsymbol{\sigma})/3$ and identified as $p = p_0 - \eta_2 \boldsymbol{\nabla} \cdot \boldsymbol{u}$.

The fluid whose stress tensor is described by Equation (2.54) is known as a Newtonian non-Stokesian fluid. When the Stokes hypothesis is valid, i.e. $\eta_2 \approx 0$, the fluid is called a Newtonian Stokesian fluid.

2.1.13 Navier-Stokes Equation

Using the stress tensor for a Newtonian non-Stokesian fluid, Equation (2.54), in Cauchy's Equation (2.35), we obtain that

$$\rho \frac{D\boldsymbol{u}}{Dt} = -\nabla p_0 + \boldsymbol{\nabla}\left(\eta_2 \boldsymbol{\nabla} \cdot \boldsymbol{u}\right) + \eta \nabla^2 \boldsymbol{u} + \frac{1}{3}\eta \boldsymbol{\nabla}\left(\boldsymbol{\nabla} \cdot \boldsymbol{u}\right) + \boldsymbol{b}. \tag{2.55}$$

Equation (2.55) is known as the Navier-Stokes equation, which together with continuity Equation (2.28) describes the dynamics of Newtonian non-Stokesian fluids. In the special case of a incompressible fluid, Navier-Stokes equation reduces to

$$\rho \frac{D\boldsymbol{u}}{Dt} = -\nabla p + \eta \nabla^2 \boldsymbol{u} + \boldsymbol{b}, \tag{2.56}$$

where $p = p_0$.

2.1.13.1 Permanent Incompressible Unidirectional Flows

Consider now an steady[7] incompressible unidirectional flow in the x direction, the way that $\boldsymbol{u} = u\hat{\boldsymbol{e}}_x$. Then, continuity Equation (2.28) states that $\boldsymbol{u} = \boldsymbol{u}(y, z)$ and, by consequence,

$$\boldsymbol{u} \cdot \boldsymbol{\nabla} \boldsymbol{u} = \boldsymbol{0}. \tag{2.57}$$

[7] $\partial/\partial t = 0$ for any continuum's quantity.

This way, Navier-Stokes Equation (2.55) reduces to

$$\boldsymbol{\nabla} p = \eta \boldsymbol{\nabla}^2 \boldsymbol{u} + \boldsymbol{b}. \tag{2.58}$$

It is important to note that Equation (2.57) shows that the unidirectional flow hypothesis is valid only when $|\rho \boldsymbol{u} \cdot \boldsymbol{\nabla} \boldsymbol{u}| \ll \left|\eta \boldsymbol{\nabla}^2 \boldsymbol{u}\right|$, what, in terms of a scale analysis, is equivalent to

$$Re_h \frac{h}{\ell} \ll 1, \tag{2.59}$$

where h is a characteristic length scale in a principal direction of the velocity gradient, ℓ is a length scale in the direction of the flow, $Re_h = \rho u_c h/\eta$ is the Reynolds non-dimensional number based on h and u_c is a characteristic velocity. Equation (2.59) presents the condition for a flow be considered unidirectional.

2.1.13.2 Poiseuille's Flow Between Parallel Plates

Consider the flow of a fluid between plates that are parallel to the xz plane. For a non-conductor Newtonian fluid, using the hypothesis of incompressible and unidirectional flow, the cartesian-component of Navier-Stokes Equation (2.55) in the direction of the flow, x-direction, is given by

$$\frac{d^2 u}{dy^2} = \frac{1}{\eta}\frac{dp}{dx}. \tag{2.60}$$

The other components of the equation just states that $p = p(x)$. If the plates are represented by the planes $y = \pm h$, the no-slip boundary condition states that $u(y = \pm h) = 0$. Thus, a simple double integration of Equation (2.60) and a later use of the no-slip boundary conditions gives that

$$u = -\frac{1}{2\eta}\frac{dp}{dx}\left(h^2 - y^2\right). \tag{2.61}$$

The flow rate per unit length in the z direction is given by

$$\frac{Q}{\ell} = \int_{-h}^{h} u(y)dy, \tag{2.62}$$

such that

$$\frac{Q}{\ell} = -\frac{2}{3\eta}\frac{dp}{dx}h^3. \tag{2.63}$$

Flows like this, pressure driven, are usually named Poiseuille's flows.

2.1.13.3 Poiseuille's Flow in a Circular Pipe

Consider the flow of a fluid in a pipe of center coinciding with the z-axis and radius a. For a non-conductor Newtonian fluid, using the hypothesis of incompressible and unidirectional flow, the polar-component of Navier-Stokes Equation (2.55) in the direction of the flow, z-direction, is given by

$$\frac{d}{dr}\left(r\frac{du}{dr}\right) = \frac{r}{\eta}\frac{dp}{dz}. \tag{2.64}$$

The other components of the equation just states that $p = p(z)$. The no-slip boundary condition applied for this case states that $u(r = a) = 0$. Also, we must impose that the velocity field is finite at the center of the tube to eliminate the singularity generated by integration of Equation (2.64). Therefore,

$$u(r) = -\frac{1}{4\eta}\frac{dp}{dz}\left(a^2 - r^2\right). \tag{2.65}$$

The flow rate is calculated from

$$Q = \int_0^{2\pi}\int_0^a urdrd\theta, \tag{2.66}$$

such that

$$Q = -\frac{1}{8\eta}\frac{dp}{dz}\pi a^4. \tag{2.67}$$

Equation (2.67) is also known as Hagen-Poiseuille's law.

2.2 Electrodynamics

In this section, we construct the basic tools of classical electrodynamics and give a glimpse of special relativity and Lorentz transformation, as all electrodynamic equations are not Galilean invariant, but Lorentz invariant.

2.2.1 Lorentz Transformations and 4-vectors

Great part of classical mechanics occurs in limits where the field equations are simply Galilean invariant[8], the way that quantities change accordingly to a Galilean trans-

[8] Invariant under Galilean transformations.

formation[9],

$$\boldsymbol{x}' = \boldsymbol{x} - \boldsymbol{v}t, \tag{2.68}$$

$$t' = t, \tag{2.69}$$

under change from an inertial frame to another inertial frame, $\mathcal{K} \to \mathcal{K}'$. Here, $\boldsymbol{v}$ is a constant vector that represents the relative velocity of the frames and $\boldsymbol{x}'$ is the position vector $\boldsymbol{x}$ in the new inertial reference frame. This kind of transformation leaves the three-dimensional distance defined by $dx^2 + dy^2 + dz^2$ invariant, i.e.

$$dx^2 + dy^2 + dz^2 = dx'^2 + dy'^2 + dz'^2. \tag{2.70}$$

Nonetheless, electromagnetic theory is incompatible with Galilean transformations, as it involves characteristic velocities comparable with the speed of light. Its field equations are intrinsically Lorentz invariant[10] (EINSTEIN, 1905), the way that quantities change accordingly to a Lorentz transformation,

$$\boldsymbol{x}' = \boldsymbol{x} + (\gamma - 1)\,\frac{\boldsymbol{\beta}\cdot\boldsymbol{x}}{\beta^2}\boldsymbol{\beta} - \gamma c\boldsymbol{\beta}t, \tag{2.71}$$

$$t' = \gamma\left(t - \frac{\boldsymbol{\beta}\cdot\boldsymbol{r}}{c}\right), \tag{2.72}$$

where c is the speed of light, $\gamma = (1 - v^2/c^2)^{-1/2}$ is known as gamma factor, $\boldsymbol{\beta}$ is the non-dimensional velocity defined by $\boldsymbol{\beta} = \boldsymbol{v}/c$ and $\beta = |\boldsymbol{\beta}|$. In contrast to Galilean transformation, Lorentz transformation leaves the four-dimensional distance defined by

$$d\chi^2 = -cdt^2 + dx^2 + dy^2 + dz^2 \tag{2.73}$$

invariant, i.e.

$$-cdt^2 + dx^2 + dy^2 + dz^2 = -cdt'^2 + dx'^2 + dy'^2 + dz'^2. \tag{2.74}$$

The 4-dimensional distance defined by $d\boldsymbol{\chi}$ naturally induces a 4-dimensional space-time with a position four-vector defined by

$$\begin{aligned}\boldsymbol{\chi} &= x^\mu\hat{\boldsymbol{e}}_\mu \\ &= x^0\hat{\boldsymbol{e}}_0 + x^1\hat{\boldsymbol{e}}_1 + x^2\hat{\boldsymbol{e}}_2 + x^3\hat{\boldsymbol{e}}_3 \\ &= ct\hat{\boldsymbol{e}}_0 + x\hat{\boldsymbol{e}}_1 + y\hat{\boldsymbol{e}}_2 + z\hat{\boldsymbol{e}}_3,\end{aligned} \tag{2.75}$$

9 This specific form of the transformation do not includes rotation.
10 Invariant under Lorentz transformations.

where x^μ are called the contravariant components of the 4-position and we are using the general index notation for non-orthogonal basis (see section A.1). It is important to note that, in this work, latin letters indexes varies from 1 to 3 and greek letters indexes varies from 0 to 3[11]. In such formalism, the internal product $d\boldsymbol{\chi} \cdot d\boldsymbol{\chi} = d\chi^2$ is defined by

$$\begin{aligned} d\chi^2 &= \hat{\boldsymbol{e}}_\mu \cdot \hat{\boldsymbol{e}}_\nu d\chi^\mu d\chi^\nu \\ &= g_{\mu\nu} d\chi^\mu d\chi^\nu, \end{aligned} \tag{2.76}$$

where $g_{\mu\nu} = \hat{\boldsymbol{e}}_\mu \cdot \hat{\boldsymbol{e}}_\nu$ is the metric tensor of the metric space. In the case of the space-time defined by Equation (2.73), the metric tensor is identified to be

$$(g_{\mu\nu}) = \begin{pmatrix} -1 & 0 & 0 & 0 \\ 0 & 1 & 0 & 0 \\ 0 & 0 & 1 & 0 \\ 0 & 0 & 0 & 1 \end{pmatrix}, \tag{2.77}$$

where the notation $(g_{\mu\nu})$ is used to represent the matrix representation of the tensor with components $g_{\mu\nu}$. This metric is known as Minkowski metric and is the metric of Einstein's special theory of relativity (EINSTEIN, 1905). We also can define the so-called covariant components of a vector in this space accordingly to

$$\chi_\mu = g_{\mu\nu}\chi^\nu, \tag{2.78}$$

the way that $x^0 = -x_0$ and $x^i = x_i$. In terms of this notation, a general Lorentz transformation can be synthesized by

$$x'^\mu = \Lambda^\mu{}_\nu x^\nu, \tag{2.79}$$

where Λ^μ_ν are the coefficients of the Lorentz transformation general matrix (BARUT, 1980). It is noticeable that the 4-nabla obeys the Lorentz transformations in Minkowski metric, i.e.

$$\frac{\partial}{\partial x'_\mu} = \Lambda^\mu{}_\nu \frac{\partial}{\partial x_\nu}, \tag{2.80}$$

the way that combinations of 4-nabla and 4-tensors generates Lorentz invariant equations.

[11] For example, x^μ can be x^0, x^1, x^2 or x^3, but x^i can be only x^1, x^2 or x^3.

2.2.2 Electromagnetic 4-potential

It is known that electromagnetic theory can be described in terms of the so called electromagnetic potentials (WALD, 2022), defined by

$$\boldsymbol{E} = -\boldsymbol{\nabla}\phi_e - \frac{\partial \boldsymbol{A}}{\partial t}, \tag{2.81}$$

$$\boldsymbol{B} = \boldsymbol{\nabla} \times \boldsymbol{A}, \tag{2.82}$$

where $\boldsymbol{E}$ is the total electric field, ϕ_e is the scalar potential and $\boldsymbol{A}$ is the vector potential.

Furthermore, these potentials are even more fundamental than the electromagnetic field strengths, statement that is discussed in more details by Wald (2022). These potentials drastically simplify the description of electromagnetism, as one can defined a 4-potential by

$$\boldsymbol{\mathcal{A}} = \frac{\phi_e}{c}\hat{\boldsymbol{e}}_0 + A^i\hat{\boldsymbol{e}}_i, \tag{2.83}$$

such that the field equations can be constructed in terms of only one 4-vector, $\boldsymbol{\mathcal{A}}$, as ϕ_e and $\boldsymbol{A}$ together fully describe the theory. The potential is constructed observing the transformation laws for the potentials under change of inertial frames, such that the 4-vector combined obeys the general Lorentz transformation, Equation (2.79). This is done recognizing that electromagnetic theory is intrinsically Lorentz invariant[12] (EINSTEIN, 1905).

2.2.3 Electromagnetic 4-current

The electric current density vector field, $\boldsymbol{J}(\boldsymbol{x}, t)$, is a field that describes the current of charge in each point in space-time. As the stress in a material, it depends of the properties of the materials and needs a constitutive equation to be described. Similarly to what was done in subsection 2.2.2, we can define a 4-vector including both charge and current densities by

$$\boldsymbol{\mathcal{J}} = c\rho_e\hat{\boldsymbol{e}}_0 + J^i\hat{\boldsymbol{e}}_i, \tag{2.84}$$

which acts as a font of the field $\boldsymbol{\mathcal{A}}$. Here ρ_e is a positive integrable function $\rho_e : \mathcal{V} \times \mathbb{R}^+ \to \mathbb{R}^+$ known as electric charge density

[12] Even by experiments.

2.2.4 Electrical Charge Balance Equation

A fundamental statement of electromagnetism is that charge must not be created or destroyed. This is manifested in the fact that, for an arbitrary volume of the continuum $\Omega(t)$ with surface $\partial\Omega(t)$, the temporal change in its total charge equals the flux of charge into the volume, i.e.

$$\frac{dQ_e}{dt} = \frac{d}{dt}\int_{\Omega} \rho_e dV = -\int_{\partial\Omega} \boldsymbol{J} \cdot \hat{\boldsymbol{n}} dS, \tag{2.85}$$

where Q_e is the total electric charge in the volume $\Omega(t)$. Thus, using divergence theorem (ARIS, 1989) and localization theorem,

$$\frac{\partial \rho_e}{\partial t} + \boldsymbol{\nabla} \cdot \boldsymbol{J} = 0, \tag{2.86}$$

which is known as continuity of charge equation. Note that Equation (2.86) can be rewritten, in the notation presented for Lorentz invariant theory, as

$$\frac{\partial (c\rho_e)}{\partial (ct)} + \frac{\partial J^i}{\partial x^i} = 0 \tag{2.87}$$

or

$$\frac{\partial \mathcal{J}^\mu}{\partial x^\mu} = 0. \tag{2.88}$$

2.2.5 Maxwell's Equations

To deduce the field equations for the electromagnetic field, we will state six premises based on known facts about the electrodynamics and construct the field equations for the 4-potential based on them. These are:

(i) Electrically charged matter has long range interactions. This means that the decay of field strength must obey a power law, not a exponential one;

(ii) By experience, electromagnetic phenomena obey the superposition principle, so the field equations must also obey it. Hence, field equations must be linear;

(iii) Field equations must be Lorentz invariant, i.e. they must be composed of quantities that obey Lorentz transformation when a change of inertial frame is done;

(iv) Field equations must have as fonts the charge and current densities. Note that the 4-vector $\boldsymbol{\mathcal{J}}$ can be used as a font of the equation, as it obeys Lorentz transformation;

(v) The principle of conservation of electric charge is valid, so that $\partial \mathcal{J}^\mu / \partial x^\mu = 0$;

(vi) As classical waves must be solution of the field equations, we impose these to be differential equations of second order.

To adhere to premise (iii), we will only utilize combinations and derivatives of $\boldsymbol{\mathcal{A}}$ and $\boldsymbol{\mathcal{J}}$ to construct the field equations, as they transform accordingly to Lorentz transformations. This way, using the premise (iv) we have a general form of the field equations given by

$$\text{sum of terms involving } \mathcal{A}^\mu \propto \mathcal{J}^\mu. \tag{2.89}$$

From premises (ii) and (vi), the left-hand side of Equation (2.89) can only contain components of 4-vectors of the form

$$\frac{\partial^2 \mathcal{A}^\mu}{\partial x^\nu \partial x_\nu}, \quad \frac{\partial^2 \mathcal{A}^\nu}{\partial x_\mu \partial x^\nu} \quad \text{and/or} \quad A^\mu. \tag{2.90}$$

Thus, we rewrite Equation (2.89) in the most general form as

$$\frac{\partial^2 \mathcal{A}^\mu}{\partial x^\nu \partial x_\nu} + b\frac{\partial^2 \mathcal{A}^\nu}{\partial x_\mu \partial x^\nu} + aA^\mu = k\mathcal{J}^\mu, \tag{2.91}$$

where a, b and k are constants to be determined by the premises. Using premise (i) and the 0-component of Equation (2.91), we conclude that $a = 0$. On the other hand, applying $\partial/\partial x^\mu$ on both sides of Equation (2.91) and using the continuity of charge $\partial \mathcal{J}^\mu/\partial x^\mu$ we obtain that $b = -1$. Finally, the constant k can be obtained just comparing the phase velocity of the wave solutions, the way that $k = \mu_0$, with μ_0 being the vacuum magnetic permeability. Therefore, the field equations given by Equation (2.91) reduces to

$$\frac{\partial \mathcal{F}^{\nu\mu}}{\partial x^\nu} = \mu_0 \mathcal{J}^\mu, \tag{2.92}$$

where the electromagnetic field strength tensor $\boldsymbol{\mathcal{F}}$ is defined by

$$\mathcal{F}^{\mu\nu} = \frac{\partial A^\nu}{\partial x_\mu} - \frac{\partial A^\mu}{\partial x_\nu}. \tag{2.93}$$

Equations (2.92) are known as the non-homogeneous Maxwell's equations. To complete the set, one must use the definition of the electromagnetic field strength, the way that

$$\frac{\partial \mathcal{F}^{\mu\nu}}{\partial x^\alpha} + \frac{\partial \mathcal{F}^{\nu\alpha}}{\partial x^\mu} + \frac{\partial \mathcal{F}^{\alpha\mu}}{\partial x^\nu} = 0 \tag{2.94}$$

or

$$\epsilon_{\mu\nu\sigma\tau}\frac{\partial \mathcal{F}^{\sigma\tau}}{\partial x_\nu} = 0, \tag{2.95}$$

where $\epsilon_{\mu\nu\sigma\tau}$ is the 4-dimensional Levi-Civita's permutation symbol. Equations (2.94) are called homogeneous Maxwell's equations. Note that the homogeneous Maxwell's equations are just a consequence of the geometrical structure of electromagnetism. Indeed, in Riemann's differential geometry, equations like Equation (2.94) are named Bianchi identities and are consequences of the definition of Riemann's curvature tensor in a specific kind of space. In modern formulations of electromagnetism, it is viewed as a gauge theory, a formal geometrical theory where $\boldsymbol{\mathcal{F}}$ is its curvature tensor and the homogeneous field equations are just the associated Bianchi identities. One can have a glimpse of this modern formulation noting that Equations (2.91) resembles curvature equations.

Although Equations (2.92) and (2.94) describes the full dynamics of the electromagnetic field, it is important to write these equations in a less enigmatic way. We first note that, using the definition of the 4-potential, the magnetic field is just the dual-vector (see Appendix A.3 for details) associated with the spacial part of electromagnetic tensor $F^{ij}\hat{\boldsymbol{e}}_{\boldsymbol{i}} \otimes \hat{\boldsymbol{e}}_{\boldsymbol{j}}$, i.e.

$$B_i = \epsilon_{ijk}\frac{\partial A^k}{\partial x_j} = \frac{1}{2}\epsilon_{ijk}\mathcal{F}^{jk}, \tag{2.96}$$

and the electric field is related with the electromagnetic field tensor by

$$E_i = -\frac{\partial \phi_e}{\partial x^i} - \frac{\partial A_i}{\partial t} = -c\frac{\partial \mathcal{A}^0}{\partial x^i} - c\frac{\partial A_i}{\partial x^0} = c\mathcal{F}_{0i}. \tag{2.97}$$

Thus, substituting these relations in non-homogeneous Maxwell's equations, Equation (2.92), we obtain

$$\boldsymbol{\nabla} \cdot \boldsymbol{E} = \frac{\rho_e}{\varepsilon_0}, \tag{2.98}$$

$$\boldsymbol{\nabla} \times \boldsymbol{B} - \frac{1}{c^2}\frac{\partial \boldsymbol{E}}{\partial t} = \mu_0 \boldsymbol{J}, \tag{2.99}$$

where ε_0 is the vacuum permittivity. On the other hand, substituting in Maxwell's homogeneous equations, Equation (2.94), we obtain

$$\boldsymbol{\nabla} \cdot \boldsymbol{B} = 0, \tag{2.100}$$

$$\boldsymbol{\nabla} \times \boldsymbol{E} + \frac{\partial \boldsymbol{B}}{\partial t} = 0. \tag{2.101}$$

The set of Equations (2.98), (2.99), (2.100) and (2.101) are the full set of Maxwell's equations in classical notation, a set that describes the dynamics of the electromagnetic fields. Equation (2.98) is known as Gauss law for the electric field, Equation (2.99) as Ampere's law, Equation (2.100) as Gauss law for magnetic field and Equation (2.101) as

Faraday's law.

2.2.6 Constitutive Law for the Electric Current Density (Ohm's Law)

The electric current density vector field $\boldsymbol{J}(\boldsymbol{x}, t)$ describes the electric charge flux in each space-time point of the continuum. Thus, $\boldsymbol{J}$ must be defined by a constitutive equation, as the way that electric charges moves through the continuum is intrinsically dependent on the type of the material, on its molecular nature. For an electric current be established, a driving force is necessary to generate the movement of charges, which in general is the electromagnetic force. Hence,

$$\boldsymbol{J} \propto \boldsymbol{F}_L, \tag{2.102}$$

where $\boldsymbol{F}_L$ is the electromagnetic force, also known as Lorentz force. As magnetic fields are a relativistic manifestation of electric fields (BARUT, 1980), we first use a inertial frame of reference in which the charges are at rest, the way the current density is linear to the electric field. Hence,

$$\boldsymbol{J} \propto \boldsymbol{E_r}, \tag{2.103}$$

where $\boldsymbol{E}_r$ represents the electric field observed by such frame of reference. We note that, in general, even in a rest frame the charges should be influenced by a magnetic field. But for the majority of materials, it is known that for a conductor at rest the electric force on charges is much more significant than the magnetic force (GRIFFITHS, 1999). This way, the linear constitutive relation given by Equation (2.103) is observed for most of electrically conducting materials, including the materials explored in this work in the context of magnetohydrodynamics. The most general form of relating two vectors linearly is through a second order tensor (ARIS, 1989). Then

$$\boldsymbol{J} = \boldsymbol{\sigma}_e \cdot \boldsymbol{E}_r, \tag{2.104}$$

where $\boldsymbol{\sigma}_e$ is called the electric conductivity tensor. In the special case of the material being homogeneous and isotropic, $\boldsymbol{\sigma}_e$ must also be a homogeneous and isotropic tensor-valued function, the way that $\boldsymbol{\sigma}_e = \sigma_e \boldsymbol{I}$, where σ_e is the electric conductivity material constant. Therefore, in this special case,

$$\boldsymbol{J} = \sigma_e \boldsymbol{E}_r. \tag{2.105}$$

Equation (2.105) is known as Ohm's law.

To generalize Equation (2.105) to more general frame of references, where the conductor is not at rest, we apply a Lorentz transformation to a frame where the conductor has velocity vector field $\boldsymbol{u}(\boldsymbol{x}, t)$. The transformation law for the electric field through Lorentz transformations can be obtained through the transformation for the 4-potential, i.e. $\mathcal{A}'^{\mu} = \Lambda^{\mu}_{\nu}\mathcal{A}^{\nu}$. Therefore (DAVIDSON, 2017),

$$\boldsymbol{J} = \sigma_e \left(\boldsymbol{E} + \boldsymbol{u} \times \boldsymbol{B}\right). \tag{2.106}$$

Equation (2.106) is the form of Ohm's law that will be used throughout this work for a electrically conductor fluid.

2.2.7 Lorentz Force

It is known, from Coulomb's law, that in a frame of reference where a point particle with electric charge is at rest, the force under it is

$$\boldsymbol{F}_{Lr} = q\boldsymbol{E}_r, \tag{2.107}$$

where q is the electric charge of the particle. Analogous to what was done in subsection 2.2.6, performing a Lorentz transformation to a general frame of reference, we obtain the Lorentz force:

$$\boldsymbol{F}_L = q(\boldsymbol{E} + \boldsymbol{v} \times \boldsymbol{B}), \tag{2.108}$$

where $\boldsymbol{v}$ is the velocity of the particle. In the case of a continuum of material particles, we have a velocity field $\boldsymbol{u}(\boldsymbol{x}, t)$ and the Lorentz force can be written per unit volume as

$$\boldsymbol{f}_L = \rho_E \left(\boldsymbol{E} + \boldsymbol{u} \times \boldsymbol{B}\right). \tag{2.109}$$

2.3 Magnetohydrodynamics

In this section, we couple the equations of fluid dynamics and electrodynamics and use some approximations to reach the equations governing magnetohydrodynamic flows.

2.3.1 MHD Approximations

The equations of electromagnetic theory can be simplified in the context of non-relativistic magnetohydrodynamic flows, in regimes where the flow characteristic velocity is small compared to the velocity of electrons traveling relatively to the conductor. The flows explored throughout this work are included in this case, as the charge relaxation time in the typical conductors is notably small compared with the characteristic times of the flows explored.

Substituting Ohm's law for conducting fluids, Equation (2.106), and Gauss law, Equation (2.98), in charge continuity Equation (2.86), we obtain that

$$\frac{\partial \rho_e}{\partial t} + \frac{\rho_e}{\tau_e} + \sigma_e \nabla \cdot (\boldsymbol{u} \times \boldsymbol{B}) = 0, \tag{2.110}$$

where $\tau_e = \frac{\varepsilon_0}{\sigma_e}$ is a electric charge relaxation time. Now, in the case where $\boldsymbol{u} = \boldsymbol{0}$, i.e. rest case, we have that

$$\frac{\partial \rho_e}{\partial t} = -\frac{\rho_e}{\tau_e}. \tag{2.111}$$

Hence,

$$\rho_e(t) = \rho_e(0) e^{-t/\tau_e}. \tag{2.112}$$

Equation (2.112) shows that, given the necessary time, any free charge in the interior of the conductor is moved to the surface. The characteristic time of this process is τ_e, which can be interpreted as the characteristic time necessary to any electric charge unbalance be relaxed. In the case of typical metallic conductors, the charge relaxation time is approximately 10^{-18} s (DAVIDSON, 2017). Hence, charges move to the surface almost immediately. In the general MHD case we have that

$$\left| \frac{\partial \rho_e}{\partial t} \right| \ll \left| \frac{\rho_e}{\tau_e} \right|. \tag{2.113}$$

Returning to the general case where the conductor have movement, Equation (2.110) can be rewritten, in the case of typical conductors, as

$$\rho_e = -\varepsilon_0 \boldsymbol{\nabla} \cdot (\boldsymbol{u} \times \boldsymbol{B}). \tag{2.114}$$

From Equations (2.114) and (2.106) we obtain by a scale analysis that

$$\rho_e |\boldsymbol{E}| \sim \frac{u_c \tau_e}{\ell_c} J_c B_c, \tag{2.115}$$

where u_c, ℓ_c, J_c e B_c are, respectively, characteristics velocity, length, current density and magnetic field. Thus, as $\rho_e |\boldsymbol{E}| \ll |\boldsymbol{J} \times \boldsymbol{B}|$, we have that the Lorentz force reduces to

$$\boldsymbol{f}_L = \boldsymbol{J} \times \boldsymbol{B}. \tag{2.116}$$

We note from Equation (2.114) that, in the case with movement, the flow can maintain charges inside the conductor and not in the surface. Nonetheless, this effect is so weak that that the electric force is negligible in relation to the magnetic force.

On the other hand, as τ_e is very small, we show by the Ohm's law, Equation (2.106) that

$$\varepsilon_0 \left|\frac{\partial \boldsymbol{E}}{\partial t}\right| \sim \tau_e \left|\frac{\partial \boldsymbol{J}}{\partial t}\right| \ll |\boldsymbol{J}| \,. \tag{2.117}$$

Hence, charge continuity Equation (2.86) and Ampere-Maxwell law, Equation (2.99), in the MHD context reduces to, respectively,

$$\nabla \cdot \boldsymbol{J} = 0, \tag{2.118}$$

$$\nabla \times \boldsymbol{B} = \mu_0 \boldsymbol{J}. \tag{2.119}$$

We note that, in this context, Equation (2.118) is equivalent to

$$\frac{\partial \rho_e}{\partial t} = 0. \tag{2.120}$$

2.3.2 Transport Equation for the Magnetic Field

To complete the set of magnetohydrodynamics equations, it is necessary a evolution equation for the magnetic field $\boldsymbol{B}$. To achieve this goal, we first apply the rotational operator to Ohm's law, Equation (2.106), and then substitute Faraday's law, Equation (2.101), inside it, obtaining

$$\boldsymbol{\nabla} \times \boldsymbol{J} = \sigma_e \left[-\frac{\partial \boldsymbol{B}}{\partial t} + \boldsymbol{\nabla} \times (\boldsymbol{u} \times \boldsymbol{B})\right]. \tag{2.121}$$

Now, using reduced form of Ampere's law for MHD, Equation (2.119), the last equation can be written as

$$\frac{\partial \boldsymbol{B}}{\partial t} = \boldsymbol{\nabla} \times (\boldsymbol{u} \times \boldsymbol{B}) - \frac{1}{\mu_0 \sigma_e} \boldsymbol{\nabla} \times \boldsymbol{\nabla} \times \boldsymbol{B}. \tag{2.122}$$

By Gauss law for magnetism, Equation (2.100), $\boldsymbol{B}$ is solenoidal (i.e. $\boldsymbol{\nabla} \cdot \boldsymbol{B} = 0$), the way that[13]

$$\frac{\partial \boldsymbol{B}}{\partial t} = \nabla \times (\boldsymbol{u} \times \boldsymbol{B}) + \nu_m \nabla^2 \boldsymbol{B}, \tag{2.123}$$

where $\nu_m = 1/\mu_0 \sigma_e$ is the magnetic diffusion coefficient. Using the vector calculus identity for $\nabla \times (\boldsymbol{u} \times \boldsymbol{B})$[14] and, again, the fact that $\boldsymbol{B}$ is solenoidal, Equation (2.123) is shown to

13 Using $\boldsymbol{\nabla} \times \boldsymbol{\nabla} \times \boldsymbol{B} = \boldsymbol{\nabla}(\boldsymbol{\nabla} \cdot \boldsymbol{B}) - \boldsymbol{\nabla}^2 \boldsymbol{B}$.

14 $\nabla \times (\boldsymbol{u} \times \boldsymbol{B}) = \boldsymbol{u}(\nabla \cdot \boldsymbol{B}) - \boldsymbol{B}(\nabla \cdot \boldsymbol{u}) + (\boldsymbol{B} \cdot \nabla)\boldsymbol{u} - (\boldsymbol{u} \cdot \nabla)\boldsymbol{B}$

be equivalent to

$$\frac{D\boldsymbol{B}}{Dt} = \boldsymbol{B} \cdot \nabla \boldsymbol{u} - \boldsymbol{B} \left(\nabla \cdot \boldsymbol{u} \right) + \nu_m \nabla^2 \boldsymbol{B}. \tag{2.124}$$

Equation (2.124) dictates the evolution of the magnetic vector field and is known as the magnetic induction equation. Its terms can be interpreted as follows:

- $\dfrac{D\boldsymbol{B}}{Dt}$: Temporal change of $\boldsymbol{B}$ felt by a material particle;
- $\boldsymbol{B} \cdot \nabla \boldsymbol{u}$: Stretching and rotation of the magnetic field lines by the flow;
- $\boldsymbol{B} \left(\nabla \cdot \boldsymbol{u} \right)$: Effect of the volumetric expansion of the material element on the magnetic field lines;
- $\nu_m \nabla^2 \boldsymbol{B}$: Diffusive transport of $\boldsymbol{B}$.

2.3.3 A Consequence of the Induction Equation

Let S_0 be an arbitrary material surface in the continuum in the time t_0 and $S(t)$ its form carried to a time t. Therefore, the derivative of the flux of the magnetic field $\boldsymbol{B}$ through $S(t)$ can be calculated using Equation (2.13) as

$$\frac{d}{dt} \int_S \boldsymbol{B} \cdot \hat{\boldsymbol{n}} dS = \int_S \frac{D\boldsymbol{B}}{Dt} \cdot \hat{\boldsymbol{n}} dS + \int_{S_0} \boldsymbol{B} \cdot \frac{DJ}{Dt} \boldsymbol{F}^{-T} \cdot \boldsymbol{N} dS_0 + \int_{S_0} \boldsymbol{B} \cdot J \frac{D\boldsymbol{F}^{-T}}{Dt} \cdot \boldsymbol{N} dS_0. \tag{2.125}$$

Using Equations (2.18) and (A.17), we obtain that

$$\frac{d}{dt} \int_S \boldsymbol{B} \cdot \hat{\boldsymbol{n}} dS = \int_S \left[\frac{D\boldsymbol{B}}{Dt} + \boldsymbol{B}(\boldsymbol{\nabla} \cdot \boldsymbol{u}) - \boldsymbol{B} \cdot \nabla \boldsymbol{u} \right] \cdot \hat{\boldsymbol{n}} dS. \tag{2.126}$$

Thus, as a consequence of the magnetic induction Equation (2.124),

$$\frac{d}{dt} \int_S \boldsymbol{B} \cdot \hat{\boldsymbol{n}} dS = \int_S \nu_m \nabla^2 \boldsymbol{B} \cdot \hat{\boldsymbol{n}} dS. \tag{2.127}$$

In the special case where the fluid is a perfect conductor (its magnetic diffusivity goes to zero), this relation states that

$$\int_{S_0} \boldsymbol{B}(t_0) \cdot \hat{\boldsymbol{n}} dS = \int_S \boldsymbol{B}(t) \cdot \hat{\boldsymbol{n}} dS. \tag{2.128}$$

The last equation states that the magnetic field lines are frozen into a perfect conductor fluid [15]. This way, if we take a specific material surface, the flux of $\boldsymbol{B}$ through this surface

[15] If one define a 4-velocity by $u^\mu = dx^\mu/d\tau$, where τ is the invariant parameter of time evolution, this result can be stated in a mathematical elegant way. In the context on differentiable manifolds, this results states that Lie derivative of electromagnetic field strength $\boldsymbol{F} = F^{\mu\nu} \hat{\boldsymbol{e}}_\mu \otimes \hat{\boldsymbol{e}}_\nu$ is null along the

will remain the same at any time. We note that this exact behavior occurs to the vorticity in perfect fluids (with no viscosity).

2.3.4 Hydromagnetic Waves

Consider the case of a perfect conductor and remember the result presented in subsection 2.3.3. As the magnetic field lines are frozen in the fluid, it can be viewed as elastic strings carrying fluid elements (mass). These elastic strings are under magnetic tension given by B_0^2/μ_0 (DAVIDSON, 2017), where B_0 is the intensity of the magnetic field acting on the fluid. Therefore, any disturbance on the fluid will cause this *magnetic string* to oscillate (the particles in it oscillate) normal to the line. These waves are named Alfvén waves, as it was first pointed to exist by (ALFVÉN, 1942), and are well known to be incompressible waves (DAVIDSON, 2017), i.e. they do not modify the mass density of the fluid. Also as a consequence, compression and expansion of the fluid elements in the direction of the magnetic field will give rise to waves in this direction. These are named magnetoacoustic waves and are known to be compressible waves, as they are originated by compression and expansion of the fluid in this direction. The conjunction of these two kinds of waves are known as magnetohydrodynamic waves.

2.3.5 Magnetohydrodynamics Governing Equations

The set of equations that rules the magnetohydrodynamics is formed by the coupling of fluid dynamics laws, the electrodynamics laws and the appropriate approximations. As the microstructure of the fluid is not changed in MHD general applications, the only change in Navier-Stokes is Lorentz force, that is a body force. Thus, the governing equations of magnetohydrodynamics is given by modified Navier-Stokes equation, continuity equation and the transport equation for the magnetic field, respectively given by

$$\rho\frac{D\boldsymbol{u}}{Dt} = -\nabla p_0 + \boldsymbol{\nabla}\left(\eta_2\boldsymbol{\nabla}\cdot\boldsymbol{u}\right) + \eta\nabla^2\boldsymbol{u} + \frac{1}{3}\eta\boldsymbol{\nabla}\left(\boldsymbol{\nabla}\cdot\boldsymbol{u}\right) + \boldsymbol{J}\times\boldsymbol{B} + \rho\boldsymbol{g}, \tag{2.129}$$

$$\frac{\partial\rho}{\partial t} + \boldsymbol{\nabla}\cdot(\rho\boldsymbol{u}) = 0, \tag{2.130}$$

flow defined by u^μ, i.e. $\pounds_u\boldsymbol{F} = \boldsymbol{0}$, where $\pounds_u$ is the Lie derivative along the flow of the vector field given by u^μ.

$$\frac{D\boldsymbol{B}}{Dt} = \boldsymbol{B} \cdot \nabla \boldsymbol{u} - \boldsymbol{B} \left(\nabla \cdot \boldsymbol{u} \right) + \nu_m \nabla^2 \boldsymbol{B}. \qquad (2.131)$$

All of the electromagnetic equations in MHD context, given by Equation (2.106), (2.98), (2.99), (2.101), (2.118) e (2.119) acts as auxiliary equations.

2.3.6 Non-dimensional Physical Parameters of MHD

Some important non-dimensional physical parameters are of most interest in magnetohydrodynamics context, giving the balance between important mechanisms of this kind of flow. The principal ones are presented by Table 1. We note that the Reynolds

Table 1 – Non-dimensional physical parameters that govern magnetohydrodynamics. Here u_c is a characteristic velocity, ℓ_c ia characteristic length, ν is the hydrodynamic diffusivity and B_c is a characteristic magnetic field.

Parameter Name Symbol and Definition	**Physical meaning**
Reynolds number $Re = u_c \ell_c / \nu$	Ratio between inertial and viscous forces
Hartman number $Ha = B_c \ell_c \sqrt{\sigma_e / \rho\nu}$	Ratio between Lorentz and viscous forces
Interaction parameter $N = Ha^2 / Re$	Ratio between Lorentz and inertial forces
Magnetic Reynolds number $Re_m = u_c \ell_c / \nu_m$	Ratio between diffusion and advection times of $\boldsymbol{B}$
Euler magnetic number $E_m = B_0^2 / \mu_0 p_0$	Ratio between magnetic and characteristic flow pressures

magnetic number defines the magnetic regime. If $Re_m \gg 1$, the fluid is a perfect conductor, i.e. there is no molecular diffusion of magnetic field and we say that the magnetic field lines are frozen in the fluid. This is analogous to vorticity lines frozen in the fluid in the case of an ideal fluid. In the case that $Re_m \ll 1$, we have pure molecular diffusion of $\boldsymbol{B}$, where its evolution equation is given simply by a diffusion equation.

3 BULK VISCOSITY ON MHD WAVES

3.1 Landau's Model for the Bulk Viscosity

Second viscosity or bulk viscosity is directly related to compression and expansion of the material volumes in a fluid, as it appears accompanied by $\boldsymbol{\nabla} \cdot \boldsymbol{u}$, that measure the volumetric expansion of a fluid element (BATCHELOR, 1967). Indeed, if we consider a material volume under real compression or expansion, as any rapid thermodynamic process, it ceases the local equilibrium momentarily and immediately an internal process to restore equilibrium position is set up inside the material element. As this process is not quasi-static, it is irreversible, involving energy dissipation and increasing entropy. If the relaxation time (the time to restore equilibrium) is large compared to the frequency of compression/expansion, bulk dissipation can be significant, resulting in the second viscosity coefficient having values comparable to the dynamic viscosity. Therefore, in flows that involve high frequencies (i.e. the product of the frequency by a relaxation time is $\mathcal{O}(1)$), the second viscosity effects can be significant and must be included in the formulation (in these cases the Stokes hypothesis is not valid). Throughout this section, a methodology first explored by Mandelshtam and Leontovich (1937) and and later discussed by Landau and Lifshitz (1987) will be discussed to present a model for the second viscosity coefficient.

Let ζ be a physical quantity that characterizes the state of a material element in the neighborhood of its local thermodynamic equilibrium value ζ_0. If the physical property is tending to equilibrium, we can expand ζ in a Taylor series, the way we obtain that

$$\zeta = \zeta_0 - \frac{d\zeta}{dt}(t - t_0) + \mathcal{O}[(t - t_0)^2], \tag{3.1}$$

where t is a generic time and t_0 is the time that ζ reaches equilibrium. As the oscillations are in the neighborhood of the equilibrium value, we can despise second order terms and rearrange the expression to reach

$$\frac{d\zeta}{dt} = \frac{(\zeta_0 - \zeta)}{\tau}, \tag{3.2}$$

where $\tau = t - t_0$ is a relaxation time, i.e. the time needed to reach equilibrium.

Next we consider the continuum where this material element is contained to be under adiabatic compression and expansion, disturbing the media periodically. Thus, the local equilibrium values of physical quantities changes periodically, such that

$$\zeta_0 = \zeta_{00} + \zeta_0', \tag{3.3}$$

where ζ_0' have the form $Ae^{i\omega t}$, with A being some constant amplitude of oscillation, ω the frequency of the continuum's oscillation and i the imaginary unit. We now write, for convenience, that $\zeta = \zeta_{00} + \zeta'$, with ζ' being a generic function. Using Equations (3.2) and (3.3) and noting that $\zeta - \zeta_0 = \zeta' - \zeta_0'$, we can write that

$$\frac{d\zeta'}{dt} + \frac{\zeta'}{\tau} = \frac{-Ae^{i\omega t}}{\tau}. \tag{3.4}$$

The ordinary differential Equation (3.4) is simply integrated multiplying both sides by $e^{t/\tau}$, the integration factor. This way we obtain

$$\zeta' = \frac{\zeta_0'}{1 - i\omega t}. \tag{3.5}$$

Equation (3.5) shows that ζ' is also a periodic function of time.

Now we turn to a specific property, the pressure p. For this case, where this media is being disturbed by compression and expansion, we have that $p = p(\rho, \zeta(\rho))$. Then

$$\frac{dp}{d\rho} = \left(\frac{\partial p}{\partial \rho}\right)_\zeta + \left(\frac{\partial p}{\partial \zeta}\right)_\rho \frac{d\zeta}{d\rho}. \tag{3.6}$$

Using Equation (3.5), the last equation can be rewritten as

$$\frac{dp}{d\rho} = \frac{1}{(1 - i\omega t)} \left[\left(\frac{\partial p}{\partial \rho}\right)_{eq} - i\omega\tau \left(\frac{\partial p}{\partial \rho}\right)_\zeta\right], \tag{3.7}$$

where

$$\left(\frac{dp}{d\rho}\right)_{eq} = \left(\frac{\partial p}{\partial \rho}\right)_\zeta + \left(\frac{\partial p}{\partial \zeta}\right)_\rho \frac{\partial \zeta_0}{\partial \rho} \tag{3.8}$$

is just the derivative of p with respect to ρ in a quasi-static process, such that $\xi \approx \xi_0$.

Alternatively, using that

$$\delta p_0 = \left(\frac{dp}{d\rho}\right)_{eq} \delta\rho, \tag{3.9}$$

$$\delta p = \frac{dp}{d\rho}\delta\rho, \tag{3.10}$$

we obtain that

$$p - p_0 = \left[\frac{dp}{d\rho} - \left(\frac{dp}{d\rho}\right)_{eq}\right] \delta\rho. \tag{3.11}$$

Therefore, combining Equations (3.7) and (3.11) and rearranging the terms,

$$p - p_0 = \frac{i\omega\tau}{1 - i\omega\tau} \left[\left(\frac{dp}{d\rho}\right)_{eq} - \left(\frac{dp}{d\rho}\right)_{\zeta}\right] \delta\rho. \tag{3.12}$$

As we are working with a continuum, we can relate $\delta p = \rho - \rho_{00} = Ce^{-i\omega t}$ with the velocity field through continuity Equation (2.28), the way we can write that

$$\frac{D\delta\rho}{Dt} + \rho\boldsymbol{\nabla}\cdot\boldsymbol{u} = 0 \tag{3.13}$$

or, performing the derivative,

$$\delta\rho = \frac{\rho}{i\omega}\boldsymbol{\nabla}\cdot\boldsymbol{u}. \tag{3.14}$$

Finally, substituting Equation (3.14) in Equation (3.12), we obtain that

$$p - p_0 = \frac{\tau\rho}{1 - i\omega\tau}(c_0^2 - c_\infty^2)\boldsymbol{\nabla}\cdot\boldsymbol{u} \tag{3.15}$$

and, using the constitutive equation for the mechanical pressure $p - p_0 = -\eta_2\boldsymbol{\nabla}\cdot\boldsymbol{u}$,

$$\eta_2 = \frac{\tau\rho}{1 - i\omega\tau}(c_\infty^2 - c_0^2). \tag{3.16}$$

Here c_0 is the sound velocity in equilibrium condition and c_∞ is the sound velocity in a fixed thermodynamic state. Equation (3.16) represents a model for the second viscosity coefficient for small oscillations. If we make Landau's model for η_2 non-dimensional, we obtain that

$$\eta_2^* = \frac{1}{Re_k}\left(\frac{\tilde{c}^2 - 1}{1 - i\omega\tau}\right), \tag{3.17}$$

where $\tilde{c} = c_\infty/c_0$ and $Re_k = \ell_c/(\tau c_0)$ is the expansional Reynolds number, which gives the ratio between the flow time, which in this case is the acoustic time, and the relaxation time. This non-dimensional physical parameter measure the relative importance of the bulk viscosity effects in this model.

3.2 Governing Equations

As the effects of the standard viscosity on hydromagnetic waves are well known, we only intend to investigate the effects of the second viscosity coefficient in our analysis. Thus, we use a Euler's fluid with second viscosity, i.e. we will use Euler's equation of motion with an additional term for the bulk viscosity. Therefore, the equations of motion are given by

$$\rho\left(\frac{\partial \boldsymbol{u}}{\partial t}+\boldsymbol{u}\cdot\boldsymbol{\nabla}\boldsymbol{u}\right)=-\nabla p_0+\boldsymbol{\nabla}\left[\eta_2(\rho)\boldsymbol{\nabla}\cdot\boldsymbol{u}\right]-\frac{1}{\mu_0}\boldsymbol{B}\times\left(\boldsymbol{\nabla}\times\boldsymbol{B}\right), \tag{3.18}$$

$$\frac{\partial \rho}{\partial t}+\boldsymbol{\nabla}\cdot\left(\rho\boldsymbol{u}\right)=0. \tag{3.19}$$

where we have used Ampere's law for $\boldsymbol{J}$, given by Equation (2.119). As we want to investigate the hydromagnetic waves and the effect of second viscosity on it and not the mechanisms that prevent this kind of waves in low conductivity fluids, the fluid will be considered as a perfect conductor. Hence, induction Equation (2.124) simply becomes

$$\frac{\partial \boldsymbol{B}}{\partial t}=\boldsymbol{\nabla}\times\left(\boldsymbol{u}\times\boldsymbol{B}\right). \tag{3.20}$$

In addition, as we are not interested in temperature, we will consider a barotropic fluid, such that $p_0=p_0(\rho)$. Therefore, we also have the barotropic equation:

$$\frac{D}{Dt}\left(\frac{p_0}{\rho^\gamma}\right)=0, \tag{3.21}$$

where γ is just a barotropic coefficient. The set of Equations (3.18), (3.19), (3.20) and (3.21) is the governing set equations for the hydromagnetic waves we intend to construct.

3.3 Non-dimensional Governing Equations

In order to make the governing equations non-dimensional, the following new quantities are defined in terms of characteristic quantities of the flow problem:

$$\boldsymbol{\nabla}^*=\ell_c\boldsymbol{\nabla},\;\;\boldsymbol{u}^*=\frac{\boldsymbol{u}}{c_0},\;\;t^*=\frac{c_0 t}{\ell_c},\;\;\rho^*=\frac{\rho}{\rho_0},\;\;p_0^*=\frac{p_0}{p_{00}},\;\;\text{and}\;\;\boldsymbol{B}^*=\frac{\boldsymbol{B}}{B_0}, \tag{3.22}$$

where the variables with * are the non-dimensional version of the variables, ρ_0 is the equilibrium value of the mass density, ℓ_c is a characteristic length of the flow, p_{00} is the equilibrium value of the thermodynamic pressure and B_0 is the norm of the magnetic field in equilibrium. Note that η_2 scales with $\tau \rho_o {c_o}^2$. In this way, recalling that $k = k(\rho)$, the non-dimensional governing equations can be written as

$$\frac{\partial \rho}{\partial t} + \boldsymbol{\nabla} \cdot (\rho \boldsymbol{u}) = 0, \tag{3.23}$$

$$\rho \left(\frac{\partial \boldsymbol{u}}{\partial t} + \boldsymbol{u} \cdot \boldsymbol{\nabla} \boldsymbol{u} \right) = -\nabla p_0 + \eta_2 \left[\boldsymbol{\nabla} \rho \left(\boldsymbol{\nabla} \cdot \boldsymbol{u} \right) + \rho \boldsymbol{\nabla} \left(\boldsymbol{\nabla} \cdot \boldsymbol{u} \right) \right] - E_m \boldsymbol{B} \times \left(\boldsymbol{\nabla} \times \boldsymbol{B} \right), \tag{3.24}$$

$$\frac{D}{Dt} \left(\frac{p_0}{\rho^\gamma} \right) = 0, \tag{3.25}$$

$$\frac{\partial \boldsymbol{B}}{\partial t} = \boldsymbol{\nabla} \times \left(\boldsymbol{u} \times \boldsymbol{B} \right), \tag{3.26}$$

where E_m is defined as the Euler magnetic number, given by

$$E_m = \frac{B_0^2}{\mu_0 p_{00}}. \tag{3.27}$$

The non-dimensional physical parameter gives a ratio between the magnetic pressure and the thermodynamic pressure. Note that in this step the asterisks were removed from non-dimensional variables for simplicity in notation. This notation change will remain till the end of the chapter.

3.4 Linearization of the Equations

As we want to study hydromagnetic waves, that are oscillations around an equilibrium value of the physical quantities, we assume the relevant physical quantities to have the form given by

$$\boldsymbol{B} = \boldsymbol{B_0} + \boldsymbol{B_1}, \tag{3.28}$$

$$\boldsymbol{u} = \boldsymbol{0} + \boldsymbol{u_1}, \tag{3.29}$$

$$p_0 = 1 + p_1, \tag{3.30}$$

$$\rho = 1 + \rho_1. \tag{3.31}$$

Here the variables with subscript 1 represents the fluctuation of small amplitude of the respective quantity around the equilibrium and $\boldsymbol{B}_0$ is the equilibrium magnetic field. Substituting these forms of the variables in the non-dimensional governing Equations

(3.23), (3.24), (3.25) and (3.26), we obtain the following set of linearized equations:

$$\frac{\partial \rho_1}{\partial t} + \boldsymbol{\nabla} \cdot \boldsymbol{u_1} = 0, \tag{3.32}$$

$$\frac{\partial \boldsymbol{u_1}}{\partial t} + \nabla p_1 - \eta_2 \left[\boldsymbol{\nabla}\left(\boldsymbol{\nabla} \cdot \boldsymbol{u_1}\right)\right] + E_m \boldsymbol{B_0} \times \left(\boldsymbol{\nabla} \times \boldsymbol{B_1}\right) = 0, \tag{3.33}$$

$$\frac{\partial p_1}{\partial t} - \gamma \frac{\partial \rho_1}{\partial t} = 0, \tag{3.34}$$

$$\frac{\partial \boldsymbol{B_1}}{\partial t} - \boldsymbol{\nabla} \times \left(\boldsymbol{u_1} \times \boldsymbol{B_0}\right) = 0. \tag{3.35}$$

The last set of equations are the governing equations for small fluctuations around equilibrium values.

3.5 Plane Wave Solutions and Dispersion Relations

Consider solutions of plane waves traveling in the z direction to the disturbances and a constant magnetic field $\boldsymbol{B}_0$ given by

$$\boldsymbol{B_0} = \sin\alpha \boldsymbol{\hat{e}_x} + \cos\alpha \boldsymbol{\hat{e}_z}, \tag{3.36}$$

where α is the angle between the magnetic field $\boldsymbol{B}_0$ and the wave number vector $\boldsymbol{k}$. This configuration is shown by Figure 2. Hence, if G is some general physical quantity, its fluctuation can be written as

$$G_1 = G_a e^{ikz+st}, \tag{3.37}$$

where G_a is the amplitude of oscillation and s is a complex valued function given by

$$s = \xi - i\omega. \tag{3.38}$$

Here ξ is called the amplification factor and ω is the frequency of the fluctuations. If

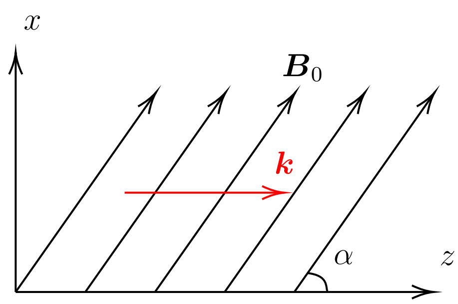

Figure 2 – Scheme for the waves and the magnetic field.

the amplification factor is negative or zero, the waves are said to be stable under small oscillations, as they will not grow with time. On the other hand, the amplification factor being positive implies that the amplitude of the waves grows exponentially. In this case the waves are said to be unstable under small oscillations.

Substituting these solutions in Equations (3.32), (3.33), (3.34) and (3.35) and noting that for this kind of solutions $\boldsymbol{\nabla} = i\boldsymbol{k}$ and $\partial/\partial t = s$, we obtain the following set of equations in the wave-space:

$$s\rho_a + iku_{az} = 0, \tag{3.39}$$

$$su_{ax} - ikE_m B_{az} B_{ax} = 0, \tag{3.40}$$

$$su_{ay} - ikE_m B_{az} B_{ay} = 0, \tag{3.41}$$

$$su_{az} + ikp_a + \eta_2 k^2 u_{az} + ikE_m B_{ax} B_{ax} = 0, \tag{3.42}$$

$$sB_{ax} + iku_{az} B_{ax} - iku_{ax} B_{az} = 0, \tag{3.43}$$

$$sB_{ay} - iku_{ay} B_{az} = 0, \tag{3.44}$$

$$sB_{az} = 0, \tag{3.45}$$

$$sp_a - \gamma s\rho_a = 0. \tag{3.46}$$

The consistency condition for Equation (3.41) and Equation (3.44) gives

$$s^2 + k^2 E_m \cos^2\alpha = 0. \tag{3.47}$$

The relation given by Equation (3.47) is a quadratic equation representing Alfvén waves (DAVIDSON, 2017). The consistency condition for Equations (3.39), (3.40), (3.42), (3.43) and (3.46) gives us

$$\eta_2\left(sk^4 E_m \cos^2\alpha + s^3 k^2\right) + \left(s^2 + k^2 E_m \cos^2\alpha\right)\left(s^2 + k^2\gamma\right) + k^2 s^2 E_m \sin^2\alpha = 0. \tag{3.48}$$

The relation given by Equation (3.48) is a equation that have two pair of roots. They correspond to fast and slow magnetoacoustic waves (BITTENCOURT, 2004).

3.6 Results with Landau's Model for the Bulk Viscosity

Equation (3.47) represents Alfvén waves. In this case, the amplification factor (ξ) is always null, what means that the Alfvén waves have a neutral value for the amplification factor. Under this condition, this kind of wave is always stable in the ideal MHD context considered here. Besides that, it is also clear from this relation that the expansional viscosity does not have any influence on the behavior of this type of waves. This was expected as these disturbance are basically incompressible waves. Moreover, the dispersion relation obtained for this kind of wave is given by

$$\omega^2 - k^2 E_m \cos^2 \alpha = 0, \tag{3.49}$$

which is completely independent of the extensional Reynolds number.

In contrast, Equation (3.48) makes clear that the expansional Reynolds number, the nondimensional frequency and the ratio of sound speed may exert a significant influence on the propagation of magnetoacoustic waves. Consequently, magnetoacoustic disturbances are compressible ones and the expansional effects of the fluid affects directly the wave dispersion relation and its stability.

Also from the equation that represents the magnetoacoustic waves, Equation (3.48), we obtain four roots for s, from which the values of the real part, the amplification factor, and the values for the imaginary part, the frequency ω, can be evaluated for different values of the physical parameters and different wave numbers, showing what is the influence of these physical parameters on the stability and on the phase velocity ω/k of the waves. By varying the physical parameters of the flow system, different graphical results for ξ and for ω/k are presented in this section.

Analyzing Figure 3, it is seen that the phase velocity of the waves, ω/k, does not depend on the value of the wave number when the high frequency expansional effects are negligible, that means that the propagation velocity at short and long wave of small amplitudes are invariant for any mode of the wave. Indeed, according to Bittencourt (2004), the magnetoacoustic waves without expansional high frequency effects are nondispersive waves (i.e. its phase velocity does not depend on k) and its dispersion relations have four roots, one corresponding to fast waves, a second one corresponding to slow waves and the others two ones representing just the first two waves propagating in the opposite direction. This behavior is clearly depicted in Figure 3. Also, for the case where the high frequency effects term is not present, Equation (3.48) is a biquadratic equation that can be solved analytically and used to validate the numerical solution. The analytical behavior expressed by

$$s^2 = \frac{1}{2} k^2 (\gamma + E_m) \pm \frac{1}{2} k^2 \left[(\gamma + E_m)^2 - 4\gamma E_m \cos^2 \alpha \right]^{1/2} \tag{3.50}$$

is exactly recovered by the numerical code solving Equation (3.48) in the asymptotic limit of $Re_k \to \infty$, as presented in Figure 3.

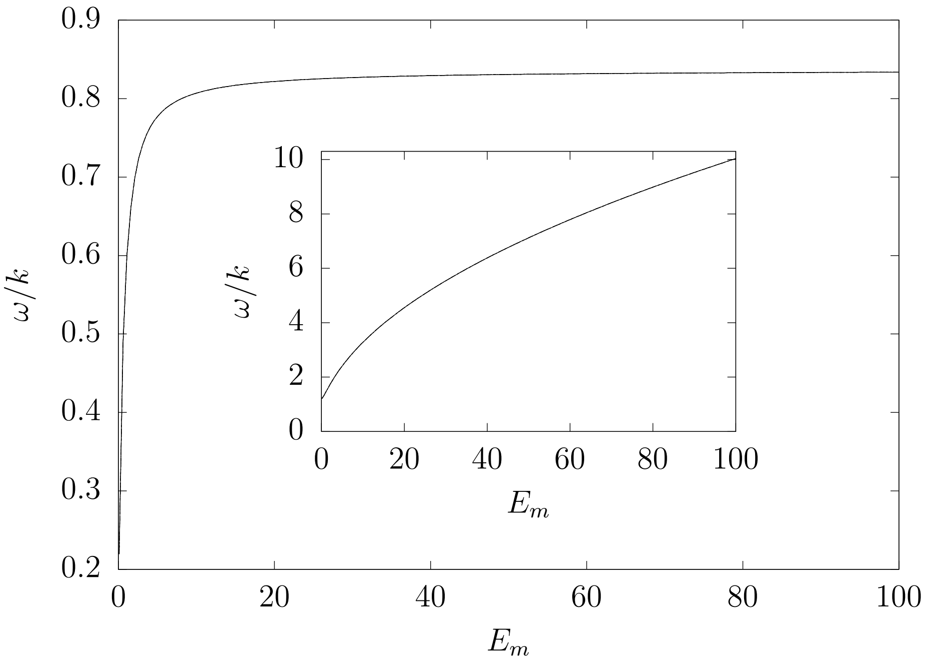

Figure 3 – Phase velocity ω/k of the slow magnetoacoustic waves as a function of E_m with $Re_k \to \infty$, $\alpha = \pi/4$ and $\gamma = 1.4$. *Inset*: The same of the main graphic, but for the root corresponding to fast waves. We note that in this graphic the phase velocity is plotted for 4 different values of k, but they all overlap.

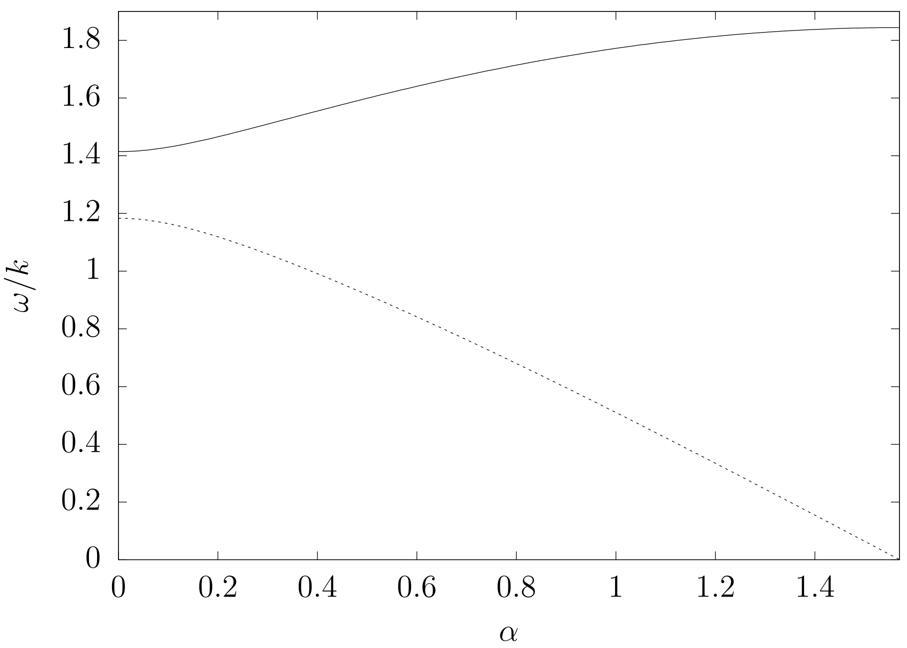

Figure 4 – Phase velocity ω/k as a function of the angle α with $Re_k \to \infty$, $Em = 2$ and $\gamma = 1.4$. In this Figure, ——— represents one root and ------ another root.

Now, varying the values of the Euler magnetic number, E_m, and the α angle, the magnitude of the phase velocity of both slow and rapid waves are affected substantially as shown in Figure 3 and Figure 4. For instance, ω/k of the slow waves increases fast with E_m for all wave numbers and it reaches a constant value for E_m around 20, i.e. as the magnetic pressure is twenty times greater than the thermodynamic one. In contrast, the root corresponding to fast waves, shown in Figure 3 (b), increases with the nondimensional magnetic pressure in the full interval of E_m with a dependence of ω/k following basically the scaling ${E_m}^{1/2}$. Again, since that the waves in the limit of very high Re_k are nondispersive, the observation here works for all spectrum of wave numbers (short and long waves). These results indicate that the ratio between magnetic pressure and thermodynamic pressure and the angle α are key physical parameters that determines the phase velocity of the wave. On the other hand, changing the angle α raises or decreases the roots representing the slow magnetoacoustic waves and the fast magnetoacoustic waves, depending on the root. For slow waves, raising α decreases the phase velocity and for fast waves raising α increases the phase velocity. So, the orientation of the applied magnetic field with respect to the direction of wave propagation change quite differently the wave speed, depending on how fast or slow is its velocity. It suggests that the orientation of a magnetic field can be used to control the propagation velocity of magnetoacoustic waves in a conductor fluid.

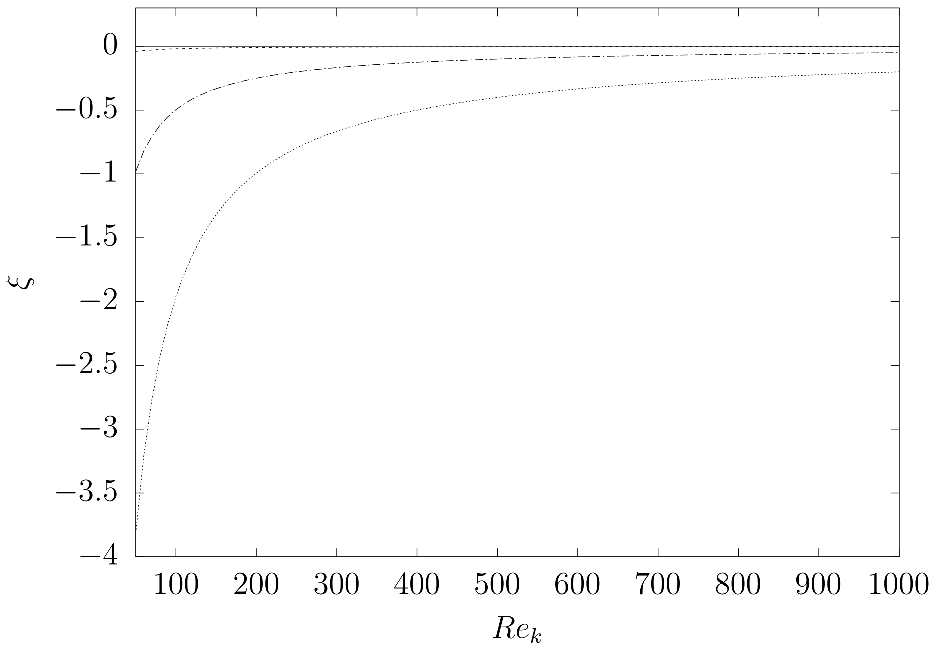

Figure 5 – Amplification factor as a function of Re_k with $\tilde{c} = 1.05$, $\omega\tau = 1$, $\alpha = \pi/4$, $Em = 2$ and $\gamma = 1.4$. In this Figure, ——— represents $k = 1$, - - - - - - $k = 10$, - · - · - · - $k = 50$, ·············· $k = 100$.

Solving s for the amplification factor (the real part) on the asymptotic case where

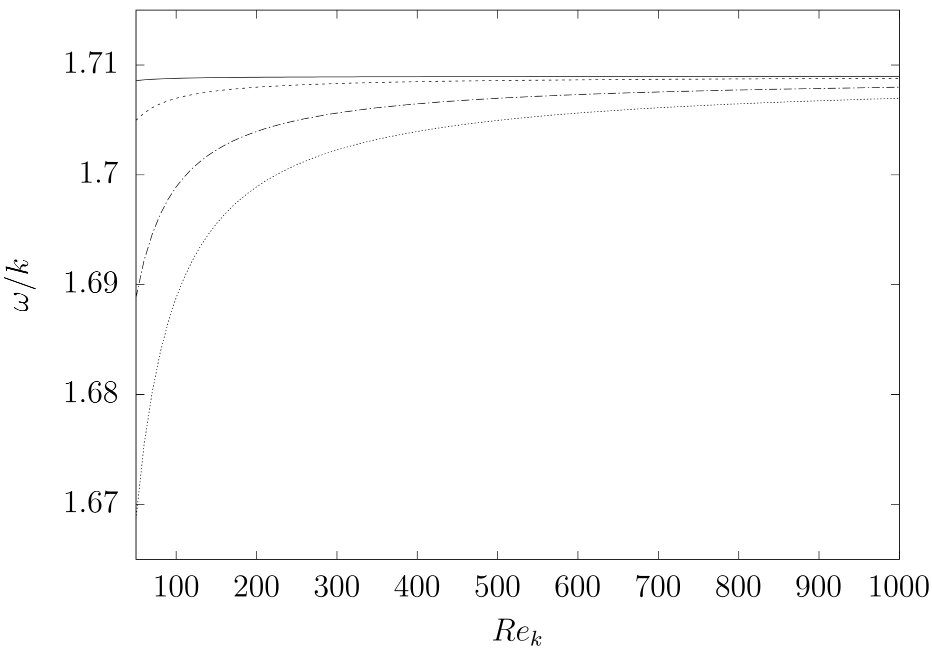

Figure 6 – Phase velocity as a function of Re_k with $\widetilde{c} = 1.05$, $\omega\tau = 1$, $\alpha = \pi/4$, $Em = 2$ and $\gamma = 1.4$. In this Figure, ——— represents $k = 1$, - - - - - - $k = 10$, -·-·-·- $k = 50$, ·········· $k = 100$.

$Re_k \to \infty$, we get from both analytical and numerical solutions that it is null for any value of the wave number, of the Euler magnetic number and of the angle α. This shows that these waves are always stable in the absence of expansional high frequency effects. On the other hand, from the numerical solution, for finite values of Re_k (i.e., when the expansional effects at high frequency take place), these effects change considerable the wave growth rate, as indicated in Figure 5. They make ξ be more negative, behavior which points out that the expansional high frequency effects tends to attenuate the wave amplitude in any mode of velocity, showing the strong dissipative effects of high frequency flows on this kind of waves. In addition, Figure 5 shows that at the asymptotic limit of very high Re_k the wave growth rate tent to a null value for both short and long waves (i.e. small and large scales of wavelengths).

Figure 6 presents a diagram for the phase velocity (ω/k) of the waves as a function of the Re_k, showing its behavior in cases where the expansional high frequency effects assumes finite values. The results indicate the importance of the expansional high frequency effects for varying the wave phase velocity as well. As in the asymptotic limit where $Re_k \to \infty$ the magnetoacoustic waves are nondispersive, from Figure 6 we see that these high frequency effects acts upon these waves making a dispersive action (i.e. they make the phase velocities have a dependence on the wave number) mainly in short waves regimes. Additionally, Figure 6 corroborates that long waves propagate faster than short waves for finite values of Re_k. It is important to notice that only one root for ω/k was shown in Figure 6, but the same physical interpretation can be obtained from the other ones, as the results are analogous.

3.7 Proposition of a Method to Estimate the Bulk Viscosity

At this point we may obtain an expression for the bulk viscosity η_2. Using the dispersion relation for magnetoacoustic waves Equation (3.48) and substituting $s = -i\omega$ gives

$$\eta_2(\omega, k; E_m, \alpha) = \frac{k^2\omega^2 E_m \sin^2\alpha - (\omega^2 - k^2 E_m \cos^2\alpha)(\omega^2 - k^2\gamma)}{i(\omega^3 k^2 - \omega k^4 E_m \cos^2\alpha)}. \tag{3.51}$$

Here η_2 is assumed to be a complex function like in the classic Landau's model. Therefore, taking the real part of Equation (3.51) we get the following expression:

$$\eta_2(\omega, k; E_m, \alpha) = \frac{(\omega^2 - k^2 E_m \cos^2\alpha)(\omega^2 - k^2\gamma) - k^2\omega^2 E_m \sin^2\alpha}{(\omega^3 k^2 - \omega k^4 E_m \cos^2\alpha)}, \tag{3.52}$$

where η_2 now is just the imaginary part of the complex bulk viscosity given in Equation (3.51). Equation (3.52) represents an explicit expression to estimate values for the bulk viscosity at high frequency MHD flows of baratropic gases in terms of the wave and fluid properties such as the wavenumber, the wave frequency, the Euler magnetic parameter, the orientation of the applied field and the barotropic coefficient of the fluid. It should be important to note that the expression of Mandelshtam and Leontovich (1937), Landau and Lifshitz (1987) for the bulk viscosity given in Equation (3.16) is not the same the one obtained in Equation (3.52). Differently, the bulk viscosity in this section is estimated based on an modal analysis of magnetoacoustic waves propagating in compressible MHD flows.

In Figure 7 we show a plot of our non-dimensional bulk viscosity η_2 as a function of the wavenumber k for two different values of the magnetic parameter E_m, i.e. 0 and 300. The case when $E_m = 0$ represents standard acoustic waves which have the maximum of the rate of energy dissipation, for a given k, due to compressional effect at high frequency with $(\eta_2)_{max} = (\omega^2 - \gamma k^2)/\omega k^2$. In addition, the result indicates a considerable decrease of the non-dimensional bulk viscosity as the magnetic parameter E_m increases from 0 to 300. For a condition of shorter waves, i.e. $k = 50$, the bulk viscosity η_2 decreases approximately 50% with respect to its value as $E_m = 0$. The insert in Figure 7 makes clear that the rate of energy dissipation per unit of volume in the flow associated with the bulk viscosity, $\eta_2(\boldsymbol{\nabla} \cdot \boldsymbol{u})^2$, can be suppressed by controlling the intensity of the applied magnetic field (i.e. in non-dimensional terms, the physical parameter E_m). The non-dimensional bulk viscosity for a MHD compressible flow at high frequency, i.e. $\omega = 10^3$ and $k = 25$ may vary from 1.6 for $E_m = 0$ to approximately 0.9 for $E_m = 10^3$. For shorter waves the value of η_2 could still go to zero, depending on the intensity of the applied magnetic field.

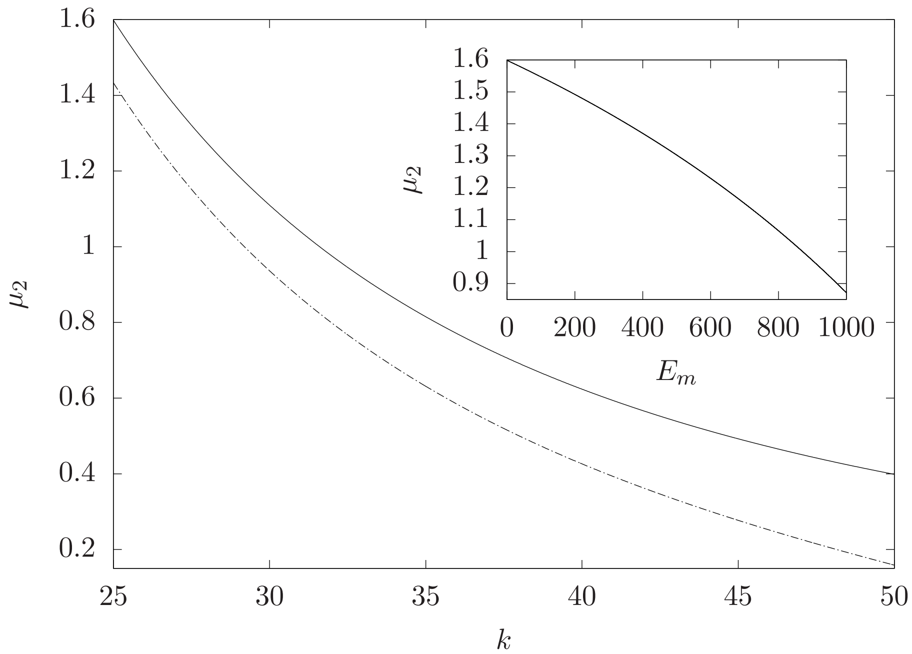

Figure 7 – Non-dimensional bulk viscosity η_2 as a function of the wavenumber k for two different values of the magnetic parameter E_m and $\gamma = 1.4$, $\omega = 10^3$ and $\alpha = \pi/4$. From top to bottom in the plot the values of E_m for the curves are: 0 and 300, respectively. For $E_m = 0$, the non-dimensional expansion viscosity has the maximum values for a given k; $(\mu_k)_{max} = (\omega^2 - \gamma k^2)/\omega k^2$. The insert depicts the η_2 decay as E_m increase for $k = 25$. The appreciable difference of the attenuation of the energy dissipation by controlling the intensity of magnetic field E_m can be clearly observed.

Figure 8 shows the bulk viscosity η_2 as a function of the wavenumber k for various values of the magnetic field orientation α with respect to direction of the wave propagation (or flow). Interestingly, an increase of the field orientation from 0 to $\pi/2$ also results in an appreciable decrease of the bulk viscosity. Clearly, the field orientation for a given wavenumber has a major effect on the bulk viscosity as $\alpha = \pi/2$, i.e. as the field is orientated crosswise the direction of wave propagation. In addition, the insert of the same plot shows a typical decrease of the bulk viscosity with field orientation α for $k = 25$,

$\omega = 10^3$ and $E_m = 300$. We can also see that there is inflection point in the bulk viscosity function at $\alpha = \pi/4$. Below the inflection point the bulk viscosity continues decreasing with the field orientation and its value saturates to $\eta_2 = 1.3$ for $\alpha = \pi/2$, corresponding to its minimum value. Under the given conditions, the effect of the bulk viscosity on the flow could be clearly attenuated by around 20% just varying the orientation of the magnetic field α from 0 to $\pi/2$.

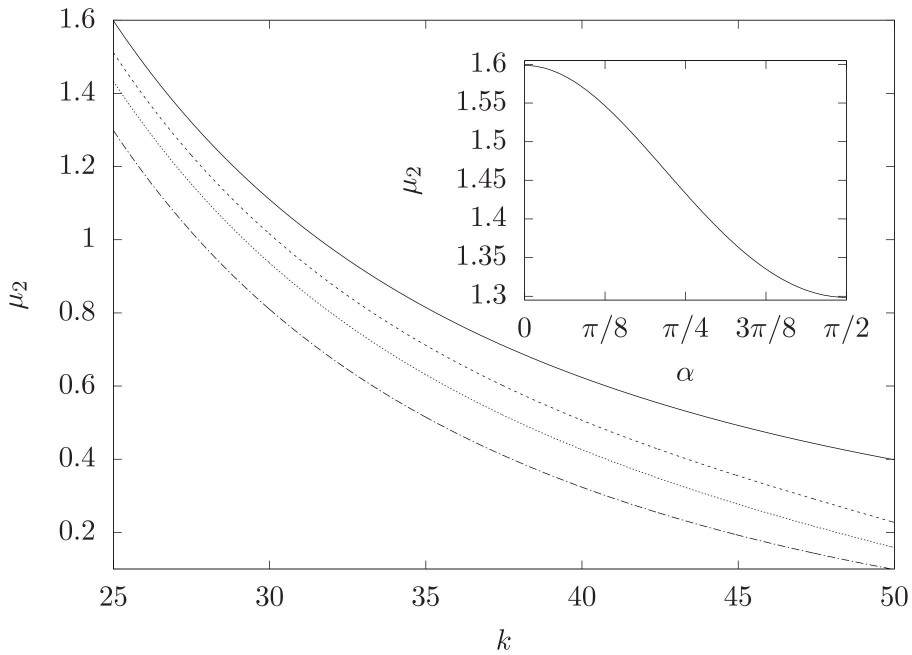

Figure 8 – Non-dimensional bulk viscosity η_2 as a function of the wavenumber k for two different values of the magnetic field orientation α. From top to bottom of the curves in the plot $\alpha = 0$, $\pi/6$, $\pi/4$ and $\pi/2$, respectively. In this plot, $\gamma = 1.4$, $\omega = 10^3$ and $E_m = 300$. The insert in the plot shows η_2 versus α for $k = 25$.

3.7.1 Wave phase velocity

At this point it is important to examine how the wave phase velocity of the magneticacoustic waves is influenced by the bulk viscosity alone. For this end, we have calculated numerically the four roots of s in the dispersion relation of magnetoacoustic wave given in Equation (3.48). Figure 9 depicts the non-dimensional wave phase velocity ω/k for fast waves (first root) as a function of the non-dimensional bulk viscosity η_2 for four different wavenumbers: $k = 25$, 50, 75 and 100, respectively. The others parameters used in the plot were $\gamma = 1.4$, $\omega = 10^3$, $E_m = 300$ and $\alpha = \pi/4$. The second root corresponding to slow magnetoacoustic waves is shown as an insert of the main plot. The other two roots give just the phase velocity of two waves propagating in the opposite direction of the one explored here, as discussed by Bittencourt (2004).

Figure 9 shows that the non-dimensional phase velocity of the fast waves decreases monotonically rapid as the bulk viscosity increases and this behavior is observed at all wavenumbers examined. However, ω/k reaches a saturation for large values of the bulk viscosity (e.g. $\eta_2 = 10$). It is interesting to note that for large values of the bulk viscosity the dispersion relation of magnetoacoustic waves described by Equation (3.48) tends to the relation of the Alfvén, the non-dispersive magnetic waves given by Equation (3.47). In this asymptotic limit of the bulk viscosity the root corresponding to fast waves is $\omega/k = \cos\alpha\sqrt{E_m}$. As expected this relation is completely independent of the bulk viscosity since these waves behaves like incompressible ones, but the intensity of the magnetic field and its orientation with respect the direction of the wave propagation still affects the propagation speed of the wave in a context of electrically conducting fluids. We also conjecture that for large values of bulk viscosity a typical time scale of the dissipation mechanism by η_2 is $\tau_0 \sim (\rho_0\ell^2)/\mu_2^0 \ll \lambda_0/c_0$, where λ_0 is a characteristic wavelength and c_o the wave speed velocity. Therefore, under this limit condition the wave does not responds to changes in the flow bulk viscosity. On the other hand, for moderate and finite values of η_2, the results presented in Figure 9 indicates that the bulk viscosity may exert a strong influence on the propagation velocity of magnetoacoustic waves. Since magnetoacoustic disturbances are in general compressible dispersive waves, compressional effects at high frequency in the flow may change drastically the wave propagation in an electrically conducting gas. Additionally, the insert of Figure 5 shows a similar behavior for the second root of Equation (3.48) in terms of ω/k versus η_2. We can see, however, that in the case of slow magnetoacoustic waves, large values of η_2 completely dissipate the motion of these second type of waves (i.e. ω/k goes to zero) for all wavenumbers. In addition, results shown in Figure 5 also corroborates that long waves propagate faster than short waves for a given finite and moderate value of the bulk viscosity. As a complementary result, Figure 10 shows a plot of ω/k versus the magnetic Euler number E_m for different values of the wavenumbers. Clearly, the applied field has a major effect on the phase velocity of magnetoacoustic waves. Longer waves propagates with higher phase velocities and an increase in the magnetic parameter substantially enhances the wave velocity. It is also interesting to note that the growth rate of ω/k is different depending on the wavelength. As can be seen, longer waves have a higher growth rate with E_m as compared to shorter waves.

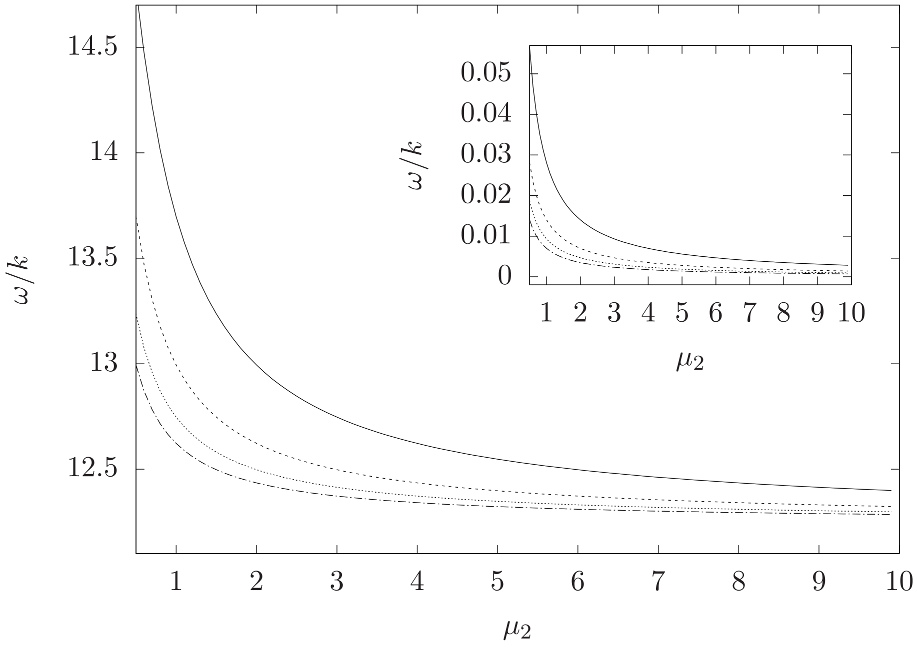

Figure 9 – Non-dimensional phase velocity for fast magnetoacoustic waves as a function of the bulk viscosity for different wavenumbers. From top to bottom the lines in the plot represent $k = 25$, 50, 75 and 100, respectively. The physical parameters used in this plot are: $\alpha = 1.4$, $E_m = 300$, and $\alpha = \pi/4$. The nondispersive asymptotic limit of ω/k for large values of η_2 is exactly predicted by Equation (3.47) as being $\omega/k = \cos\alpha\sqrt{E_m}$. The supplementary result of ω/k versus η_2 for slow magnetoacoustic waves is presented in the insert of the plot.

3.7.2 Final Remark

A interesting result of the study presented here was to find that a reduction of the energy dissipation rate associated with the bulk viscosity can be controlled by the intensity of an applied magnetic in a MHD flow. This finding may lead to a drag reduction in compressible flows of electrically conduction gases, since the mechanical energy dissipation per unit of mass, $\eta_2(\boldsymbol{\nabla}\cdot\boldsymbol{u})^2/\rho$, can be considerably attenuated by action of an applied magnetic field. For instance, while $\eta_2 \approx 0.4$ for $k = 50$ and $E_m = 0$, $\mu_k \approx 0.25$ at the same k for $E_m = 100$. This corresponds to a decrease of approximately 38% in the flow dissipation associated with the high frequency expansion of the fluid. Another interesting finding was to have established, even in a study of small amplitudes waves, a closure expression which could be used to evaluate the bulk viscosity in terms of the applied magnetic field parameter (E_m), the wave quantities (k and ω) and fluid properties. We expect that this model can be useful for estimating the bulk viscosity by experiments

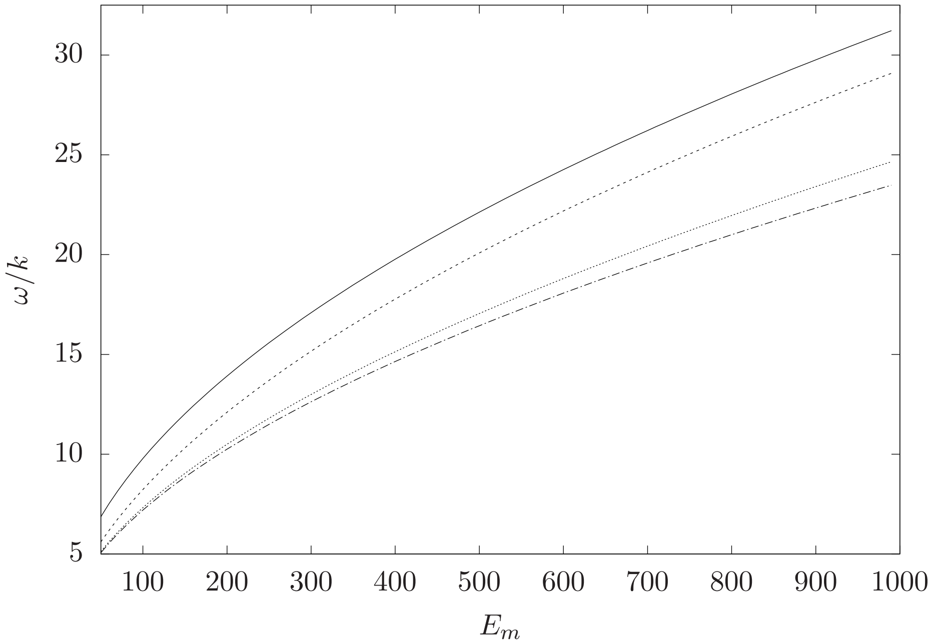

Figure 10 – Non-dimensional phase velocity for fast magnetoacoustic waves as a function of magnetic Euler number E_m for different wavenumbers. From top to bottom the lines in the plot represent $k = 25$, 50, 75 and 100, respectively. The physical parameters used in this plot are: $\alpha = 1.4$, $\eta_2 = 1$, and $\alpha = \pi/4$. The limit of $E_m = 0$ corresponds to the high frequency acoustic waves in a non-Stokesian Newtonian gas (i.e., with bulk viscosity) in the absence of magnetic effects.

involving flows of conducting gases in which typical frequencies and the wavenumbers of magnetoacoustic waves can be measured in laboratory scale.

The study presented in this chapter provide insights into the role of a bulk viscosity in the propagation of magnetoacoustic waves, which was a significant step forward in understanding how to control the phase velocity of magnetic waves and the rate of mechanical dissipation in compressible flows at high frequency by controlling field intensity and orientation. This study was even submitted to the journal Physics of Fluids and we are now in process of preparation of the revised version (CUNHA; INÁCIO, 2024). Currently, we have no experimental results with which to compare our predictions. In this way, we suggest an experimental investigation in laboratory scale involving measurements of magnetoacoustic parameters such as the wavelength and frequency in compressible MHD flow at high frequency, where the bulk viscosity become an important quantity of the flow. A next step could also be to extent our studies to explore bubble dynamics phenomenon in the presence of a bulk viscosity and a magnetic field effects on the high frequency radial oscillations of a spherical gas bubble in a liquid.

4 SHEAR INDUCED DISPERSION ON MHD FLOWS

4.1 Incompressible MHD Flow in a Channel

In this section, we construct the solution for the unidirectional flow of an incompressible electrically conducting fluid in a channel with an external longitudinal magnetic field applied. The construction includes the induction of a magnetic field in the flow direction. The solution to this problem is needed because it will serve as non-perturbed solution in further analysis of the shear induced dispersion phenomenon.

4.1.1 Governing Equations

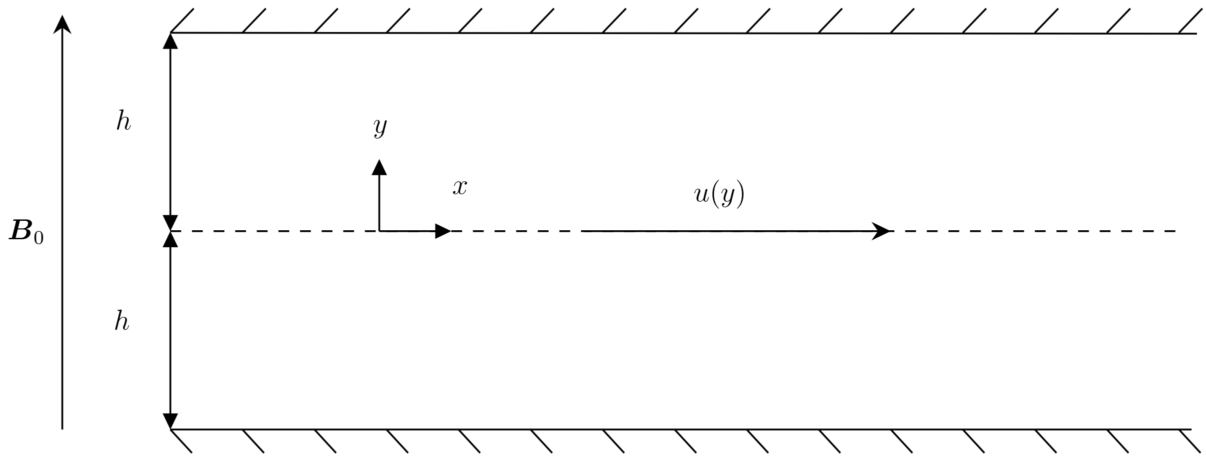

Figure 11 – Scheme for the MHD flow in channel.

The unidirectional flow between parallel plates with an external magnetic field is described by Figure 11. We observe that gravity exert only static effect on the flow, so that it can be added to the pressure, generating an modified pressure given by $p = p^* - \rho \boldsymbol{g} \cdot \boldsymbol{x}$.

In this flow, we can write the total magnetic field as a sum of a external field contribution with a induced field contribution, so that

$$\boldsymbol{B} = B_x(y)\hat{\boldsymbol{e}}_{\boldsymbol{x}} + B_0\hat{\boldsymbol{e}}_{\boldsymbol{y}}, \tag{4.1}$$

where $\boldsymbol{B}_x = B_x(y)\hat{\boldsymbol{e}}_{\boldsymbol{x}}$ is the induced magnetic field in the direction of the flow. This form of the induced field is obtained using the unidirectional flow condition in the induction equation. On the other hand, from Faraday's law for permanent permanent regime,

$$\nabla \times \boldsymbol{E} = \boldsymbol{0}. \tag{4.2}$$

Hence, $E_z = E_0$ is a constant. Then, as the z-component of current density is given by Ohm's law,

$$J_z = \sigma_e \left(E_0 + uB_0\right), \tag{4.3}$$

we have that Lorentz law gives that

$$\boldsymbol{f}_L = \boldsymbol{J} \times \boldsymbol{B} = \sigma_e \left(E_0 + uB_0\right)\left(-B_0\hat{\boldsymbol{e}}_{\boldsymbol{x}} + B_x\hat{\boldsymbol{e}}_{\boldsymbol{y}}\right). \tag{4.4}$$

Using Lorentz force, given by Equation (4.4), in modified Navier-Stokes Equation (2.129), we find that

$$G + \eta\frac{d^2u}{dy^2} - \sigma_e E_0 B_0 - \sigma_e u B_0^2 = 0, \tag{4.5}$$

$$-\frac{\partial p}{\partial y} + \sigma_e B_x \left(E_0 + B_0 u\right) = 0, \tag{4.6}$$

where $G = -\frac{\partial p}{\partial x}$. Equations (4.5) and (4.6) are the differential equations that determine the velocity field and the pressure field, respectively.

From the transport equation for the magnetic field for a incompressible fluid, Equation (2.131), we have that

$$B_0\frac{du}{dy} + \nu_m\frac{d^2B_x}{dy^2} = 0. \tag{4.7}$$

Equation (4.7) is the differential equation that determines the induced magnetic field.

4.1.2 Non-dimensional Governing Equations

Consider the following set of definitions of non-dimensional variables:

$$u^* = \frac{u}{U}, \quad y^* = \frac{y}{h}, \quad p^* = \frac{ph}{\eta U}, \quad B_x^* = \frac{B_x}{B_0} \quad \text{e} \quad E_0^* = \frac{E_0}{UB_0}. \tag{4.8}$$

where U is the mean velocity. Then, the governing differential equations of the problem, Equations (4.5), (4.6) and (4.7), becomes

$$G^* + \frac{d^2u^*}{dy^{*2}} - Ha^2 E_0^* - Ha^2 u^* = 0, \tag{4.9}$$

$$-\frac{\partial p^*}{\partial y^*} + Ha^2 B_x^* \left(E_0^* + u^*\right) = 0, \tag{4.10}$$

$$\frac{d^2 B_x^*}{dy^{*2}} + Re_m \frac{du^*}{dy^*} = 0. \tag{4.11}$$

Here, Ha represents the Hartmann number, which gives the ratio between Lorentz and viscous forces. Till the end of the solution for MHD flow between parallel plates, the notation of non-dimensional variables, *, will be suppressed to ease the notation.

4.1.3 Velocity Field

The non-dimensional velocity field is determined by Equation (4.9), which is an ordinary differential equation whose solution is given by a sum of the homogeneous solution with the particular solution. Hence, the general solution to u is given by

$$u = \frac{G}{Ha^2} - E_0 + C_1 \sinh\left(Ha y\right) + C_2 \cosh\left(Ha y\right), \tag{4.12}$$

where C_1 and C_2 are constants. Applying the no-slip boundary condition in the walls, these constants are determined as

$$C_1 = 0 \tag{4.13}$$

$$C_2 = \frac{E_0 - Ha^{-2} G}{\cosh\left(Ha\right)}. \tag{4.14}$$

Therefore, the velocity profile is given by

$$u(y) = \left(\frac{G}{Ha^2} - E_0\right)\left[1 - \frac{\cosh\left(Ha y\right)}{\cosh\left(Ha\right)}\right]. \tag{4.15}$$

4.1.4 Magnetic Field

The non-dimensional magnetic field is determined by Equation (4.11). Then, substituting the solution to the velocity field and integrating twice, we obtain that

$$B_x(y) = -Re_m \left(\frac{G}{Ha^2} - E_0\right)\left[y - \frac{\sinh\left(Ha\, y\right)}{Ha \cosh\left(Ha\right)}\right] + C_3 y + C_4, \tag{4.16}$$

where C_3 and C_4 are integration constants. In this case without magnetization, the magnetic boundary condition gives $B_x(y = \pm 1) = 0$, so that

$$C_3 = Re_m \left(\frac{G}{Ha^2} - E_0 \right) \left[1 - \frac{\sinh(Ha)}{Ha \cosh(Ha)} \right] \tag{4.17}$$

$$C_4 = 0. \tag{4.18}$$

Therefore, the induced magnetic field can be obtained as

$$B_x(y) = \frac{Re_m}{Ha \cosh(Ha)} \left(\frac{G}{Ha^2} - E_0 \right) \left[\sinh(Ha\, y) - \sinh(Ha)\, y \right]. \tag{4.19}$$

4.1.5 Pressure Field

In the flow treated here, the pressure gradient is what generates the flow and is imposed, i.e.

$$\frac{\partial p}{\partial x} = -G, \tag{4.20}$$

such that

$$p(x, y) = -Gx + f(y), \tag{4.21}$$

where f is a function of y that arise from integration. Taking the partial derivative in the y-direction of Equation (4.21) we are left with

$$\frac{\partial p}{\partial y} = \frac{df(y)}{dy}. \tag{4.22}$$

Substituting Equation (4.10) we obtain a differential equation for $f(y)$, given by

$$\frac{df(y)}{dy} = Ha^2 B_x (E_0 + u). \tag{4.23}$$

Substituting the results for the velocity field and for the induced magnetic field and then integrating, we obtain the pressure field as

$$\begin{aligned} p(x, y) = -Gx + p_0 + \frac{Re_m}{\cosh(Ha)} \left(\frac{G}{Ha^2} - E_0 \right) \Bigg\{ \left(\frac{G}{Ha^2} - E_0 \right) \Bigg[\frac{1 - \cosh^2(Ha\, y)}{2 \cosh(Ha)} \\ + \tanh(Ha) \sinh(Ha\, y) y + \frac{\tanh(Ha)}{Ha} (1 - \cosh(Ha\, y)) \Bigg] \\ + \frac{G}{Ha^2} \left[\cosh(Ha\, y) - \frac{Ha}{2} \sinh(Ha) y^2 - 1 \right] \Bigg\}, \end{aligned} \tag{4.24}$$

where $p_0 = p(0, 0)$.

4.1.6 Flow Rate

The non-dimensional flow rate is given by

$$Q = \frac{1}{2}\int_{-1}^{1} u(y)dy. \tag{4.25}$$

The characteristic flow rate is given by $|Q| \sim 2Uh\ell$, where ℓ is the length of the channel in the z-direction. Therefore, using the velocity field given by Equation (4.15),

$$Q = \frac{1}{2}\int_{-1}^{1}\left(\frac{G}{Ha^2} - E_0\right)\left[1 - \frac{\cosh(Hay)}{\cosh(Ha)}\right]dy. \tag{4.26}$$

Integrating we obtain that

$$Q = \left(\frac{G}{Ha^2} - E_0\right)\left[1 - \frac{\tanh(Ha)}{Ha}\right]. \tag{4.27}$$

We note that, by definition, this non-dimensional flow rate must equals 1, as the characteristic velocity is the mean velocity U.

4.1.7 Equation for the Non-dimensional Electric Field

The non-dimensional electric field present in the problem, E_0, is coupled to the magnetic field by the nature of Maxwell's equations. Even through we do not apply an external electric field, generally E_0 exists and, in this case, is the induced electric field. Then, B_x, E_0 and u are tied together. Indeed, applying an external electric field, the flow would be modified and, by consequence, the magnetic field too, so that E_0 and B_x can not be established independently. This fact is mathematically traduced using Ohm's law, Equation (2.106), in conjunction with the Ampère's law, Equation (2.119), giving that

$$\boldsymbol{E} = \frac{1}{Re_m}\nabla \times \boldsymbol{B} - \boldsymbol{u} \times \boldsymbol{B}, \tag{4.28}$$

Note that this equation is already in the non-dimensional form. Substituting the expressions obtained for the MHD parallel plates problem,

$$E_0 = \frac{1}{Re_m}\frac{dB_x}{dy} - u. \tag{4.29}$$

As E_0 is constant, it can be determined evaluating Equation (4.29) in the walls of the channel, so that we eliminate the velocity profile from the equation by the no-slip condition. Then,

$$E_0 = \frac{1}{Re_m} \frac{dB_x}{dy}\bigg|_{y=\pm 1}. \tag{4.30}$$

Therefore, substituting the expression obtained for the magnetic field,

$$E_0 = -\frac{G}{Ha^2}\left[\frac{Ha}{\tanh(Ha)} - 1\right]. \tag{4.31}$$

4.1.8 Complete Solution

Using the non-dimensional form of the electric field, given by Equation (4.31), in the Equations for the velocity field, for the magnetic field and for the pressure, we respectively obtain

$$u = \frac{G}{Ha \tanh(Ha)}\left[1 - \frac{\cosh(Ha\, y)}{\cosh(Ha)}\right], \tag{4.32}$$

$$B_x = \frac{Re_m}{Ha^2}\frac{G}{\sinh(Ha)}\left[\sinh(Ha\, y) - \sinh(Ha) y\right], \tag{4.33}$$

$$p = p_0 - Gx + \frac{Re_m}{Ha^2}G^2\left[-\frac{y^2}{2} + \frac{\sinh(Ha\, y)}{\sinh(Ha)}y - \frac{1}{2}\frac{\sinh^2(Ha\, y)}{\sinh^2(Ha)}\right]. \tag{4.34}$$

We note that as the non-dimensional flow rate was defined in the way that $Q = 1$, G can not be arbitrary and must be coupled to the rest of the problem, so that this constraint for Q is satisfied. Thus, using the equation for E_0, Equation (4.31), in the expression for the flow rate, Equation (4.27), we obtain that G must be determined by

$$G = \frac{Ha}{\left[\coth(Ha) - Ha^{-1}\right]}. \tag{4.35}$$

We note that in this case the flow is intrinsically coupled to the magnetic quantities.

4.1.9 Effective Viscosity

Although the fluid is electrically conductor, the dimensional flow rate for the case of non-conducting fluid flowing between two parallel plates can be used to defined the effective viscosity, letting

$$Q^* = \frac{2G^* h^3 \ell}{3}\frac{1}{\eta_{ef}}, \tag{4.36}$$

where Q^* and G^* represents the dimensional flow rate and pressure gradient (only till the end of this solution) and η_{ef} represents the effective viscosity. By definition, this effective viscosity represents the viscosity that a non-conducting fluid must have to have the same relation between the flow rate and the pressure gradient that the conducting fluid to a fixed Hartmann number. This way, the effective viscosity must depend on the Hartmann number Ha. From the flow rate of the electrically conducting fluid,

$$Q^* = \frac{2G^* h^3 \ell}{3} \left\{ \frac{3}{\eta Ha} \left[\frac{1}{\tanh(Ha)} - \frac{1}{Ha} \right] \right\}, \tag{4.37}$$

so that, by direct comparison, the effective viscosity non-dimensionalized by the viscosity of the conducting fluid is given by

$$\frac{\eta_{ef}}{\eta} = \frac{Ha}{3\left[\coth(Ha) - Ha^{-1}\right]}. \tag{4.38}$$

4.1.10 Results

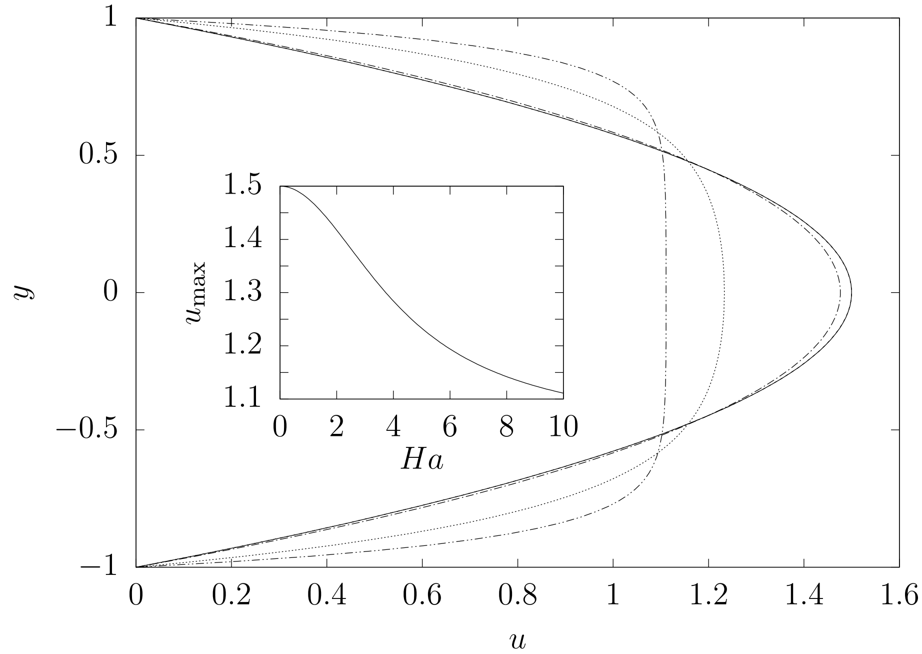

Figure 12 – Non-dimensional velocity profiles of the incompressible MHD flow between parallel plates for different Hartman numbers. In this Figure, ——— represents $Ha = 0$, - - - - - - $Ha = 0.1$, -·-·-·- $Ha = 1$, ·········· $Ha = 5$, -··-··- $Ha = 10$. *Inset*: Maximum velocity as a function of the Hartmann number.

Figures 12, 13 and 14 present graphically the results for the velocity profiles, the induced magnetic fields and for the effective viscosity respectively. From these figures, it is clear that increasing the effects of the external magnetic field (raising Hartmann number) causes a damping of the flow. This damping effect is also observed on the effective viscosity, as raising Hartmann number raises the effective viscosity. The damping effect that Lorentz force causes in the flow is well-known and have several applications in engineering. For example, NASA[1] already used this magnetic damping to brake rockets in the atmosphere entrance (CUNHA, 2021b). This kind of effect is also used in metallurgical industry to damp the motion of liquid metals, which is needed in several applications (DAVIDSON, 1999). Although the external magnetic field just brakes the flow, we note that, as a

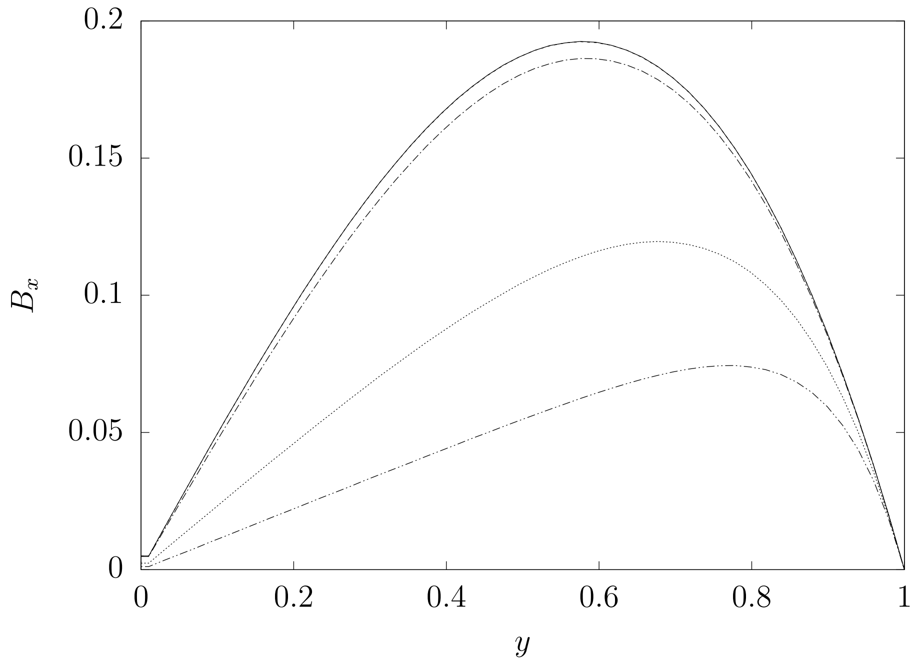

Figure 13 – Induced magnetic fields for the incompressible MHD flow between parallel plates with different Hartmann numbers and $Re_m = 1$. In this Figure ——— represents $Ha = 0.1$, - - - - - - $Ha = 1$, - · - · - · $Ha = 5$, ·············· $Ha = 10$.

consequence of the coupling between the velocity field, the magnetic field and the electric field, the existence of a flow with a magnetic field induces a electric field. This is a hint that one can generate a flow using an external electric field in a electrically conducting fluid, characterizing a MHD pump (MULLER; BUHLER, 2001). Indeed, the MHD pumping is a known effect vastly applied in specific cases in the industry (DAVIDSON, 1999).

4.2 Transport Equation for the Concentration of Particles

Let $\phi(\boldsymbol{x}, t)$ be a local volumetric concentration of particles scalar field, $\boldsymbol{N}$ the local flux vector field or current of this concentration, V an arbitrary volume on the continuum and S the surface of V. Hence, as the time variation of the quantity of particles in V must

[1] National Aeronautics and Space Administration

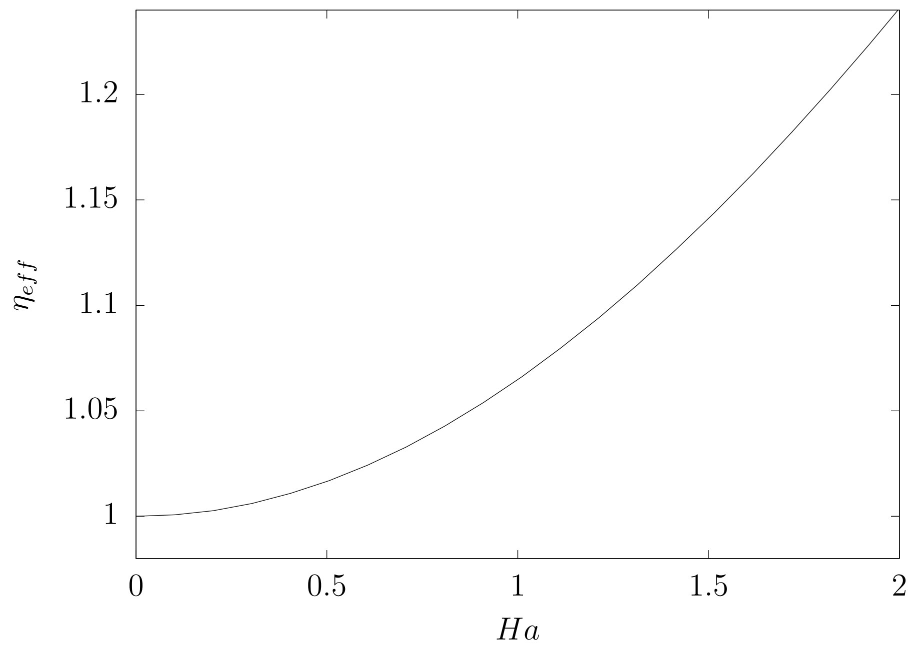

Figure 14 – Effective viscosity as a function of the Hartmann number for the incompressible MHD flow between parallel plates.

equals the flux of this quantity entering V through its boundary S, we have that

$$\frac{d}{dt}\int_V \phi dV = -\int_S \boldsymbol{N}\cdot\hat{\boldsymbol{n}} dS. \tag{4.39}$$

Using divergence theorem (ARIS, 1989) and Reynolds transport theorem, given by Equation (2.21), it follows that

$$\int_V \left[\frac{\partial \phi}{\partial t} + \boldsymbol{\nabla}\cdot(\boldsymbol{u}\phi) + \boldsymbol{\nabla}\cdot\boldsymbol{N}\right] dV = 0. \tag{4.40}$$

Finally, using the localization theorem, Equation (4.40) reduces to

$$\frac{\partial \phi}{\partial t} + \boldsymbol{\nabla}\cdot(\boldsymbol{u}\phi) = -\boldsymbol{\nabla}\cdot\boldsymbol{N} \tag{4.41}$$

Equation (4.41) is the general diffusion equation and can be used to model the transport of concentration of particles. In the special case of an incompressible fluid, it reduces to

$$\frac{D\phi}{Dt} = -\boldsymbol{\nabla}\cdot\boldsymbol{N} \tag{4.42}$$

or

$$\frac{\partial \phi}{\partial t} + \boldsymbol{u}\cdot\boldsymbol{\nabla}\phi = -\boldsymbol{\nabla}\cdot\boldsymbol{N}. \tag{4.43}$$

It is worthwhile to note that continuity equation is a special case of the last equation. If we take the volumetric mass concentration, i.e. the mass density, we have no net mass flux and Equation (4.41) would be simply the mass continuity equation. Also, much of the fluxes are Fickian, meaning that we can write a linear relation between $\boldsymbol{N}$ and the gradient of ϕ.

4.3 Shear-Induced Dispersion

In a suspension, we expect a dispersion of particles to occur. This dispersion is, generally, composed of different diffusions, each coming from a different underlying mechanism. In the rest of this section, we discuss these diffusions and the associated mechanisms.

The first is the bulk effect of Brownian motion. Depending on the size of the particles in a suspension, the molecules of the fluid medium hitting these particle can generate a *random walk* in the particles, characterizing the Brownian motion. In macroscopic analysis, the bulk effect of this *random walk* can generate a flux of particles. The second order tensor associated with this self-diffusivity of a single particle is called self-diffusivity tensor $\boldsymbol{\mathcal{D}}_s$. Its important to note that this kind of diffusion is independent of particle interactions.

The second mechanism is the shear induced or hydrodynamic dispersion. Consider two particles colliding in a suspension, if these particles are in creeping flow, are perfectly smooth and spherical and have no magnetic moment, the trajectories should be reversible, i.e. after the interaction the particles should get back to the original streamline it was. On the other hand, some mechanisms can break the reversibility of these interactions, like surface roughness of the particles, deformation of the particles, geometry of the particles and magnetic force interactions. When this reversibility is broken, the particles deviate from its original streamline after collisions, generating a bulk effect viewed as a dispersion of the particles (DAVIS, 1996). As the collisions are introduced by the shear, this effect is called shear induced dispersion, as cited before.

4.4 Fick's Law and the Down-Gradient Diffusivity

In general, diffusion arise macroscopically from a microscopic random process. Due to the randomness of the process, a net flux characterizing this diffusion must be from regions of higher concentration to regions of lower concentrations, the way the flux have a linear relation with the gradient of concentration. Therefore, a general expression for this flux is given by

$$\boldsymbol{N}_c = \boldsymbol{\mathcal{D}}_c \cdot \boldsymbol{\nabla}\phi, \tag{4.44}$$

where $\boldsymbol{\mathcal{D}}_c$ is the down-gradient diffusivity tensor. Equation (4.44) is known as Fick's law. We note that, when there is no irreversible particle-particle interactions, the down-gradient diffusion is just the self-diffusion. On the other hand, when irreversible interactions takes place, a flux contribution must enter the relation. For a monodisperse dilute suspension of non-Brownian rigid rough particles under shear flows, Cunha and Hinch (1996) showed through theoretical calculations a exact relation between the diffusivity tensors discussed, this is given by

$$\boldsymbol{\mathcal{D}}_c = 2\boldsymbol{\mathcal{D}}_s + \boldsymbol{\mathcal{D}}_f, \tag{4.45}$$

where $\boldsymbol{\mathcal{D}}_f$ is a flux contribution. Cunha and Hinch (1996) also show that $\mathcal{D}_c$ have order of magnitude of $10\mathcal{D}_s$.

Besides these ordinary fluxes[2] described, a gradient of shear and also a gradient of viscosity should generate a diffusion, as higher shear rates induces more collisions of particles and higher viscosity should also influence the dispersion. Indeed, in the next sections a model to these fluxes will be deduced, in which this flux proportional to $\boldsymbol{\nabla}\dot{\gamma}$ will appear naturally in the construction. Here $\dot{\gamma}$ represents the shear rate. The diffusion due to gradient of shear rate is named hydrodynamic migration and the associated flux is named particle migration.

4.5 Equation for the Shear-Induced Particle Flux

Phillips et al. (1992) were the first to construct a constitutive relation for the shear-induced particle flux, basing their work on the previous experimental work of Leighton and Acrivos (1987b). Therefore, throughout this work, we will follow closely this constitutive model. It is important to note that shear-induced dispersion is highly anisotropic. Thus, the model that will be deduced here with isotropic diffusivities can only be used properly in unidirectional flows.

Consider a dilute mono-dispersed suspension, so that only two-particles interactions can arise. As the higher shear rate and higher concentrations imply more collisions, the collision frequency of a particle scales with $\dot{\gamma}\phi$. On the other hand, each collision im-

[2] Ordinary in the sense that they are linearly related to the gradient of concentration.

plies a displacement of the particle $\mathcal{O}(a_p)$, where a_p is the radius of the particle, thus the particle's migration velocity scales with $a_p\dot{\gamma}\phi$. In this sense, the gradient of the migration velocity should induce a net flux of particles, as adjacent layers of fluid with different migration velocity should push a different number of particle to each other, which characterizes a net flux. Therefore,

$$\boldsymbol{N}_c \propto \phi\boldsymbol{\nabla}(a_p\dot{\gamma}\phi), \tag{4.46}$$

where no self-diffusivity of a single particle alone is taken into account. The shear-induced dispersion is quite anisotropic, but as we will only work in unidirectional flows, the proportion relation given by Equation (4.46) can be substituted by a equality simply by a scalar diffusivity. Hence,

$$\boldsymbol{N}_c = -K_c a_p^2 \phi\boldsymbol{\nabla}(\dot{\gamma}\phi), \tag{4.47}$$

where an extra a_p is added via the proportion coefficient to make K_c have dimension of diffusivity. Equation (4.47) can be rewritten as

$$\boldsymbol{N}_c = -K_c a_p^2 \left(\phi^2\boldsymbol{\nabla}\dot{\gamma} + \dot{\gamma}\phi\boldsymbol{\nabla}\phi\right), \tag{4.48}$$

where the first term on the right hand side represents hydrodynamic migration (flux from regions of higher shear rate to regions of lower shear rate) and the second term represents hydrodynamic dispersion (flux from regions of higher concentrations to regions of lower concentrations). It is important to note that both fluxes have the same diffusion coefficient because they both have the same underlying mechanism. On the other hand, a gradient of viscosity should also generate a flux, as this gradient produces a change in the particle pairs center of rotation and, by consequence, a displacement. This flux should depend on the concentration ϕ, on the frequency of collision $\dot{\gamma}\phi$ and on the relative spacial variation of the viscosity. Thus,

$$\boldsymbol{N}_\eta = -K_\eta a_p^2 \dot{\gamma}\phi^2 \frac{\boldsymbol{\nabla}\eta}{\eta}, \tag{4.49}$$

where K_η is a diffusivity associated with the gradient of viscosity mechanism. Equation (4.49) can also be written as

$$\boldsymbol{N}_\eta = -K_\eta a_p^2 \dot{\gamma}\phi^2 \frac{1}{\eta}\frac{d\eta}{d\phi}\boldsymbol{\nabla}\phi, \tag{4.50}$$

as η can be written, in general, as a function of the concentration of particles.

We must also include a Brownian flux, as it is the mechanism that balances the hydrodynamic dispersion. Indeed, the shear tends to disperse the particles to regions of lower shear rate, while the Brownian motion tends to randomize the suspension, homogenizing the suspension. Using a homogeneous and isotropic diffusivity tensor, the diffusivity for the Brownian motion is simply the translational Brownian diffusivity, given by (GRAHAM, 2018)

$$D_t = \frac{kT}{6\pi\eta_0 a_p}. \tag{4.51}$$

Therefore, the flux associated with the Brownian motion is

$$\boldsymbol{N}_b = -\frac{kT}{6\pi\eta_0 a}\boldsymbol{\nabla}\phi. \tag{4.52}$$

Here k is the Boltzmann constant, T is the temperature of the base liquid of the suspension and η_0 is the viscosity of the base liquid.

Finally, using the fluxes given by Equations (4.48) and (4.50) in the diffusion Equation for a incompressible suspension, Equation (4.42), we obtain that

$$\begin{aligned}\frac{D\phi}{Dt} &= -\boldsymbol{\nabla}\cdot(\boldsymbol{N}_b + \boldsymbol{N}_c + \boldsymbol{N}_\eta)\\ &= \boldsymbol{\nabla}\cdot\left[\frac{kT}{6\pi\eta_0 a}\boldsymbol{\nabla}\phi + K_c a_p^2\left(\phi^2\boldsymbol{\nabla}\dot{\gamma} + \dot{\gamma}\phi\boldsymbol{\nabla}\phi\right) + K_\eta a_p^2\dot{\gamma}\phi^2\frac{1}{\eta}\frac{d\eta}{d\phi}\boldsymbol{\nabla}\phi\right].\end{aligned} \tag{4.53}$$

Equation (4.53) is a closure equation to the problem of a suspension in which hydrodynamic dispersion and Brownian flux are present.

4.6 MHD Flow in Channel with Shear-Induced Dispersion

In this section, we will model the problem of the incompressible MHD flow of a monodisperse suspension of spherical particles in a channel (flow between parallel plates). We will also construct solutions to this flow and discuss these solutions.

4.6.1 Formulating the Problem

Consider the permanent incompressible flow of an electrically conductive suspension in a channel under the action of a external magnetic field. This problem is analogous to the ordinary MHD channel flow, but in the presence of particles in the fluid and diffusion of them. The flow is unidirectional in x-direction, i.e. $\boldsymbol{u} = u\hat{\boldsymbol{e}}_x$, and the external magnetic field is constant in the y-direction.

The movement equation is just Cauchy equation simplified to this case, i.e.

$$\boldsymbol{\nabla} \cdot \boldsymbol{\tau} + \boldsymbol{J} \times \boldsymbol{B} = \boldsymbol{\nabla} p, \tag{4.54}$$

where $\boldsymbol{\tau} = 2\eta(\phi)\boldsymbol{D}$ is the shear stress tensor. We note that we can not use directly Navier-Stokes Equation (2.56) because now η is not a constant, as assumed before. Calculating $\boldsymbol{\nabla} \cdot \boldsymbol{\tau}$ we obtain that

$$\boldsymbol{\nabla} \cdot \boldsymbol{\tau} = \left(\frac{d\eta}{d\phi} \frac{d\phi}{dy} \frac{du}{dy} + \eta \frac{d^2 u}{dy^2} \right) \hat{\boldsymbol{e}}_x. \tag{4.55}$$

On the other hand, the magnetic field is given by $\boldsymbol{B} = B_x(y)\hat{\boldsymbol{e}}_x + B_0\hat{\boldsymbol{e}}_y$, where $B_x\hat{\boldsymbol{e}}_x$ is the induced field in flow's direction and $B_0\hat{\boldsymbol{e}}_y$ is the external constant magnetic field. The Lorentz force $\boldsymbol{J} \times \boldsymbol{B}$ is the same obtained in the ordinary MHD channel flow. Therefore, the two components of the movement equation are

$$-\sigma_e B_0 \left(E_0 + uB_0\right) + \eta \frac{d^2 u}{dy^2} + G + \frac{d\eta}{d\phi} \frac{d\phi}{dy} \frac{du}{dy} = 0, \tag{4.56}$$

$$\sigma_e B_x(E_0 + uB_0) - \frac{\partial p}{\partial y} = 0, \tag{4.57}$$

where $G = -\partial p/\partial x$ is the pressure gradient in x-direction and $E_0 = \nu_m dB_x/dy - uB_0$. Since the transport equation does not change explicitly due to the diffusion of particles, just implicitly by $\boldsymbol{u}$, the transport of magnetic field equation is equal to the one deduced in the ordinary problem, it is given by

$$B_0 \frac{du}{dy} + \nu_m \frac{d^2 B_x}{dy^2} = 0. \tag{4.58}$$

Now, in the presence of hydrodynamic dispersion, Equations (4.56), (4.57) and (4.58) must be coupled to a diffusion equation to the concentration of particles, given by Equation (4.53). In the case of this permanent and unidirectional flow,

$$\frac{D\phi}{Dt} = 0, \tag{4.59}$$

so that $\boldsymbol{\nabla} \cdot \boldsymbol{N} = 0$. Thus, as the flow quantities only vary in y-direction and $\dot{\gamma} = du/dy$,

$$\frac{d}{dy} \left[\left(\frac{kT}{6\pi\eta_0 a_p^3} - K_c \frac{du}{dy}\phi - K_\eta \frac{\phi^2}{\eta} \frac{du}{dy} \frac{d\eta}{d\phi} \right) \frac{d\phi}{dy} - K_c \phi^2 \frac{d^2 u}{dy^2} \right] = 0. \tag{4.60}$$

4.6.2 Full Set of Governing Equations

Collecting Equations (4.56), (4.57), (4.58), (4.60) and the Equation for E_0 (an auxiliary equation), we obtain the following set of equations:

$$-\sigma_e B_0 \left(E_0 + uB_0\right) + \eta \frac{d^2u}{dy^2} + G + \frac{d\eta}{d\phi}\frac{d\phi}{dy}\frac{du}{dy} = 0, \tag{4.61}$$

$$\sigma_e B_x(E_0 + uB_0) - \frac{\partial p}{\partial y} = 0, \tag{4.62}$$

$$B_0 \frac{du}{dy} + \nu_m \frac{d^2 B_x}{dy^2} = 0, \tag{4.63}$$

$$\frac{d}{dy}\left[\left(\frac{kT}{6\pi\eta_0 a_p^3} - K_c \frac{du}{dy}\phi - K_\eta \frac{\phi^2}{\eta}\frac{du}{dy}\frac{d\eta}{d\phi}\right)\frac{d\phi}{dy} - K_c\phi^2 \frac{d^2u}{dy^2}\right] = 0, \tag{4.64}$$

$$\nu_m \frac{dB_x}{dy} - uB_0 = E_0. \tag{4.65}$$

This set of equations closes the problem in question. It is important to note that the continuity equation is already embedded in the fact that $u = u(y)$.

4.6.3 Boundary Conditions

The boundary conditions of the problem are, simply, the no-slip condition, given by

$$u(y = \pm h) = 0, \tag{4.66}$$

the condition that there is no flux through the walls of the channel, given by

$$\left(\frac{kT}{6\pi\eta_0 a_p^3} - K_c \frac{du}{dy}\phi - K_\eta \frac{\phi^2}{\eta}\frac{du}{dy}\frac{d\eta}{d\phi}\right)\frac{d\phi}{dy} - K_c\phi^2 \frac{d^2u}{dy^2} = 0, \quad y = \pm h, \tag{4.67}$$

and the condition that the induced magnetic field is equal to the external magnetic field on the walls, so that

$$B_x(y = \pm h) = 0. \tag{4.68}$$

The Equation (4.67) is just a consequence of $\boldsymbol{N} \cdot \hat{\boldsymbol{n}}$ being 0 on the walls of the channel. Also, if we have a imposed mean velocity or a imposed flow rate,

$$\int_A u dS = \overline{u} A, \tag{4.69}$$

can be used as a closure condition. Here A is the transversal area of the channel and $\overline{u}$ is the mean velocity. Finally, the mean value of the particle volume fraction distribution,

$\phi(y)$, must be equal the volume fraction on the a half of symmetry of the fluid, ϕ_0. Thus,

$$\overline{\phi} = \frac{1}{h}\int_0^h \phi dy = \phi_0, \tag{4.70}$$

where $\overline{\phi}$ is the mean value of ϕ.

4.6.4 Non-dimensional Set of Governing Equations and Boundary Conditions

Consider the the non-dimensional variables defined by

$$p^* = \frac{ph}{\eta_0 U}, \quad \eta^* = \frac{\eta}{\eta_0}, \quad y^* = \frac{y}{h}, \quad u^* = \frac{u}{U}, B_x^* = \frac{B_x}{B_0}, \quad E_0^* = \frac{E_0}{UB_0}. \tag{4.71}$$

Then, the set of governing equations can be written in the non-dimensional form in the following way:

$$-Ha^2\left(E_0 + u\right) + \eta\frac{d^2u}{dy^2} + G + \frac{d\eta}{d\phi}\frac{d\phi}{dy}\frac{du}{dy} = 0, \tag{4.72}$$

$$Ha^2 B_x(E_0 + u) - \frac{\partial p}{\partial y} = 0, \tag{4.73}$$

$$Re_m\frac{du}{dy} + \frac{d^2 B_x}{dy^2} = 0, \tag{4.74}$$

$$\frac{d}{dy}\left[\left(\frac{1}{Pe} - K_c\frac{du}{dy}\phi - K_\eta\frac{\phi^2}{\eta}\frac{du}{dy}\frac{d\eta}{d\phi}\right)\frac{d\phi}{dy} - K_c\phi^2\frac{d^2u}{dy^2}\right] = 0, \tag{4.75}$$

$$\frac{1}{Re_m}\frac{dB_x}{dy} - u = E_0. \tag{4.76}$$

Note that we dropped the * notation for the non-dimensional variables in the last set of equations. This was done to ease the notation and will carried throughout this chapter. Here $Pe = 6\pi\eta_0 a_p^3\dot{\gamma}_c/kT$ is Péclet number, which gives a ratio between the Brownian diffusion time and advection time, and $\dot{\gamma}_c$ is the characteristic shear rate. The set of boundary conditions can be rewritten in the non-dimensional form as

$$u(y = \pm 1) = 0 \tag{4.77}$$

$$\left(\frac{1}{Pe} - K_c\frac{du}{dy}\phi - K_\eta\frac{\phi^2}{\eta}\frac{du}{dy}\frac{d\eta}{d\phi}\right)\frac{d\phi}{dy} - K_c\phi^2\frac{d^2u}{dy^2} = 0, \quad y = \pm 1, \tag{4.78}$$

$$B_x(y = \pm 1) = 0, \tag{4.79}$$

$$\int_{-1}^{1} u dy = 1, \tag{4.80}$$

$$\int_0^1 \phi dy = \phi_0. \tag{4.81}$$

4.6.5 Regular Perturbation Analysis

In here we intend to work only with small effects of the hydrodynamic dispersion. Hence, to solve the problem for the shear induced dispersion in a channel containing an electrically conducting suspension, we use a regular perturbation analysis of the problem. To proceed to the solution, it also needed a few simplifications, they are:

- Viscosity gradient terms are neglected, since this effect is very small for dilute suspensions (SINZATO; CUNHA, 2020; SINZATO; CUNHA, 2021; CUNHA; SINZATO; PEREIRA, 2022);
- The velocity profile u is set to u_0 (without hydrodynamic dispersion effects, but still electrically conducting) in the diffusion equation, as even more drastic simplifications in the velocity profile of this kind of equation are shown to give a minor deviation by Sinzato (2021).

Using these simplifications, the set of governing equations is reduced to

$$\eta \frac{d^2 u}{dy^2} - Ha^2 \left(E_0 + u\right) + G = 0, \tag{4.82}$$

$$Ha^2 B_x (E_0 + u) - \frac{\partial p}{\partial y} = 0, \tag{4.83}$$

$$Re_m \frac{du}{dy} + \frac{d^2 B_x}{dy^2} = 0, \tag{4.84}$$

$$\frac{d}{dy}\left[\frac{d\phi}{dy} - PeK_c \frac{du_0}{dy}\phi\frac{d\phi}{dy} - PeK_c \frac{d^2 u_0}{dy^2}\phi^2\right] = 0, \tag{4.85}$$

$$\frac{1}{Re_m}\frac{dB_x}{dy} - u = E_0. \tag{4.86}$$

Note that the second simplification completely decouples the diffusion equation from the movement equation. This is necessary to solve the system of equation. Using a perturbation expansion in terms of the small parameter PeK_c, the quantities involved in this system of equations can be written as

$$\phi = \phi_0 + PeK_c\phi_1 + \mathcal{O}(Pe^2 K_c^2), \tag{4.87}$$

$$u = u_0 + PeK_c u_1 + \mathcal{O}(Pe^2 K_c^2), \tag{4.88}$$

$$B_x = B_{x0} + PeK_c B_{x1} + \mathcal{O}(Pe^2 K_c^2). \tag{4.89}$$

We note that the choice of the parameter PeK_c to be small is a consequence of Equation (4.85). From it is clear that the shear induced effect is small when PeK_c is small. The induced magnetic field is not perturbed as it is a direct consequence of the velocity field. Substituting these in the governing Equations (4.82), (4.83), (4.84) and (4.85) and matching the terms with the same power of K_c, we obtain a set of equations for each of the contributions on Equations (4.87) and (4.89). These are

$$\mathcal{O}(1)\begin{cases}\phi_0 = \text{constant} = \overline{\phi},\\ \eta_e \dfrac{d^2 u_0}{dy^2} = Ha^2(E_0 + u_0) - G,\\ \dfrac{d^2 B_{x0}}{dy^2} = -Re_m \dfrac{du_0}{dy},\end{cases} \tag{4.90}$$

$$\mathcal{O}(PeK_c)\begin{cases}\dfrac{d\phi_1}{dy} = \dfrac{d^2 u_0}{dy^2}\phi_0^2,\\ \eta_e \dfrac{d^2 u_1}{dy^2} = -\dfrac{5}{2}\phi_1 \dfrac{d^2 u_0}{dy^2},\\ \dfrac{d^2 B_{x1}}{dy^2} = -Re_m \dfrac{du_1}{dy},\end{cases} \tag{4.91}$$

$$\mathcal{O}(Pe^2K_c^2)\begin{cases}\dfrac{d\phi_2}{dy} = \dfrac{du_0}{dy}\phi_0 \dfrac{d\phi_1}{dy} + 2\dfrac{d^2 u_0}{dy^2}\phi_0\phi_1,\\ \eta_e \dfrac{d^2 u_2}{dy^2} = -\dfrac{5}{2}\left[\phi_1 \dfrac{d^2 u_1}{dy^2} + \phi_2 \dfrac{d^2 u_0}{dy^2}\right],\\ \dfrac{d^2 B_{x2}}{dy^2} = -Re_m \dfrac{du_2}{dy},\end{cases} \tag{4.92}$$

where η_e is just Einstein's non-dimensional suspension viscosity for the mean volume fraction, $1+2.5\overline{\phi}$. Also, boundary conditions given by Equations (4.77), (4.79), (4.80) and (4.81) can be written in terms of each contribution as

$$u_0(y=\pm 1) = u_1(y=\pm 1) = u_2(y=\pm 1) = 0, \tag{4.93}$$

$$B_{x0}(y=\pm 1) = B_{x1}(y=\pm 1) = B_{x2}(y=\pm 1) = 0, \tag{4.94}$$

$$\int_{-1}^{1} u_0 dy = 1 \quad \text{and} \quad \int_{-1}^{1} u_1 dy = \int_{-1}^{1} u_2 dy = 0 \tag{4.95}$$

$$\int_{0}^{1} \phi_0 dy = \overline{\phi} \quad \text{and} \quad \int_{0}^{1} \phi_1 dy = \int_{0}^{1} \phi_2 dy = 0. \tag{4.96}$$

Then, using the boundary conditions given by Equations (4.93)-(4.96), the coefficients of the expansion can be found. The leading order solution is

$$\phi_0 = \overline{\phi}, \tag{4.97}$$

$$u_0 = \frac{G_0}{\sqrt{\eta_e} Ha \tanh\left(Ha/\sqrt{\eta_e}\right)}\left[1 - \frac{\cosh\left(Hay/\sqrt{\eta_e}\right)}{\cosh\left(Ha/\sqrt{\eta_e}\right)}\right], \tag{4.98}$$

$$B_{x0} = \frac{Re_m G_0}{Ha^2 \sinh\left(Ha/\sqrt{\eta_e}\right)}\left[\sinh\left(\frac{Hay}{\sqrt{\eta_e}}\right) - y \sinh\left(\frac{Ha}{\sqrt{\eta_e}}\right)\right]. \tag{4.99}$$

Here G_0 is just the pressure gradient in the case without shear induced effects. The next order solutions, $\mathcal{O}(K_c)$, are given by

$$\phi_1 = \frac{\phi_0^2}{\left[1 - \sqrt{\eta_e}\tanh\left(Ha/\sqrt{\eta_e}\right)/Ha\right]}\left[1 - \frac{1}{\cosh\left(Ha/\sqrt{\eta_e}\right)}\left(1 + \frac{Ha}{\sqrt{\eta_e}}\sinh\left(Hay/\sqrt{\eta_e}\right)\right)\right], \tag{4.100}$$

$$\begin{aligned} u_1 = {} & \frac{5\phi_0^2}{16\eta_e\sinh^2\left(Ha/\sqrt{\eta_e}\right)}\frac{1}{\left(\coth\left(Ha/\sqrt{\eta_e}\right) - \sqrt{\eta_e}/Ha\right)^2} \\ & \times\left\{\frac{Ha}{\sqrt{\eta_e}}\left[y\sinh\left(\frac{2Ha}{\sqrt{\eta_e}}\right) - \sinh\left(\frac{2Hay}{\sqrt{\eta_e}}\right)\right] + 8\left[\cosh\left(\frac{Ha}{\sqrt{\eta_e}}\right) - 1\right]\cosh\left(\frac{Hay}{\sqrt{\eta_e}}\right)\right. \\ & \left. -8\left[\cosh\left(\frac{Ha}{\sqrt{\eta_e}}\right) - 1\right]\cosh\left(\frac{Ha}{\sqrt{\eta_e}}\right)\right\}, \end{aligned} \tag{4.101}$$

$$\begin{aligned} B_{x1} = {} & \frac{5Re_m\phi_0^2}{32Ha\sqrt{\eta_e}\sinh^2\left(Ha/\sqrt{\eta_e}\right)}\frac{1}{\left(\coth\left(Ha/\sqrt{\eta_e}\right) - \sqrt{\eta_e}/Ha\right)^2} \\ & \times\left\{\frac{Ha^2}{\eta_e}\sinh\left(\frac{2Ha}{\sqrt{\eta_e}}\right) - \frac{Ha^2}{\eta_e}y^2\sinh\left(\frac{2Ha}{\sqrt{\eta_e}}\right) + 16\sinh\left(\frac{Hay}{\sqrt{\eta_e}}\right)\right. \\ & - 16y\sinh\left(\frac{Ha}{\sqrt{\eta_e}}\right) - 16\cosh\left(\frac{Ha}{\sqrt{\eta_e}}\right)\sinh\left(\frac{Hay}{\sqrt{\eta_e}}\right) \\ & \left.\frac{Ha}{\sqrt{\eta_e}}\cosh\left(\frac{2Hay}{\sqrt{\eta_e}}\right) - \frac{Ha}{\sqrt{\eta_e}}\cosh\left(\frac{2Ha}{\sqrt{\eta_e}}\right) + 8y\sinh\left(\frac{2Ha}{\sqrt{\eta_e}}\right)\right\}. \end{aligned} \tag{4.102}$$

The pressure gradient G can be found through the equation $\int_{-1}^{1} u dy = 1$, so that

$$\begin{aligned} G = {} & \frac{Ha\sqrt{\eta_e}}{\left(\coth\left(Ha/\sqrt{\eta_e}\right) - \sqrt{\eta_e}/Ha\right)} \\ & + \frac{5\phi_0^2 PeK_c}{2\sinh\left(Ha/\sqrt{\eta_e}\right)\tanh\left(Ha/\sqrt{\eta_e}\right)\left(\coth\left(Ha/\sqrt{\eta_e}\right) - \sqrt{\eta_e}/Ha\right)^3} \\ & \times\left[\cosh\left(\frac{Ha}{\sqrt{\eta_e}}\right) - 1\right]\left[\frac{Ha}{\sqrt{\eta_e}} - \tanh\left(\frac{Ha}{\sqrt{\eta_e}}\right)\right]. \end{aligned} \tag{4.103}$$

4.6.6 Results

Figure 15 shows the results of the local volume fraction of particles distribution for different values of K_c in a half of symmetry of the flow. This figure shows that in the presence of hydrodynamic dispersion the particle tends to migrate to the y-center of the channel. When there is no hydrodynamic dispersion, the volume fraction is homogeneous across y-direction. These behaviours were expected, as in the presence of such dispersion the particles tend to migrate from regions of higher shear rate to regions of lower shear rate. Indeed, regions of higher shear rate produces more collisions, making particles in such regions migrate more. Hence, as they migrate more, after some time these particles happen to be in regions of lower shear rate, where the migration effect is lower. Looking the net flux, particles from higher shear rate regions migrate more and particles from lower shear rate regions have lower migration coefficients, generating a net flux towards the regions of lower shear rate. Although in small scales, this is the exactly behavior observed in Figure 15.

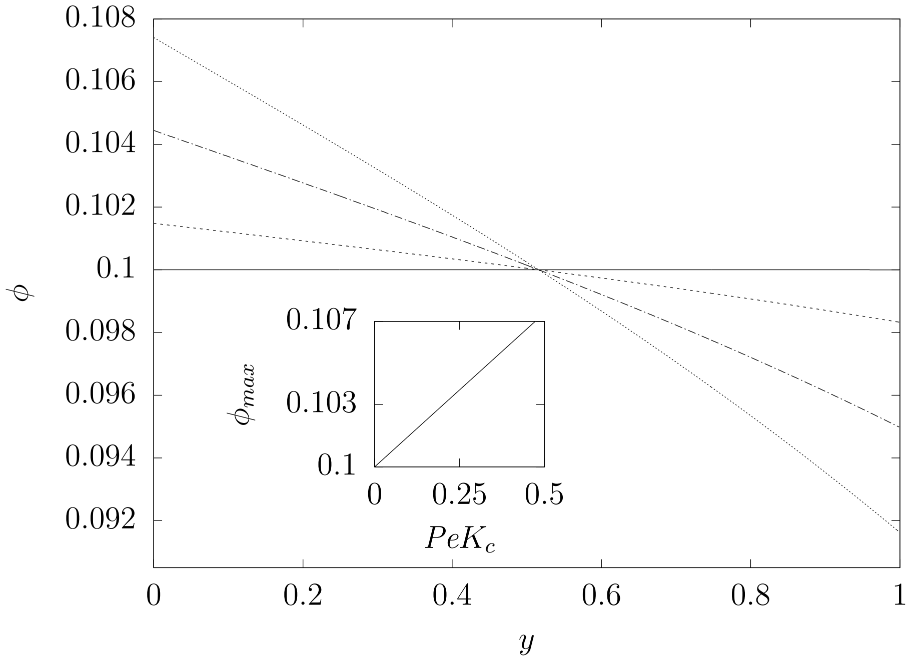

Figure 15 – Local volume fraction of particles on the upper half of symmetry of the channel for $\phi_0 = 0.1$ and $Ha = 1$. In this Figure, ——— represents $PeK_c = 0$, ------ $PeK_c = 0.1$, -·-·-·- $PeK_c = 0.3$ and ·········· $PeK_c = 0.5$. *Inset*: Maximum of the local volume fraction as a function of the parameter PeK_c.

On the other hand Figure 16 shows the effect of the magnetic field on the volume fraction distribution, as it shows this volume fraction distribution for a half of symmetry of the flow for some values of the Hartmann number. It is evident that the magnetic field tends to homogenize the suspension distribution of particles in the channel, except in the walls. Indeed, as we increase the magnetic field, the particle distribution is homogenized from $y = -0.8$ to $y = 0.8$. This also shows that the magnetic field expels particles from the regions near the walls (y from -1 to -0.8 and 0.8 to 1). This behavior is not trivial and indicates that a external magnetic field can be used to control the particle distribution on a electrically conducting suspension. For example, an external magnetic field can be used to expel particles from the regions near wall when it is needed, as particles interacting with the wall can be a problem depending on the application. Also, when a more homogeneous flow in the core of the channel is needed, a external magnetic field can be used to induce this configuration. One can note that the magnetic field can help the shear induced near the walls, between $y = 0.8$ and $y = 1$, but it helps differently in the core flow. Indeed, Figure 17 gives a glimpse of this non-linear behavior. It shows that the magnetic field changes substantially the shear rate, such that it is no longer linear on the half of symmetry of the channel, it is non-linear, so that the gradient of shear rate is substantially increased in some regions of the channel. As the shear induced can be direct influenced by the gradient of shear rate, this change in the magnetic field must contribute to the shear-induced dispersion. These results indicates the need of a solution that can achieve a wider range of parameters, as these effects of the magnetic field could be explored better, such that the effects of this non-linearity could generate some different physical insights. We note that in a wider range of the parameters, the shear-induced effect associated with the gradient of shear rate can grow considerably, as the flux coefficient in the equation for ϕ scales with $\phi_0^2 PeK_c$. The way that the combined mechanism of the gradient of shear rate with the action of the magnetic field can generate different physical results in these wider ranges.

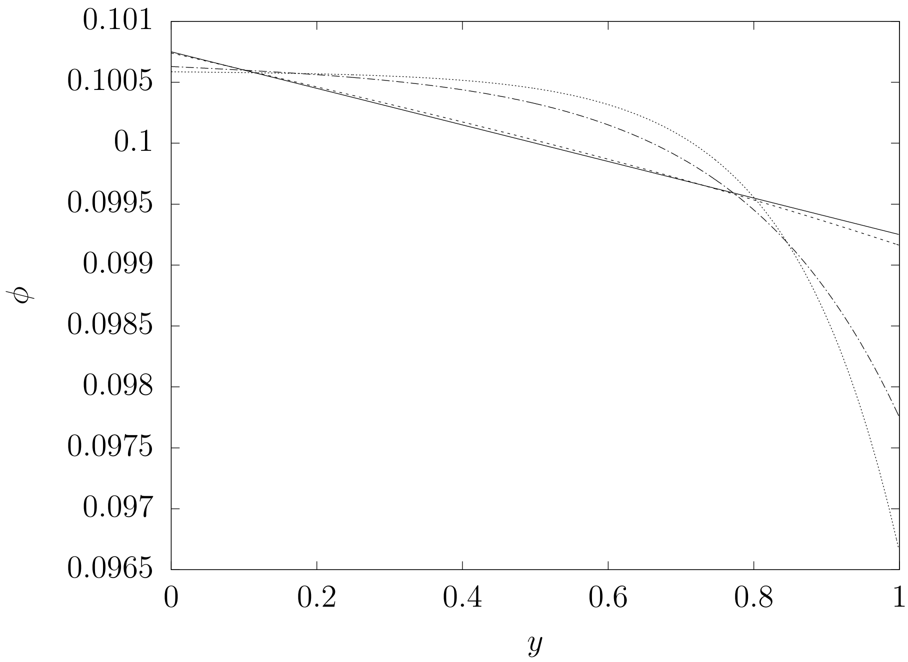

Figure 16 – Local volume fraction of particles on the upper half of symmetry of the channel for $\phi_0 = 0.1$ and $PeK_c = 0.05$. In this Figure, ——— represents $Ha = 0.01$, - - - - - - $Ha = 1$, -·-·-·- $Ha = 5$ and ·········· $Ha = 7.5$.

From Figure 18 we see the behavior of the velocity profile for different K_c. As the

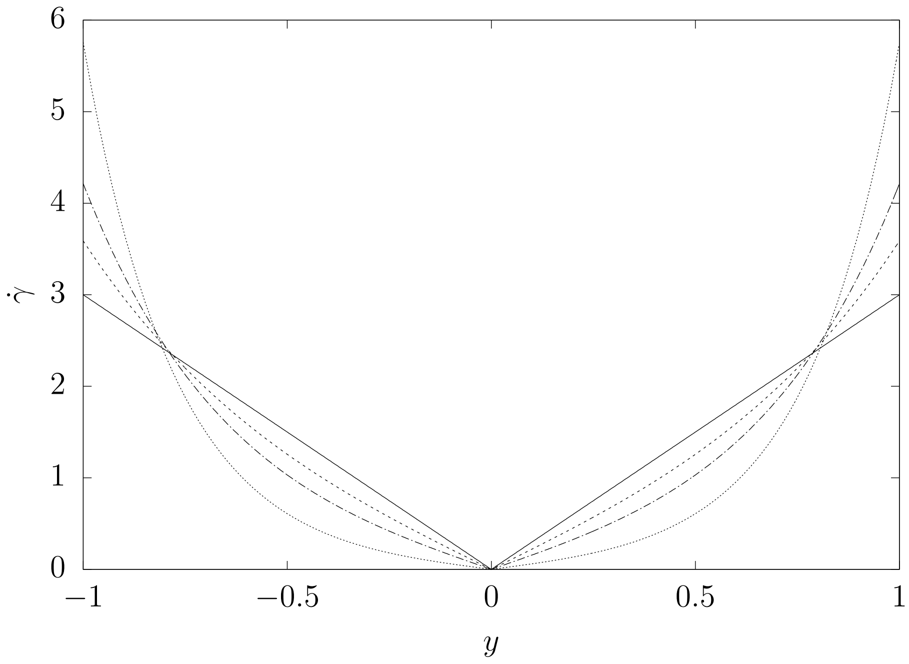

Figure 17 – Shear rate for $\phi_0 = 0.1$, $PeK_c = 0.05$ and different values of Hartmann number. In this Figure, ——— represents $Ha = 0$, - - - - - - $Ha = 2$, -·-·-·- $Ha = 3$ and ··········· $Ha = 5$.

hydrodynamic dispersion tends to concentrate particles on the center of the channel, the change in the local volume fraction indicates that this kind of dispersion will increase the viscosity of the suspension on the center, decreasing the flow velocity and the flow rate more on this region. Hence, the velocity profile is lower on the center of the channel. Note that this behavior is observed on Figure 18. This result is also observed in Figure 20, as the result of the dispersion is to increase the effective viscosity, i.e. to the flow rate increasing K_c has the same effect of increasing the viscosity. This behavior of the effective viscosity and of the velocity profile makes the possibility of controlling the dispersion via an external magnetic field even more important, as it is shown here that the dispersion present in flow of suspensions can decrease the flow rate, which can be a undesired effect in many applications. Figure 19 shows the induced magnetic field for different values of PeK_c. As expected by Equations (4.90)-(4.92), the magnetic field is a direct consequence of the velocity profile. As the velocity is lower on the profile due to shear-induced effects, it induces less intense magnetic field.

Although the analysis presented here shows exciting results, it was done for small effects of the hydrodynamic dispersion. In more general range of the parameters, the solution can present behaviors not observed here, like non-linear ones. Hence, the results presented here emboldens a more general solution, a numerical one, to analyze the effect of

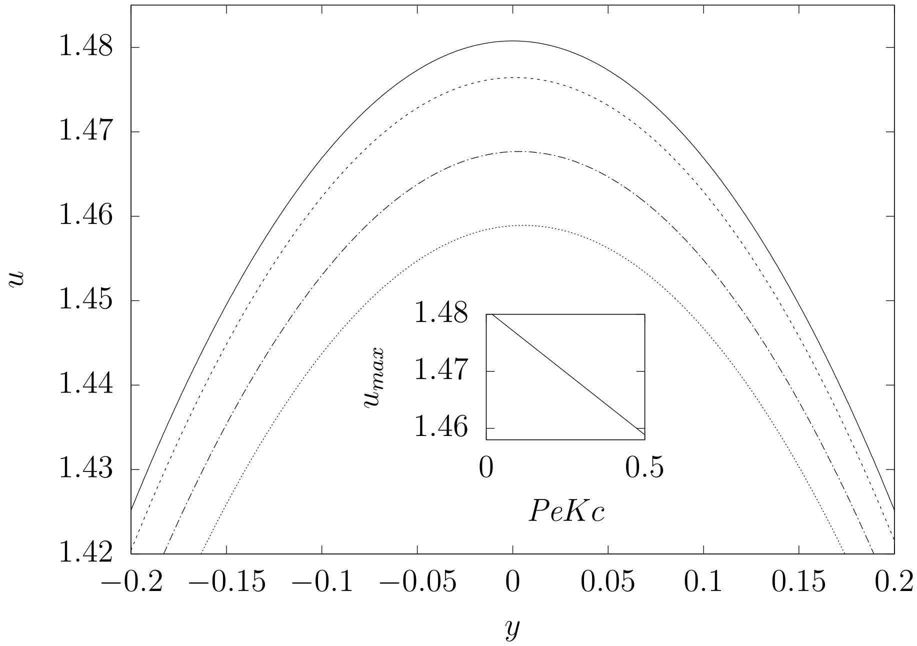

Figure 18 – Velocity profile for $\phi_0 = 0.1$ and $Ha = 1$. In this Figure, ——— represents $PeK_c = 0$, - - - - - - $PeK_c = 0.1$, -·-·-·- $PeK_c = 0.3$ and ·········· $PeK_c = 0.5$. *Inset*: The maximum of the velocity profile as a function of the parameter PeK_c.

hydrodynamic dispersion on electrically conducting suspensions on more general range of parameters, including situations that the hydrodynamic dispersion effect is substantially more intense. Indeed, although the perturbation analysis provides great insights on the flow of an electrically conducting suspension in the presence of hydrodynamic dispersion effects, only a small range of the parameters could be analyzed and on some different configurations even more interesting effects could appear. This way, as a next work, we are looking forward to do a numerical study of the equations solved here with regular perturbation analysis.

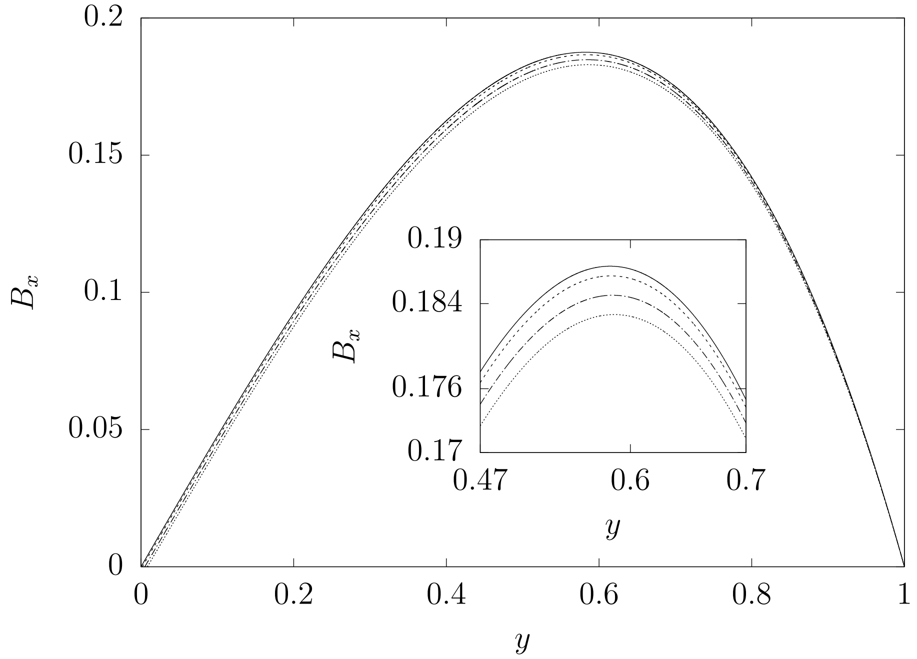

Figure 19 – Magnetic field profile for $\phi_0 = 0.1$ and $Ha = 1$. In this Figure, ——— represents $PeK_c = 0$, - - - - - - $PeK_c = 0.1$, -·-·-·- $PeK_c = 0.3$ and ·········· $PeK_c = 0.5$.

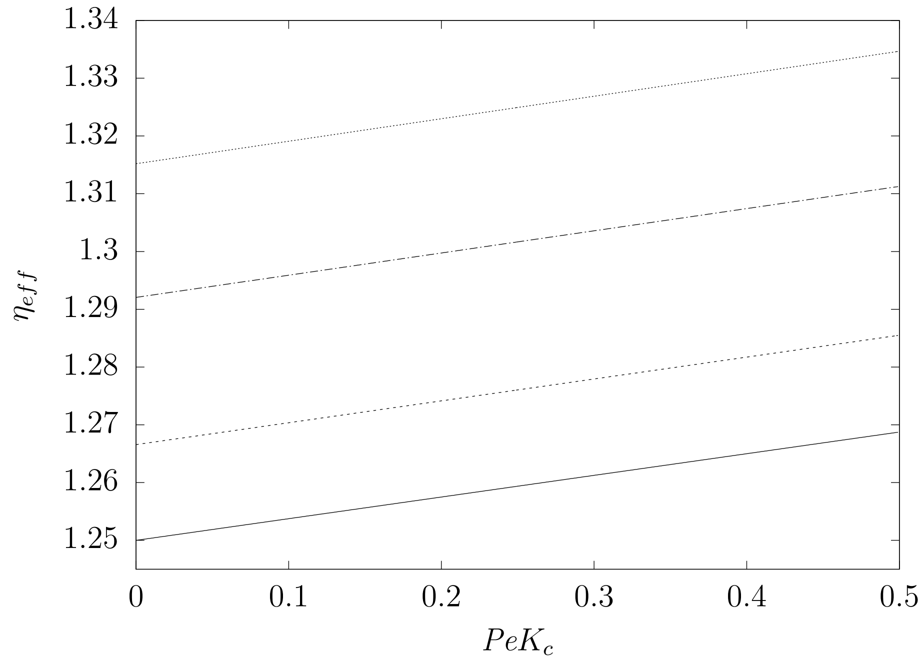

Figure 20 – Effective viscosity for $\phi_0 = 0.1$. In this Figure, ——— represents $Ha = 0$, - - - - - - $Ha = 0.5$, -·-·-·- $Ha = 0.8$ and ·········· $Ha = 1$.

5 CONCLUSION

In this dissertation, two fronts of work were explored. In the first, we studied the effects of a bulk viscosity in magnetohydrodynamic waves traveling in a barotropic gas, like Alfvén's and magnetoacoustic waves. In the second, we explored the hydrodynamic dispersion in the flow of an electrically conducting suspension in a channel.

Regarding the first front, we formulated and nondimensionalized the governing equations for the flow of a barotropic gas, considering dissipation solely from the bulk viscosity, given the well-established impact of standard viscosity on the waves under examination. These equations were perturbed with oscillations of small amplitude around the equilibrium, the way that linearized equations in wave space were obtained. These could be combined in a way that the dispersion relations for magnetohydrodynamic waves arise. Firstly, stability and phase velocity of these waves were analyzed in aid of a already existing model for the bulk viscosity. The results showed that the high frequency effects accounted by the bulk viscosity have no influence under Alfvén's waves, as these are incompressible. On the other hand, it was clear that this bulk viscosity has an influence on magnetoacoustic waves. The magnetoacoustic waves was shown to obtain dispersive effects under the effects of the bulk viscosity, i.e. in the a high frequency context, the phase velocity of these waves depends on the wave number. Also, we have shown that the magnetoacoustic waves are stable perturbations on the fluid. We even showed that the bulk viscosity helps this stability, i.e. it makes the amplification factor more negative, showing that this bulk viscosity indeed has a dissipative effect on magnetoacoustic waves, as expected. Secondly, a model to estimate the bulk viscosity on laboratory based on MHD waves properties was proposed. The equation of this model was analyzed graphically. This analysis have shown how the dissipation of energy associated with the bulk viscosity can be controlled by a external magnetic field on magnetohydrodynamic flows. In special, this control can lead to a drag reduction in compressible flows of electrically conducting gases.

Regarding the second front, an in-depth discussion on hydrodynamic dispersion mechanism was made first. Each mechanism involved was discussed separately, making possible a construction for a flux model for each of these mechanism. This flux is shown to be associated with the gradient of particle concentration in the suspension and the gradient of shear rate. These constructions were based on an already existing constitutive model for shear-induced dispersion, which had been previously tested and compared with experimental results. Subsequently, a diffusive equation was proposed based on these fluxes. This equation, along with momentum and induction equations, constituted the governing equations of the problem. They were analyzed for the case of channel flow and made non-dimensional, thereby highlighting the non-dimensional physical parameters governing the problem. To solve the resulting coupled system of differential equations, a regular perturbation analysis was proposed, along with justified simplifications. Initially, it was demonstrated that the external magnetic field could control the volume fraction of particle distribution along the channel, which was an interesting finding. Specifically, the external magnetic field was shown to expel particles from regions near the wall while simultaneously homogenizing the particle distribution outside this wall region, which constituted 80% of the volume of the core flow. It was also discussed that the velocity profile and effective viscosity are affected, as hydrodynamic dispersion causes the flow to be slower in the core and reduces the flow rate. This last result was emphasized to highlight the usefulness of the possibility of controlling the local volume fraction with the application of an external magnetic field in this type of suspension.

5.1 Future Work

As briefly discussed in earlier sections, there is still room for further development to build upon the findings presented in this dissertation. Therefore, we propose several points to be addressed in future work:

- Use the model proposed to the bulk viscosity to analyze a concrete problem in the context of electrically conducting gases, like the problem of an oscillating bubble;
- Solve the channel flow of an electrically conducting non-dilute suspension with hydrodynamic dispersion effects numerically, allowing a much more vast range of parameters. To start this study, we propose using other model for the suspension viscosity, as Einstein's model account only for dilute suspensions. For example, the

model by Krieger and Dougherty (1959), which proposes that, for a non-dilute suspension,

$$\eta = \eta_0 \left(1 - \frac{\phi}{\phi_m}\right)^{-\{\eta\}\phi_m}, \tag{5.1}$$

where $\{\eta\}$ is denominated intrinsic viscosity and ϕ_m is the maximum packing volume fraction. Note that $\{\eta\}$ is non-dimensional and the values of $\{\eta\}$ and ϕ_m are determined empirically.

Bibliography

ACRIVOS, A. et al. Longitudinal shear-induced diffusion of spheres in a dilute suspension. *Journal of Fluid Mechanics*, v. 240, p. 651–657, 1992. Cited on page 4.

ACRIVOS, A.; MAURI, R.; FAN, X. Shear-induced resuspension in a couette device. *International Journal of Multiphase Flow*, v. 19, n. 5, p. 797–802, 1993. ISSN 0301-9322. Cited on page 4.

ALFVÉN, H. Existence of electromagnetic-hydrodynamic waves. *Nature*, v. 150, p. 405–406, 1942. Cited 2 times on pages 3 and 33.

ALLEN, T. K. et al. Experimental generation of plasma alfven waves. *Phys. Rev. Lett.*, American Physical Society, v. 2, p. 383–384, May 1959. Cited on page 3.

ARIS, R. *Vectors, tensors and the basic equations of fluid mechanics*. New York: Dover, 1989. Cited 5 times on pages 14, 15, 25, 28, and 61.

BANERJEE, D. et al. Magnetohydrodynamic waves in open coronal structures. *Space Science Reviews*, v. 217, p. 76, september 2021. Cited on page 3.

BARUT, A. O. *Electrodynamics and classical theory of fields and particles*. New York: Dover, 1980. Cited 2 times on pages 23 and 28.

BATCHELOR, G. K. *Introduction to fluid dynamics*. Cambridge: Cambridge University Press, 1967. Cited 2 times on pages 19 and 35.

BITTENCOURT, J. A. *Fundamentals of plasma physics*. New York: Springer, 2004. Cited 3 times on pages 41, 42, and 49.

CHANDRASEKHARAIAH, D. S.; DEBNATH, L. *Continuum mechanics*. San Diego: Academic Press, 1994. Cited on page 10.

CHANG, C. C.; LUNDGREN, T. S. Duct flow in magnetohydrodynamics. *Zeitschrift für angewandte Mathematik und Physik*, v. 12, p. 100–114, 1961. Cited on page 4.

CUNHA, F. R. *Fundamentos da hidrodinâmica de fluidos magnéticos*. 2012. Turbulência (B. S. Carmo, G. R. Assi, J. R. Meneghini, J. A. P. Aranha, e E. V. Volpe, eds.), vol. 8, cap. 7, pp. 257–339, Brasil: ABCM. Cited on page 2.

CUNHA, F. R. *Notas de aula do curso Dinâmica dos Fluidos Não-Newtonianos, Pós-Graduação em Ciências Mecânicas*. Brasília: Departamento de Engenharia Mecânica, Universidade de Brasília, 2021. Cited 2 times on pages 17 and 18.

CUNHA, F. R. *Notas de aula do curso Magnetohidrodinâmica, Pós-Graduação em Ciências Mecânicas*. Brasília: Departamento de Engenharia Mecânica, Universidade de Brasília, 2021. Cited 2 times on pages 16 and 60.

CUNHA, F. R.; INÁCIO, L. A. S. A theoretical study on the bulk viscosity in a compressible flow of an electrically conducting gas in the presence of magnetoacoustic waves. *Physics of Fluids (Revised version in preparation)*, 2024. Cited on page 51.

CUNHA, F. R.; SINZATO, Y. Z.; PEREIRA, I. D. O. An experimental investigation on the magnetoviscous effect and shear rate-dependent viscosity of a magnetic suspension under longitudinal and transverse magnetic fields. *Physics of Fluids*, v. 34, n. 9, p. 093314, 09 2022. ISSN 1070-6631. Cited 2 times on pages 5 and 69.

CUNHA, F. R. D.; HINCH, E. J. Shear-induced dispersion in a dilute suspension of rough spheres. *Journal of Fluid Mechanics*, v. 309, p. 211–223, 1996. Cited 2 times on pages 4 and 63.

DAVIDSON, P. A. Magnetohydrodynamics in materials processing. *Annual Review of Fluid Mechanics*, v. 31, p. 273–300, 1999. Cited 3 times on pages 1, 2, and 60.

DAVIDSON, P. A. *Introduction to magnetohydrodynamics*. Cambridge: Cambridge University Press, 2017. Cited 5 times on pages 1, 29, 30, 33, and 41.

DAVIS, R. H. Hydrodynamic diffusion of suspended particles: a symposium. *Journal of Fluid Mechanics*, v. 310, p. 325–335, 1996. Cited on page 62.

ECKSTEIN, E. C.; BAILEY, D. G.; SHAPIRO, A. H. Self-diffusion of particles in shear flow of a suspension. *Journal of Fluid Mechanics*, v. 79, n. 1, p. 191–208, 1977. Cited on page 4.

EINSTEIN, A. On the electrodynamics of moving bodies. *Annalen der Physik*, p. 891–921, 1905. Cited 3 times on pages 22, 23, and 24.

FRAIM, F. W.; HEISER, W. H. The effect of a strong longtitudinal magnetic field on the flow of mercury in a circular tube. *Journal of Fluid Mechanics*, Cambridge University Press, v. 33, n. 2, p. 397–413, 1968. Cited on page 4.

FÄLTHAMMAR, C.-G. The discovery of magnetohydrodynamic waves. *Journal of Atmospheric and Solar-Terrestrial Physics*, v. 69, n. 14, p. 1604–1608, 2007. ISSN 1364-6826. Cited on page 3.

GOLD, R. R. Magnetohydrodynamic pipe flow. *Journal of Fluid Mechanics*, v. 13, p. 505, 1962. Cited on page 4.

GOOSSENS, M.; ERDéLYI, R.; RUDERMAN, M. S. Resonant mhd waves in the solar atmosphere. *Space Science Reviews*, v. 158, p. 289–338, july 2011. Cited on page 3.

GOOSSENS, M. et al. On the nature of kink mhd waves in magnetic flux tubes. *Astronomy & Astrophysics (A&A)*, v. 503, n. 1, p. 213–223, june 2009. Cited on page 3.

GRAHAM, M. D. *Microhydrodynamics, Brownian Motion and Complex Fluids*. Cambridge: Cambridge University Press, 2018. Cited on page 65.

GREGORY, T. S. et al. The magnetohydrodynamic effect and its associated material designs for biomedical applications: A state-of-the-art review. *Advanced Functional Materials*, v. 26, n. 22, p. 3942–3952, 2016. Cited on page 1.

GRIFFITHS, D. J. *Introduction to electrodynamics*. New Jersey: Prentice Hall, 1999. Cited on page 28.

HARTMANN, J. Theory of the laminar flow of an electrically conductive liquid in a homogeneous magnetic field. *Mathematisk-fysiske Meddelelser*, v. 6, p. 1–27, 1937. Cited on page 3.

HARTMANN, J.; LAZARUS, F. Experimental investigations of the flow of mercury in a homogeneous magnetic field. *Mathematisk-fysiske Meddelelser*, XV, 1937. Cited on page 4.

HUDSON, S. D. Wall migration and shear-induced diffusion of fluid droplets in emulsions. *Physics of Fluids*, v. 15, n. 5, p. 1106–1113, 05 2003. ISSN 1070-6631. Cited on page 4.

HUNT, J. C. R.; MALCOLM, D. G. Some electrically driven flows in magnetohydrodynamics part 2. theory and experiment. *Journal of Fluid Mechanics*, Cambridge University Press, v. 33, n. 4, p. 775–801, 1968. Cited on page 4.

IBáNEZ, M. H. Damping of hydromagnetic waves by bulk viscosity. *Waves and Oscillation in the Solar Atmosphere - Proceedings IAU Symposium*, v. 247, p. 337–343, 2007. Cited on page 3.

IHARA, S.; MATSUSHIMA, A.; TAJIMA, K. The flow of conducting fluids in circular pipes with finite conductivity under uniform transverse magnetic fields. *Journal of Applied Mechanics*, v. 39, p. 29, 1967. Cited on page 4.

JEPHCOTT, D. F. Alfvén waves in a gas discharge. *Nature*, v. 183, p. 1652–1654, 1959. Cited on page 3.

KAPOOR, B.; ACRIVOS, A. Sedimentation and sediment flow in settling tanks with inclined walls. *Journal of Fluid Mechanics*, v. 290, p. 39–66, 1995. Cited on page 4.

KARNIS, A.; GOLDSMITH, H.; MASON, S. The kinetics of flowing dispersions: I. concentrated suspensions of rigid particles. *Journal of Colloid and Interface Science*, v. 22, n. 6, p. 531–553, 1966. ISSN 0021-9797. Cited on page 4.

KIM, J. M.; LEE, S. G.; KIM, C. Numerical simulations of particle migration in suspension flows: Frame-invariant formulation of curvature-induced migration. *Journal of Non-Newtonian Fluid Mechanics*, v. 150, n. 2, p. 162–176, 2008. ISSN 0377-0257. Cited on page 5.

KNAEPEN, B.; MOREAU, R. Magnetohydrodynamic turbulence at low magnetic Reynolds number. *Annual Review of Fluid Mechanics*, v. 40, p. 25–45, 2008. Cited 2 times on pages 1 and 2.

KRIEGER, I. M.; DOUGHERTY, T. J. A mechanism for non-newtonian flow in suspensions of rigid sphere. *Transactions of the Society of Rheology*, v. 3, p. 137–152, 1959. Cited on page 79.

KRISHNAN, G. P.; BEIMFOHR, S.; LEIGHTON, D. T. Shear-induced radial segregation in bidisperse suspensions. *Journal of Fluid Mechanics*, v. 321, p. 371–393, 1996. Cited on page 5.

LANDAU, L. D.; LIFSHITZ, E. M. *Course of Theoretical Physics Volume 6: Fluid Mechanics*. Oxford: Pergamon Press, 1987. Cited 4 times on pages 5, 19, 35, and 46.

LEHNERT, B. Magneto-hydrodynamic waves in liquid sodium. *Phys. Rev.*, American Physical Society, v. 94, p. 815–824, May 1954. Cited on page 3.

LEIGHTON, D.; ACRIVOS, A. Measurement of shear-induced self-diffusion in concentrated suspensions of spheres. *Journal of Fluid Mechanics*, v. 177, p. 109–131, 1987. Cited on page 4.

LEIGHTON, D.; ACRIVOS, A. The shear-induced migration of particles in concentrated suspensions. *Journal of Fluid Mechanics*, v. 181, p. 415–439, 1987. Cited 3 times on pages 4, 5, and 63.

LIU, I.-S. *Continuum Mechanics*. Berlin: Springer-Verlag, 2002. Cited 3 times on pages 11, 14, and 18.

LUNDQUIST, S. Experimental demonstration of magneto-hydrodynamic waves. *Nature*, v. 164, p. 145–146, 1949. Cited on page 3.

LUNDQUIST, S. Experimental investigations of magneto-hydrodynamic waves. *Phys. Rev.*, American Physical Society, v. 76, p. 1805–1809, Dec 1949. Cited on page 3.

MANDELSHTAM, L. I.; LEONTOVICH, M. A. To the sound absorption theory in liquids. *JETP*, v. 7, p. 438–444, 1937. Cited 3 times on pages 5, 35, and 46.

MOORTEL, I. D.; NAKARIAKOV, V. M. Magnetohydrodynamic waves and coronal seismology: an overview of recent results. *Philosophical Transactions of the Royal Society A: Mathematical, Physical and Engineering Sciences*, v. 370, n. 1970, p. 3193–3216, 2012. Cited on page 3.

MORLEY, N. B. et al. Liquid magnetohydrodynamics — recent progress and future directions for fusion. *Fusion Engineering and Design*, v. 51-52, p. 701–713, 2000. ISSN 0920-3796. Cited on page 1.

MULLER, U.; BUHLER, L. *Magnetofluiddynamics in channels and containers*. Berlin: Springer-Verlag, 2001. Cited on page 60.

MURGATROYD, W. Cxlii. experiments on magneto-hydrodynamic channel flow. *The London, Edinburgh, and Dublin Philosophical Magazine and Journal of Science*, Taylor & Francis, v. 44, n. 359, p. 1348–1354, 1953. Disponível em: <https://doi.org/10.1080/14786441208520404>. Cited on page 4.

NAGAO, S.; SATO, T. Some experiments on plasma alfvén waves. *Journal of the Physical Society of Japan*, v. 15, n. 4, p. 735–735, 1960. Cited on page 3.

NAKAHARA, M. *Geometry, Topology and Physics*. Philadelphia: IOP Publishing, 2003. Cited on page 89.

NAKARIAKOV, V. M.; KOLOTKOV, D. Y. Magnetohydrodynamic waves in the solar corona. *Annual Review of Astronomy and Astrophysics*, v. 58, n. 1, p. 441–481, 2020. Cited on page 3.

NIR, A.; ACRIVOS, A. Sedimentation and sediment flow on inclined surfaces. *Journal of Fluid Mechanics*, v. 212, p. 139–153, 1990. Cited on page 4.

OKAMOTO, T. J. et al. Coronal transverse magnetohydrodynamic waves in a solar prominence. *Science*, v. 318, n. 5856, p. 1577–1580, 2007. Cited on page 3.

PHILLIPS, R. J. et al. A constitutive equation for concentrated suspensions that accounts for shear-induced particle migration. *Physics of Fluids A: Fluid Dynamics*, v. 4, n. 1, p. 30–40, 01 1992. ISSN 0899-8213. Cited 2 times on pages 5 and 63.

PTUSKIN, V. S. et al. Dissipation of magnetohydrodynamic waves on energetic particles: Impact on interstellar turbulence and cosmic-ray transport. *The Astrophysical Journal*, v. 642, n. 2, p. 902, may 2006. Cited on page 3.

RASHIDI, S.; ESFAHANI, J. A.; MASKANIYAN, M. Applications of magnetohydrodynamics in biological systems-a review on the numerical studies. *Journal of Magnetism and Magnetic Materials*, v. 439, p. 358–372, 2017. ISSN 0304-8853. Cited on page 1.

ROURE, G. A.; CUNHA, F. R. Hydrodynamic dispersion and aggregation induced by shear in non-Brownian magnetic suspensions. *Physics of Fluids*, v. 30, n. 12, p. 122002, 12 2018. ISSN 1070-6631. Cited 2 times on pages 4 and 5.

SAMAD, A. The flow of conducting fluids through circular pipes having finite conductivity and finite thickness under uniform transverse magnetic fields. *International Journal of Engineering Science*, v. 19, p. 1221–1232, 1981. Cited on page 4.

SCHAFLINGER, U.; ACRIVOS, A.; ZHANG, K. Viscous resuspension of a sediment within a laminar and stratified flow. *International Journal of Multiphase Flow*, v. 16, n. 4, p. 567–578, 1990. ISSN 0301-9322. Cited on page 4.

SHERCLIFF, J. A. Steady motion of conducting fluids in pipes under transverse magnetic fields. *Mathematical Proceedings of the Cambridge Philosophical Society*, v. 49(01), p. 136, 1952. Cited on page 3.

SHERCLIFF, J. A. Magnetohydrodynamic pipe flow. *Journal of Fluid Mechanics*, v. 1, p. 644, 1956. Cited on page 4.

SINZATO, Y. Z. *Hydrodynamic Dispersion in Capillary Flow of Magnetic Fluids*. Dissertação (Mestrado) — University of Brasília, Brasília, 2021. Cited on page 69.

SINZATO, Y. Z.; CUNHA, F. R. Modeling and experiments of capillary flow of non-symmetric magnetic fluids under uniform field. *Journal of Magnetism and Magnetic Materials*, v. 508, p. 166867, 2020. ISSN 0304-8853. Cited 2 times on pages 5 and 69.

SINZATO, Y. Z.; CUNHA, F. R. Capillary flow of magnetic fluids with effect of hydrodynamic dispersion. *Physics of Fluids*, v. 33, p. 10, 2021. Cited 2 times on pages 5 and 69.

SOKOLOV, I. V. et al. Magnetohydrodynamic waves and coronal heating; unifying empirical and mhd turbulence models. *The Astrophysical Journal*, The American Astronomical Society, v. 764, n. 1, p. 23, jan 2013. Disponível em: <https://dx.doi.org/10.1088/0004-637X/764/1/23>. Cited on page 3.

TANAZAWA, I. The flow of conducting fluids through circular pipes having finite conductivity and finite thickness under uniform transverse magnetic fields. *Transactions of the Japan Society of Mechanical Engineers*, v. 27, 1962. Cited on page 4.

TRUESDELL, C. *A first course in rational continuum mechanics*. [S.l.]: Academic Press, 1977. Cited on page 17.

UHLENBUSCH, J.; FISCHER, E. Hydromagnetische stromung im kreiszylindrischen rohr. *Zeitschrift fur Physik*, v. 164, p. 190–198, 1961. Cited on page 4.

URATA, N. Stability of aluminum reduction cell. In: *1st International Symposium on Electromagnetic Processing of Materials*. [S.l.: s.n.], 1994. Cited on page 2.

VIGEESH, G. et al. Three-dimensional simulations of magnetohydrodynamic waves in magnetized solar atmosphere. *The Astrophysical Journal*, The American Astronomical Society, v. 755, n. 1, p. 18, jul 2012. Cited on page 3.

WALD, R. M. *Advanced Classical Electromagnetism*. Princeton: Princeton University Press, 2022. Cited 2 times on pages 12 and 24.

WANG, Y.; MAURI, R.; ACRIVOS, A. Transverse shear-induced gradient diffusion in a dilute suspension of spheres. *Journal of Fluid Mechanics*, v. 357, p. 279–287, 1998. Cited on page 4.

WILCOX, J. M.; BOLEY, F. I.; SILVA, A. W. D. Experimental Study of Alfvén-Wave Properties. *The Physics of Fluids*, v. 3, n. 1, p. 15–19, 01 1960. ISSN 0031-9171. Cited on page 3.

YIWEN, L. et al. Applications and prospects of magnetohydrodynamics in aeronautical engineering. *Advances in Mechanics*, v. 47, n. lxjz-47-1-452, p. 452, 2017. ISSN 1000-0992. Cited on page 1.

ZARRAGA, I. E.; LEIGHTON DAVID T., J. Measurement of an unexpectedly large shear-induced self-diffusivity in a dilute suspension of spheres. *Physics of Fluids*, v. 14, n. 7, p. 2194–2201, 07 2002. ISSN 1070-6631. Cited on page 4.

Appendix

A Mathematical Constructions

A.1 Non-orthogonal Coordinate Systems

Consider a n-dimensional (finite) real inner product space $\mathcal{V}$ (a vector space equipped with a inner product $\boldsymbol{g}$) that have a basis $\{\hat{\boldsymbol{e}}_1, \hat{\boldsymbol{e}}_{\boldsymbol{2}}, ..., \hat{\boldsymbol{e}}_n\}$, such that any vector $\boldsymbol{u}$ in this space can be written as

$$\boldsymbol{u} = \sum_{i=1}^{n} u^i \hat{\boldsymbol{e}}_i \tag{A.1}$$

$$= u^i \hat{\boldsymbol{e}}_i, \tag{A.2}$$

where u^i are said to be the components of $\boldsymbol{u}$ in the basis $\{\hat{\boldsymbol{e}}_i\}$ and in the second line we have used Einstein summation convention[1]. The inner product is a positive-definite symmetric bilinear map $g : \mathcal{V} \times \mathcal{V} \to \mathbb{R}$. The inner product of two vectors $\boldsymbol{u}$ and $\boldsymbol{v}$ is

$$g(\boldsymbol{u}, \boldsymbol{v}) = \boldsymbol{u} \cdot \boldsymbol{v} = u^i v^j \hat{\boldsymbol{e}}_i \cdot \hat{\boldsymbol{e}}_j. \tag{A.3}$$

The tensor-valued functions $\hat{\boldsymbol{e}}_i \cdot \hat{\boldsymbol{e}}_j$ are usually represented by g_{ij} and are named the metric of the space. The norm of a vector $\boldsymbol{u}$ can be defined by its inner product, by

$$|\boldsymbol{u}| = \sqrt{\boldsymbol{u} \cdot \boldsymbol{u}}. \tag{A.4}$$

Now, note that we can construct a set of vectors orthogonal to $\hat{\boldsymbol{e}}_i$ at each point. Hence, given the basis $\{\hat{\boldsymbol{e}}_i, ...\hat{\boldsymbol{e}}_n\}$, we can construct a set of vectors $\{\hat{\boldsymbol{e}}^i, ...\hat{\boldsymbol{e}}^n\}$ such that

$$\hat{\boldsymbol{e}}^i \cdot \hat{\boldsymbol{e}}_{\boldsymbol{j}} = \delta^i{}_j, \tag{A.5}$$

where $\delta^i{}_j$ is the Kronecker delta. To prove that $\{\hat{\boldsymbol{e}}^i\}$ form a basis to $\mathcal{V}$, we have to prove that this set of vectors is linearly independent and that it spans $\mathcal{V}$. First note that this

[1] This convention states that every repeated index implies summation on this index.

set is linearly independent, as if $u_i\hat{\boldsymbol{e}}^i = \mathbf{0}$, then

$$u_i\hat{\boldsymbol{e}}^i \cdot \hat{\boldsymbol{e}}_j = a_i\delta^i{}_j = a_j = 0. \tag{A.6}$$

We can also see that this set spans $\mathcal{V}$. To see this, first note that

$$\hat{\boldsymbol{e}}^i \cdot \boldsymbol{v} = \hat{\boldsymbol{e}}^i \cdot (v^j\hat{\boldsymbol{e}}_j) = v^j\delta^i{}_j = v^i. \tag{A.7}$$

Then,

$$\boldsymbol{u} \cdot \boldsymbol{v} = g_{ij}u^iv^j = g_{ij}u^i(\hat{\boldsymbol{e}}^j \cdot \boldsymbol{v}) = (g_{ij}u^i\hat{\boldsymbol{e}}^j) \cdot \boldsymbol{v}, \tag{A.8}$$

which implies that $\boldsymbol{u}$ can be written as

$$\boldsymbol{u} = u_j\hat{\boldsymbol{e}}^j, \tag{A.9}$$

where $u_j = g_{ij}u^i$. Therefore, as $\{\hat{\boldsymbol{e}}^i\}$ are linearly independent and spans $\mathcal{V}$, it is proved that it is also a basis for $\mathcal{V}$. We say that the bases $\{\hat{\boldsymbol{e}}^i\}$ and $\{\hat{\boldsymbol{e}}_i\}$ are a pair of dual bases for $\mathcal{V}$. The components u^j are called contravariant components of $\boldsymbol{u}$, while u_j are called the covariant components of $\boldsymbol{u}$.

Note that the metric act as a map between contravariant and covariant components. Indeed, in more general treatments, one can construct vector spaces without a defined inner product or metric. This way, to obtain a operation on vectors returning real numbers, one construct the space of linear functionals (also a linear space) on $\mathcal{V}$, the so-called dual space $\mathcal{V}^*$. A element of $\mathcal{V}^*$ is a linear functional $\boldsymbol{\omega}$ such that $\boldsymbol{\omega} : \mathcal{V} \to \mathbb{R}$. If $\hat{\boldsymbol{e}}^j$ is a basis of $\mathcal{V}^*$, any linear functional (also called 1-forms) can be written as

$$\boldsymbol{\omega} = \omega_i\hat{\boldsymbol{e}}^i, \tag{A.10}$$

and acts on a vector $\boldsymbol{u}$ by

$$\boldsymbol{\omega}(\boldsymbol{u}) = \omega_iu^j\hat{\boldsymbol{e}}^i(\hat{\boldsymbol{e}}_j). \tag{A.11}$$

As $\hat{\boldsymbol{e}}^i$ are linear functionals on a vector space $\mathcal{V}$, they are completely defined by the action on the basis of $\mathcal{V}$. This way we can choose a basis for $\mathcal{V}^*$ satisfying $\hat{\boldsymbol{e}}^i(\hat{\boldsymbol{e}}_j) = \delta^i{}_j$. Note that in this general construction, the elements with basis $\{\hat{\boldsymbol{e}}^i\}$ are completely different mathematical elements from vectors with basis $\{\hat{\boldsymbol{e}}_i\}$, the way that they action can not be identified as an inner product, as inner products acts between elements of the same space. To reduce this general treatment to the case presented before, where the dual vectors belonged to the same space of the vectors, we must simply introduce the metric. Indeed, the metric acts as a natural isomorphism between $\mathcal{V}$ and $\mathcal{V}^*$ (a linear bijector map between

$\mathcal{V}$ and $\mathcal{V}^*$). For example, through the metric we can defined a map from $\mathcal{V}$ to $\mathcal{V}^*$ by

$$\boldsymbol{g}(\boldsymbol{u}) = g_{ij} u^j \hat{\boldsymbol{e}}^i. \tag{A.12}$$

The inverse mapping, from $\mathcal{V}^*$ to $\mathcal{V}$, can be defined with aid of the components of the inverse of the metric, which must be proved to exist by the properties of the metric. Hence, to the dual basis be also vectors as the natural basis, we must introduce extra structure to the vector space, the metric (the inner product). More details on this general approach can be found in (NAKAHARA, 2003).

A.2 Material Derivative of the Deformation Gradient Tensor

Applying the material derivative operator on F_{ij} and using its definitions,

$$\frac{DF^i_j}{Dt} = \left[\frac{\partial}{\partial t}\left(\frac{\partial x^i}{\partial X^j}\right)\right]_{\boldsymbol{X}} = \frac{\partial}{\partial X^j}\left(\frac{\partial x^i}{\partial t}\right)_{\boldsymbol{X}} = \frac{\partial}{\partial X^j} u^i(\boldsymbol{X}, t). \tag{A.13}$$

Thus, using the i-th component of the velocity field of the continuum, $u^i = u^i(\boldsymbol{x}(\boldsymbol{X}, t), t)$, we obtain that

$$\frac{DF^i_j}{Dt} = \left[\frac{\partial}{\partial x^k} u^i(\boldsymbol{x}, t)\right] \frac{\partial x^k}{\partial X^j}, \tag{A.14}$$

or, multiplying both sides of the equation by $\hat{\boldsymbol{e}}_i \otimes \hat{\boldsymbol{e}}^j$ and applying summations on the indexes i and j,

$$\frac{D\boldsymbol{F}}{Dt} = (\nabla \boldsymbol{u})^T \cdot \boldsymbol{F}. \tag{A.15}$$

We can also find the material derivative of the inverse of the deformation gradient tensor. Applying the material derivative on $\boldsymbol{F} \cdot \boldsymbol{F}^{-1} = \boldsymbol{I}$, we are left with

$$-\boldsymbol{F} \cdot \frac{D\boldsymbol{F}^{-1}}{Dt} = \frac{D\boldsymbol{F}}{Dt} \cdot \boldsymbol{F}^{-1}. \tag{A.16}$$

Thus, using Equation (A.15),

$$\frac{D\boldsymbol{F}^{-1}}{Dt} = -\boldsymbol{F}^{-1} \cdot (\nabla \boldsymbol{u})^T. \tag{A.17}$$

A.3 Exterior Product and Dual Relations

Consider two vectors, $\boldsymbol{u}$ and $\boldsymbol{v}$, on a vector space $\mathcal{V}$. Let us define a new operation $\wedge : \mathcal{V} \times \mathcal{V} \to \mathcal{V} \otimes \mathcal{V}$ by

$$\boldsymbol{u} \wedge \boldsymbol{v} = \boldsymbol{u} \otimes \boldsymbol{v} - \boldsymbol{v} \otimes \boldsymbol{u}, \tag{A.18}$$

known as exterior or wedge product. Note that the resultant tensor is skew-symmetric. Thus, we can represent the space of skew-symmetric tensors by $\mathrm{Skw}(\mathcal{V} \otimes \mathcal{V}) = \mathcal{V} \wedge \mathcal{V}$. The basis for $\mathcal{V} \otimes \mathcal{V}$ is $\{\hat{\boldsymbol{e}}_i \otimes \hat{\boldsymbol{e}}_j\}$, what implies that the basis for $\mathcal{V} \wedge \mathcal{V}$ is just $\{\hat{\boldsymbol{e}}_i \wedge \hat{\boldsymbol{e}}_j\}$.

In three-dimensional spaces, skew-symmetric tensors have only 3 independent components, the way that dimension($\mathcal{V}$) = dimension($\mathcal{V} \wedge \mathcal{V}$). Thus, in a Euclidean three-dimensional space, we can define a linear map $\tau : \mathcal{V} \wedge \mathcal{V} \to \mathcal{V}$, called duality map, by

$$\tau(\hat{\boldsymbol{e}}_i \wedge \hat{\boldsymbol{e}}_j) = \epsilon_{ijk} \hat{\boldsymbol{e}}^k. \tag{A.19}$$

If $\hat{\boldsymbol{e}}_i$ is orthogonal, the duality map τ establishes the correspondence given by

$$\hat{\boldsymbol{e}}_1 \wedge \hat{\boldsymbol{e}}_2 = \hat{\boldsymbol{e}}_3, \tag{A.20}$$

$$\hat{\boldsymbol{e}}_2 \wedge \hat{\boldsymbol{e}}_3 = \hat{\boldsymbol{e}}_1, \tag{A.21}$$

$$\hat{\boldsymbol{e}}_3 \wedge \hat{\boldsymbol{e}}_1 = \hat{\boldsymbol{e}}_2. \tag{A.22}$$

Thus, if $\boldsymbol{W}$ is a skew-symmetric tensor, i.e.

$$\boldsymbol{W} = W^{ij} \hat{\boldsymbol{e}}_i \otimes \hat{\boldsymbol{e}}_j = \frac{1}{2} W^{ij} \hat{\boldsymbol{e}}_i \wedge \hat{\boldsymbol{e}}_j, \tag{A.23}$$

the correspondent vector is given by

$$\begin{aligned} \boldsymbol{w} &= \tau(\boldsymbol{W}) \\ &= \frac{1}{2} W^{ij} \tau(\hat{\boldsymbol{e}}_i \wedge \hat{\boldsymbol{e}}_j) \\ &= \frac{1}{2} \epsilon_{ijk} W^{ij} \hat{\boldsymbol{e}}^k. \end{aligned} \tag{A.24}$$

If the basis is orthonormal, we have

$$w_i = \frac{1}{2} \epsilon_{ijk} W_{jk}, \tag{A.25}$$

$$W_{ij} = \epsilon_{ijk} w_k. \tag{A.26}$$

Equations (A.25) and (A.26) are known as duality relations and $\boldsymbol{w}$ is called the dual vector of $\boldsymbol{W}$.